12-15-2014

Climatic Controls on Organic Matter Decomposition in Boreal Peatlands

Michael J. Philben
University of South Carolina - Columbia

CLIMATIC CONTROLS ON ORGANIC MATTER DECOMPOSITION IN BOREAL PEATLANDS

by

Michael J. Philben

Bachelor of Arts
Northwestern University, 2010

Submitted in Partial Fulfillment of the Requirements

For the Degree of Doctor of Philosophy in

Marine Science

College of Arts and Sciences

University of South Carolina

2014

Accepted by:

Ronald H. Benner, Major Professor

Robert C. Thunell, Committee Member

James T. Morris, Committee Member

Sharon A. Billings, Committee Member

Lacy Ford, Vice Provost and Dean of Graduate Studies

DEDICATION

To Mom and Dad for their loving support throughout my journey, and to Carrie Pernesky for being the best partner I could ask for.

ACKNOWLEDGEMENTS

I am grateful to Glen MacDonald, Dave Beilman, and James Holmquist for providing the peat samples that formed the basis of this dissertation, and Karl Kaiser for laboratory assistance and training. I also thank Sue Ziegler, Kate Edwards, and Faye Murrin for providing vegetation samples from Newfoundland, Canada, Satoru Hobara and Keisuke Koba for providing vegetation from Toolik Lake, Alaska, Frank Chapelle for providing access to an elemental analyzer, Tristan Lawson for assistance with sample preparation and Raymond Kahler for assistance with amino acid analysis. Finally, I thank the NSF for funding this work.

ABSTRACT

Boreal peatlands currently contain 550 Pg C and are located at high latitudes where mean annual temperatures are expected to increase by as much as 7°C by the end of the century. There is growing concern that warming will stimulate decomposition, transforming peatlands from a sink to a source of atmospheric carbon dioxide and accelerating climate change. A primary goal of this dissertation was to evaluate the effect of climate change on organic matter decomposition in peatlands. This was achieved by developing and employing biochemical tracers to indicate the extent of peat decomposition across a range of naturally occurring climatic conditions. First, peat cores were analyzed from a latitudinal transect from the West Siberian Lowland, Russia. Cores in the south of the transect formed with mean annual temperatures as much as 7° warmer than those in the north. However, peat accumulation rates were as much as 5 times higher in the southern cores, leading to faster burial beneath the water table where anoxic conditions generally prevail. The northern cores therefore experienced longer oxygen exposure time than the southern cores. Three independent biochemical indicators (the C:N ratio, hydroxyproline yields, and acid:aldehyde ratios of lignin phenols) all indicated the northern cores were more extensively decomposed than the southern cores. This suggests oxygen exposure time is the primary control on the extent of peat decomposition while temperature is of secondary importance. The importance of oxygen exposure time was supported by assessing temporal changes in decomposition in a peat core from James Bay Lowland, Canada. A reconstruction of the water table based on fossil testate

amoebae indicated oxygen exposure time was longest in a 100 cm interval in the center of the core. This interval had lower yields of neutral sugars, lower C:N ratios, and higher amino acid and hydroxyproline yields than the rest of the core, indicating more extensive decomposition. The bottom 50 cm of the core was formed during the Holocene Thermal Optimum under conditions ~2°C warmer than the rest of the core, but was not more extensively decomposed. This supports the conclusion that oxygen exposure time rather than temperature is the main control on organic matter decomposition in peatlands. The low apparent sensitivity of decomposition to temperature is consistent with recent observations of a strong correlation between peat accumulation rates and mean annual temperature, suggesting contemporary warming could enhance peatland carbon sequestration.

TABLE OF CONTENTS

LIST OF TABLES

LIST OF FIGURES

List of Abbreviations

AA.....Amino Acid

Ad/Al..... Acid/aldehyde

Ara..... Arabinose

C.....Carbon

CI_{Carb} .....Carbohydrate Cyperceae Index

CI_{Phenol} ..... Phenol Cyperceae Index

DAPA.....Diaminopimelic Acid

DOM .....Dissolved Organic Matter

FID .....Flame Ionization Detector

Fuc..... Fucose

Gal.....Galactose

GC ..... Gas Chromatography

Glc..... Glucose

Hly.....Hydroxylysine

Hyp.....Hydroxyproline

HPAEC ..... High Performance Anion Exchange Chromatography

HRGP.....Hydroxyproline-Rich Glycoprotein

HTM.....Holocene Thermal Maximum

IDT.....Isodityrosine

LIA..... Little Ice Age

LI_{Carb}.....Carbohydrate Lichen Index

Man ..... Mannose

MCA ..... Medieval Climate Anomaly

N ..... Nitrogen

NMR ..... Nuclear Magnetic Resonance

NPP ..... Net Primary Production

PAD ..... Pulsed Amperometric Detection

PCA ..... Principle Component Analysis

PON ..... *p*-hydroxyacetophenone

Rha ..... Rhamnose

S ..... Syringyl

SI_{Carb} ..... Carbohydrate *Sphagnum* Index

THAA ..... Total Hydrolysable Amino Acids

THAS ..... Total Hydrolysable Amino Sugars

THNS ..... Total Hydrolysable Neutral Sugars

V ..... Vanillyl

VPI_{Phenol} ..... Phenol Vascular Plant Index

WSL ..... West Siberian Lowland

Xyl ..... Xylose

CHAPTER 1

REACTIVITY OF HYDROXYPROLINE-RICH GLYCOPROTEINS AND THEIR POTENTIAL AS BIOCHEMICAL TRACERS OF PLANT-DERIVED NITROGEN[1]

1.1 Introduction

Vascular plants represent the largest component of living biomass on Earth and are a critical component of the global biogeochemical cycles of C and N. During the decomposition of plant litter, microbes utilize plant-derived biopolymers and leave their biochemical imprint in the remaining detrital material [*Tremblay and Benner*, 2006; *Simpson et al*., 2007]. As plant detritus is typically N-poor vs. microbial biomass, decomposers incorporate exogenous N in the process of N-immobilization, increasing the N content of the detritus [*Melillo et al*., 1984; *White and Howes*, 1994; *Parton et al*., 2007]. The process is of interest, both due to the role of N as a limiting nutrient in many ecosystems and because it has been recently recognized that microbial remains constitute a major fraction of soil organic N and have a long turnover time *[Kindler et al*., 2006; *Miltner et al*., 2009].

Many current approaches for tracking the fate of plant and microbial inputs utilize isotope-labeled additions to detritus and soils [*Kindler et al*., 2006; *Miltner et al*., 2009; *Mambelli et al*., 2011]. In addition, changes in the detritus during the transition from

[1] Philben, M. and R. Benner (2013), Reactivity of hydroxyproline-rich glycoproteins and their potential as biochemical tracers of plant-derived nitrogen, *Organic Geochemistry*., *57*, 11-22, doi: 10.1016/j.orggeochem.2013.01.003.

carbohydrate-dominated plant remains to protein-rich microbial necromass duringdecomposition have been used to estimate plant and microbial contributions to the detrital N pool using nuclear magnetic resonance (NMR) spectroscopy [*Simpson et al*., 2007] andpyrolysis-gas chromatography-mass spectrometry combustion-isotope ratio mass spectrometry (Py-GC-MS-C-IRMS; [*Mambelli et al*. 2011]). While these approaches have provided valuable insights, they are not suitable for routine use in the field because they require experimental manipulations or controlled conditions.

A variety of unique compounds in the cell wall complex of bacteria, including muramic acid and D-enantiomers of amino acids (AAs), have been used to estimate bacterial contributions to the organic nitrogen pool in aquatic environments [*Tremblay and Benner*, 2006; *Kaiser and Benner*, 2008; *Lomstein et al*., 2009]. The amino sugars glucosamine, galactosamine, and muramic acid are often used as tracers of bacterial and fungal remains in soils, where fungi play a major role in decomposition [*Guggenberger et al.*, 1999; *Amelung*, 2001, 2003]. However, no such tracer of plant N is in use. Such a biochemical tracer could be used to estimate plant N contributions to soils and sediments, complementing the information on the immobilized N input gleaned from microbial tracers.

The AA 4-hydroxyproline (Hyp) is a promising candidate for a plant N tracer. It has only two major biochemical sources: hydroxyproline-rich glycoproteins (HRGPs) in plants, and collagen, a structural protein in animals. HRGPs are a family of homologous proteins in the primary cell walls of all land plants and most green algae, and include arabinogalactan proteins, extensins and solanaceous lectins [*Kieliszewski and Lamport*, 1994]. They are insoluble and play a structural role in plants by increasing the tensile

strength of the cell and contributing to pathogen defense [*Cassab*, 1998]. Animal remains are generally considered to be a relatively minor component of soils, so collagens are unlikely to contribute a significant amount of Hyp. In addition, collagen contains hydroxylysine (Hly; [*Spzak*, 2011]), another unique amino acid that can be used to identify collagen-derived Hyp.

Fungi and bacteria, the major decomposers of plant remains in soils, may synthesize small amounts of free Hyp for use in antibiotics such as etamycine [*Katz et al*., 1979] and cryptocandin [*Strobel et al*., 1999], but are believed to lack prolyl hydroxylase for the hydroxylation of peptidal proline residues [*Shibasaki et al*., 1999]. Bacteria contain collagen-like proteins that share collagen's repeated Gly-X-Y AA motif and triple helix structure, but appear to lack Hyp [*Rasmussen et al*., 2003; *Sylvestre et al*., 2003; *Xu et al.* 2002], although some fungal fimbriae may have Hyp-containing collagen [*Celerin et al*. 1996]. Since bacteria and fungi produce little Hyp and animal remains are a minor component of soils and sediments, HRGPs from plants and green algae are likely to be the only significant sources of Hyp. Thus, Hyp could be useful as a biogeochemical tracer of plant N in soils and sediments.

In this study, we have examined the reactivity of Hyp during a 4 yr decomposition experiment with plant tissue representative of the three major groups of higher plants: dicotyledonous angiosperms (dicots), monocotyledonous angiosperms (monocots), and gymnosperms. It is important to analyze tissue from different phylogenetic groups, as the HRGPs in these plant types, though closely related, can have important structural differences [*Kieliszewski and Lamport*, 1994]. We demonstrate that the reactivity of Hyp

is similar to that of bulk plant N in monocot tissue and gymnosperm tissue but is more resistant to decomposition in dicot tissue.

1.2. Material and methods

1.2.1. Decomposition experiments

A detailed description of the experiments is given elsewhere [*Opsahl and Benner*, 1995]. Briefly, green and senescent samples of black mangrove leaves (*Avicennia germainans*, a dicot), smooth cordgrass (*Spartina alterniflora*, a monocot) and cypress needles (*Taxodium distichum*, a gymnosperm) were collected in the vicinity of Port Aransas (Texas, USA). Senescent material (10-13 g) from each tissue were placed in mesh bags (60 µm opening), suspended in flow-through tanks receiving estuarine water and incubated in the dark to prevent the growth of algae. Duplicate bags were harvested at progressively longer intervals over the 4 yr period. After harvesting, bags were rinsed with deionized water and dried for 3 days at 45°C. The samples were ground and homogenized using a Wiley mill. All chemical analyses were made on material from each replicate bag.

1.2.2. Bacterial and fungal samples

To test for the presence of Hyp in bacteria and fungi, lyophilized cells of 5 bacterial cultures (*Pseudomonas fluorescence, Azobacter vinelandii, Bacillus subtilis, Micrococcus* sp., and *Aerobacter* sp.) and samples of 4 species of fungi (*Cortinarius armillatus, Albatrellus ovinus, Clitocybe* sp., and *Russula paludosa*) were analyzed for AAs. All bacteria were obtained from Sigma and fungal samples were collected from a boreal forest in Newfoundland, Canada. Fungi were oven-dried at 60 °C and ground using a Wiley mill.

1.2.3. Chemical analysis

The C content and N content were measured using a Carlo Erba EA 1108 CHN analyzer [*Opsahl and Benner*, 1995]. Stable N isotopes were measured by Coastal Science Labs (Austin, Texas, USA). Lignin-derived phenols were analyzed via CuO oxidation followed by gas chromatography (GC) with flame ionization detection (FID) and presented in Opsahl and Benner [1995]. The sum of the *p*-hydroxy phenols (*p*-hydroxybenzaldehyde, *p*-hydroxyacetophenone, *p*-hydroxybenzoic acid), syringyl phenols (syringaldehyde, acetosyringone, syringic acid), and vanillyl phenols (vanillin, acetovanillone, vanillic acid) is reported here.

Samples for total hydrolysable neutral sugar (THNS) analysis were pretreated in 12M H_2SO_4 for 2 h, followed by dilution to 1.2 M H_2SO_4 and hydrolysis at 100 °C for 3 h. The hydrolysates were derivatized using Sylon BFT (Supelco) at 60 °C for 10 min,analyzed by GC-FID, and presented in Opsahl and Benner [1999]. The following neutral sugars were measured: arabinose (Ara), fucose (Fuc), galactose (Gal), glucose (Glc), lyxose (Lyx), mannose (Man), rhamnose (Rha), ribose (Rib) and xylose (Xyl). Total hydrolysable amino sugars (THASs) were analyzed using the method of Kaiser and Benner [2000]. Samples (5 mg) were hydrolyzed in 3 M HCl at 100 °C for 5 h in sealed ampoules. Following hydrolysis, samples were neutralized with the self-absorbed AG11 A8 resin (BioRad), desalted using the cation exchanger AG50 X8 (Na^+ form; BioRad) and analyzed using high performance anion exchange chromatography (HPAEC) with pulsed amperometric detection (PAD). The three amino sugars analyzed were glucosamine (GlcN), galactosamine (GalN) and mannosamine (ManN).

Samples (10 mg) for total hydrolysable amino acid (THAA) analysis were placed in sealed ampoules with 1 ml 6 M HCl at 110 °C for 20 h. The HCl was removed under a stream of N_2 and the samples were redissolved in 200 µl deionized water. Norvaline was added to each sample as internal standard and samples were processed and derivatized using the Phenomenex EZ:faast method. AAs were separated using GC (Phenomex ZB-AAA column; 110° to 320°C at 30° min^{-1}) with FID. AA yields were quantified using the external standard method. The external standard included 16 AAs and was analyzed daily. The quantified AAs were: alanine (Ala), glycine (Gly), valine (Val), leucine (Leu), isoleucine (Ile), threonine (Thr), serine (Ser), proline (Pro), aspartic acid (Asp), methionine (Met), hydroxyproline (Hyp), glutamic acid (Glu), phenylalanine (Phe), lysine (Lys), histidine (His) and tyrosine (Tyr). Unlike the commonly used OPA derivatization for fluorometric detection, this procedure allows measurement of the heterocyclic AAs Pro and Hyp. Asparagine and glutamine are converted to aspartic acid and glutamic acid, respectively, during acid hydrolysis and are included in the reported measurements of Asp and Glu. The mean deviation for the analysis of replicate litter bag samples ranged from ±2.1-5.8% for THAA and ±2.0-4.4% for Hyp.

The lignin phenols, neutral sugar and AA yields are reported as a proportion (%) of the total C according to the equation:

$$\%C_{biochemical} = \Sigma(Yield_{biochemical}/C)*(Wt\ \%\ C_{biochemical}/100) \quad (1.1)$$

where $Yield_{biochemical}/C$ is the C-normalized yield of each measured biochemical in mg biochemical (100 mg C)$^{-1}$ and Wt % $C_{biochemical}$ is the wt. % carbon in the biochemical.

1.2.4. Calculation of %N from senescent plant tissue

The N measured is the sum of the N from the plant tissue and the N immobilized from exogenous sources. Three independent approaches were used to estimate the fraction of N derived from the plant tissue [*Tremblay and Benner*, 2006]. In the first, the "plant reactivity method", it is assumed that plant N is removed at the same rate as bulk C or lignin phenols during decomposition. The amount of plant N remaining at time *t* (N_{Plant}) was calculated using the equation:

$$N_{Plant} = N_{Plant,\ initial}\ (C_t/C_{initial}) \quad \text{or} \quad N_{Plant} = N_{Plant,\ initial}\ (\text{lignin}_t/\text{lignin}_{initial}) \tag{1.2}$$

where $N_{Plant,\ initial}$ is the wt. % N of the senescent plant tissue, C_t and lignin_t are the wt. % C and lignin phenol yield, respectively, of the detritus at time *t*, and $C_{initial}$ and $\text{lignin}_{initial}$ are the wt. % C and lignin phenol yields in the senescent tissue. The proportion of detrital N derived from the plant tissue was calculated as:

$$\%\ \text{Plant N} = 100*(N_{Plant}/N_{sample}) \tag{1.3}$$

where N_{sample} is the total N in the sample. The reported value is the mean of the results obtained using the reactivity of carbon and lignin phenols.

The second method uses N isotopes to estimate the relative contribution of plant and exogenous N sources in the detritus according to the equation:

$$\delta^{15}N_{sample} = (\%N_{plant} \times \delta^{15}N_{plant}) + (\%N_{immob} \times \delta^{15}N_{immob}) \tag{1.4}$$

It is assumed that there is no fractionation of N-isotopes during decomposition, and all changes in detrital $\delta^{15}N$ are due to differences between the $\delta^{15}N$ value of the original plant material ($\delta^{15}N_{plant}$) and the $\delta^{15}N$ value of exogenous N ($\delta^{15}N_{immob}$). $\delta^{15}N_{immob}$ is assumed to be between 8.8‰ (the most ^{15}N-rich sample observed) and 11‰, the value estimated for dissolved inorganic N in the experiments [*Tremblay and Benner*, 2006]. The calculation was performed twice, using the two alternative values for the $\delta^{15}N_{immob}$ end member and the mean result reported.

To test the usefulness of Hyp as a geochemical tracer, plant-derived N was also calculated using it as an indicator of plant N, according to the equation:

$$\%\text{Plant N} = 100\,\frac{\text{Hyp/N}_t}{\text{Hyp/N}_{initial}} \qquad (1.5)$$

where $(Hyp/N)_t$ is the N-normalized Hyp yield at time *t* and $(Hyp/N)_{initial}$ is the N-normalized yield in the senescent tissue.

1.3. Results

1.3.1. Sources of Hyp

Microbes can synthesize trace quantities of Hyp as secondary metabolites, but none of the 5 species of bacteria or 4 species of fungi tested in this study contained detectable amounts of Hyp. A literature search showed that it is found in all land plants and all green algae (*Chlorophyta* and *Charophyta*) except for the genus *Nitella* (Table 1.1). It is also found in low concentration in diatoms [*Mannino and Harvey*, 2000], where it is concentrated in soluble cellular protein rather than in the cell wall [*Gotelli and Cleland*, 1968]. It occurs in the cell walls of oomycetes (water molds) but not in the walls of true fungi [*Crook and Johnston*, 1962]. As bacteria and fungi lack significant amounts of Hyp and were the dominant decomposers during this experiment, the litter bags had no exogenous sources of Hyp.

1.3.2 Bulk parameters

All three vascular plant tissues experienced extensive decomposition over the course of the 4 yr study. Decomposition was most extensive for the mangrove leaves, which lost 97.5% of their initial C in the 4 yrs (Table 2). Cordgrass and cypress needles lost 93.0% and 87.6%, respectively. Losses during the first 42 days were attributed largely to leaching of soluble components, while subsequent losses were due mainly to microbial degradation [*Opsahl and Benner* 1995].

Bulk N loss was less than C loss for all three tissues. After 4 yrs, 10.8% of the initial N remained in the mangrove leaves, and 25.9 and 34.5% in the cordgrass and cypress needles, respectively (Table 1.2; Fig. 1.1b). For cypress needles, > 100% of the

initial N was present after 1.8 yr despite extensive mass loss, demonstrating net immobilization of exogenous N.

Senescent cypress needles had a C:N ratio of 120, approximately double that of mangrove leaves and cordgrass (Table 1.2). In mangrove leaves and cypress needles, the ratio declined throughout (Fig. 1.1a). As the wt. % OC remained relatively constant, the large decrease in C:N mostly reflects an increase in wt. % N during decomposition [*Tremblay and Benner* 2006]. The C:N ratio in cordgrass displayed a different pattern, increasing by 40% during the leaching phase before declining during microbial decomposition (Fig. 1.1a).

The stable isotope composition ($\delta^{15}N$) of mangrove leaves and cypress needles decreased during the leaching phase before increasing to above their initial values by 4 yrs (Table 1.2; Fig. 1.1c). The $\delta^{15}N$ of mangrove leaves increased from a minimum of 5.7‰ after 189 days to 8.7‰ after 4 yrs and increased from a minimum of 4.3 to 7.6‰ in cypress needles. The cordgrass $\delta^{15}N$ did not decline during the leaching phase and steadily increased from 1.2‰ in the senescent tissue to 6.1‰ after 4 yrs.

1.3.3. Yields of neutral sugars, lignin phenols, AAs and amino sugars

THAAs, neutral sugars, amino sugars and lignin phenols accounted for 19-58% of the C in the senescent tissue (Table 1.2). The largest fraction of carbon was characterized for cordgrass due to its high neutral sugar yield. The proportion of C characterized remained relatively constant in the mangrove leaves but declined from 58 to 34% in the cordgrass and from 19 to 8% in the cypress needles.

Neutral sugars were the most abundant class characterized in the senescent tissues, and they were also the most reactive component in all tissues (Fig. 1.2). By the

end of the study, the neutral sugar yield had declined 60% in mangrove leaves, 71% in cordgrass and 80% in cypress needles, relative to the yield in their respective senescent tissues. The cordgrass neutral sugar yield was at least 2.5 times the yield from the other senescent tissues. Cordgrass neutral sugars were also less reactive during the initial stages, declining to only 90% of their initial yield after 3 yrs, but then fell to 29% of initial by the end of the study.

Lignin phenols accounted for 2.5% of the C in senescent mangrove leaves, 5.3% in cordgrass and 1.9% in cypress needles (Table 1.2). In all three tissues, the lignin yield increased during the first 3 yrs (Fig. 1.2). As lignin phenols have no exogenous sources, these increases indicate that lignin was less reactive than the bulk C. However, the lignin phenol yield declined between 3 yrs and 4 yrs for all 3 tissues, indicating that during this period lignin was removed more rapidly than bulk C.

AA yields from mangrove leaves and cordgrass both declined during senescence, indicating the resorption of some AAs during senescence [*Aerts*, 1996] . The yield from senescent mangrove leaves was 68% lower than from green leaves, while the senescent cordgrass yield was 45% lower (Table 1.2). AA yield increased with decomposition for all 3 tissues, by a factor of 4 for mangrove leaves, a factor of 3 for cordgrass and a factor of 2 for cypress needles. For cordgrass, the yield decreased slightly in the leaching phase before increasing during the phase of microbial degradation.

Amino sugar yields increased 16-fold in mangrove leaves and 28-fold in cordgrass after 4 yrs of decomposition (Table 1.2). The absolute amount increased during the first year to 270% and 134% of the amount present in the senescent cordgrass and mangrove leaves, respectively (Fig. 1.3). These increases occurred despite considerable

mass loss from the two tissues, indicating extensive microbial input. There was net removal of amino sugars in both tissues after 1 yr, indicating turnover of microbial remains.

1.3.4. Hyp yield

The Hyp yield displayed very different patterns with decomposition in the 3 tissue types (Table 1.2). For mangrove leaves, the most Hyp-rich tissue, the yield increased from 17.2 nmol mg C^{-1} for the senescent tissue to 79.8 nmol mg C^{-1} after 4 yrs of decomposition, a more than 4 fold increase. As Hyp lacks a significant exogenous source, the increase in is due to selective preservation of Hyp vs. bulk carbon. The Hyp yield increased more slowly for the cordgrass, but doubled in 4 yrs. For the cypress needles, the yield initially increased for 1.8 yrs, but then declined back to its initial value.

The reactivity of Hyp is similar to that of lignin phenols in cordgrass and cypress needles (Fig. 1.2). The yield of both components increased to ca. 200% of the initial yield for the cordgrass and returned to ca. 100% for the cypress needles after an initial increase. The Hyp yield from cordgrass displayed a different pattern than the lignin yield, as the lignin yield increased for 3 yrs but declined in the 4^{th} year, while the Hyp yield continued to increase for the duration of the experiment. In the mangrove leaves, Hyp was much less reactive than lignin phenols. The Hyp yield increased to 465% of its initial value by the end of the study, while the lignin yield increased only to 143%. Thus, Hyp in mangrove leaves was more resistant to decomposition than lignin phenols.

Although Hyp was less reactive than bulk C and other major biochemicals, the absolute amount of Hyp remaining declined with decomposition in all 3 tissues (Fig. 1.3). After 4 yrs, 12% of the initial Hyp remained in the mangrove leaves and the cypress

needles, while 14% remained in the cordgrass. The removal of Hyp from mangrove leaves showed a pattern very similar to the removal of N (Fig. 1.3). For cordgrass and cypress needles, N was removed more slowly than Hyp.

The mol% Hyp of both mangrove leaves and cordgrass was higher in senescent tissue than in fresh green tissue (Table 1.2). Hyp increased from 1.3 to 3.8% of the THAAs during senescence in mangrove leaves, and from 1.2 to 1.7% in cordgrass. As the Hyp yield was lower in the senescent tissue than in the green tissue, the changes were caused by a sharp decline in AA yield in both tissues during senescence, likely due to resorption. As most Hyp is bound in insoluble structural proteins, little Hyp was resorbed during senescence. The mol% Hyp decreased during decomposition in all tissues, as the AA yield increased more rapidly than the Hyp yield due to immobilization of exogenous N not containing Hyp.

1.3.5. Proportion (%) N from senescent plant tissue

The plant reactivity method and the N isotope method gave similar estimates of the proportion of detrital N derived from the senescent plant tissue (% Plant N) after 4 yrs of decomposition in all three tissues (Fig. 1.4). The N isotope method resulted in < 100% plant N in senescent mangrove leaves and cypress needles because the $\delta^{15}N$ declined during the leaching phase. The minimum $\delta^{15}N$ value was used as $\delta^{15}N_{Plant}$, causing the senescent tissue to appear to contain immobilized N.

Using the N normalized Hyp yield to estimate the % Plant N ("Hyp method") compared well with the other two methods for cordgrass and with the plant reactivity method in cypress needles (Fig. 1.4). The N isotope method indicated higher % Plant N in cypress needles than the other two methods for the first 3 yrs of decomposition, but

converged with the other methods after 4 yrs. For the mangrove leaves, the Hyp method indicated that nearly 100% of the N in the litter bags was plant-derived throughout the experiment. This contrasted with the plant reactivity and N isotope methods, which indicated that 33% and 39%, respectively, was plant-derived.

1.3.6. Hyp-rich glycoprotein (HRGP) AA composition and reactivity

A literature review of HRGP AA composition revealed that all HRGPs are rich in the AAs Hyp, Pro and Lys (Table 1.3). In addition, almost all characterized HRGPs from dicots are rich in Tyr and Val, while monocot HRGPs are rich in Thr but have little Val or Tyr. With the exception of Val, these AAs are found in relatively low abundance in decomposers and in bulk plant tissue. This makes them useful tracers of HRGPs in the decaying tissues. In all plant types, the (Tyr+Lys):Hyp ratio never fell below 0.54, the mean ratio in dicot HRGPs (Fig. 1.5). In mangrove leaves, the ratio declined with decomposition but never dropped below the critical value of 0.54. This observation is consistent with the intact preservation of the peptide component of HRGP, as non-HRGP Tyr and Lys are removed more quickly than they are added through immobilization, leaving behind detritus with an AA composition more closely resembling HRGP.

Assuming all Hyp in the detritus is derived from HRGP and the HRGP peptides are preserved intact, the mean AA composition of HRGP from each taxonomic grouping can be used to estimate the contribution of N from HRGPs to the detrital N in each litter bag. Thus, the detrital N originating from the senescent tissue can be divided into HRGP-associated N and other plant N using the equation:

$$\%\text{Plant N as HRGP} = \frac{(\%\text{THAA as HRGP})(\%\text{N as THAA-N})}{\%\text{Plant N}} \quad (1.6)$$

To avoid circular reasoning, the Hyp method was excluded from this calculation and % Plant N was calculated using the mean of the plant reactivity and N isotope methods. The %THAA as HRGP was calculated as:

$$\%\text{THAA as HRGP} = 100 \times \frac{\sum[(\text{Hyp}_{\text{sample}}) \times (\text{mol\% AA}_{\text{HRGP}})/(\text{mol\% Hyp}_{\text{HRGP}})]}{\text{THAA}_{\text{sample}}} \quad (1.7)$$

for each of the 16 AAs constituting THAA. Hyp_{sample} and THAA_{sample} represent the C-normalized yields of Hyp and THAA, respectively. Mol% AA_{HRGP} and mol% Hyp_{HRGP} were calculated as the mean for each plant type from Table 1.3.

The calculation showed that the proportion of plant-derived N accounted for by HRGPs changed little with decomposition in the cordgrass and cypress needles, indicating that the reactivity of HRGPs was similar to that of other plant-derived N-containing components (Fig. 1.6). In mangrove leaves, HRGPs were less reactive than other mangrove-derived N, and after 4 yrs of decomposition HRGPs accounted for > 15% of the total plant-derived N.

1.3.7. HRGP glycan composition and reactivity

In vascular plant HRGP, Hyp often forms linkages with arabinose oligosaccharides, resulting in Hyp-Ara_n blocks, with *n* typically 1-4 subunits [*Lamport and Miller*, 1971]. The size of the typical block varies with taxonomic grouping. Dicot HRGP contains mostly Hyp-Ara_4 arabinosides, gymnosperms contain an even mixture of Hyp-Ara_4 and Hyp-Ara_3, and monocots have mostly unglycosylated Hyp (Table 1.4). This information can be used to calculate a mean Ara/Hyp ratio for each group. The Ara/Hyp ratio is 3.1 in dicots, 1.0 in monocots and 2.4 in gymnosperms.

The Ara/Hyp values in the senescent plant tissues were much higher than these values, as plants have many non-HRGP sources of Ara. However, these sources are more reactive than HRGP and the ratio declined with decomposition as Ara was remineralized (Fig. 1.7). The Ara/Hyp ratio in mangrove leaves declined from 25.4 to 4.8 after 189 days, and then remained fairly constant to the end of the study. Despite increasing Hyp yield, the ratio never dropped below 2.3. This suggests that association with HRGP protected arabinose from microbial degradation, as the Ara/Hyp ratio in mangrove leaves remained close to the ratio in dicot HRGPs, although this could also be caused by microbial Ara production. This trend was not visible for the cordgrass, which contained much more Ara that was not associated with HRGP.

1.4. Discussion

1.4.1. Preservation of HRGP in mangrove leaves

HRGPs in mangrove leaves appeared to be selectively preserved vs. other plant proteins, while their reactivity was similar to that of other plant proteins in cordgrass and cypress needles. Since the decomposition of all three tissues occurred under similar conditions, the apparent resistance of mangrove HRGP to microbial decomposition is most likely due to differences between mangrove leaves and the other plant tissues. It appears that either the structure of mangrove HRGP makes it inherently recalcitrant to decomposition compared with HRGP from other plants, or the physical and chemical environment of the mangrove cell wall protects the HRGP in ways that the other plant cell walls do not. We discuss below four potential mechanisms for the selective preservation of HRGP.

1.4.1.1. Association with tannins

One potential mechanism for the preservation of plant proteins is association with tannins. Tannins form hydrophobic associations and hydrogen bonds with proteins [*Hagerman et al*., 1998] and tannin-protein complexes are more resistant to microbial attack than unaltered proteins [*Howard and Howard*, 1993]. In addition, proline-rich proteins like HRGPs form complexes more readily than other proteins [*Hagerman and Butler*, 1981]. Thus, association with tannins could contribute to the observed preservation of HRGPs.

However, this hypothesis is not viable for black mangrove leaves because they lack detectable amounts of tannins. In a synthesis of colorimetric and protein precipitation tannin assays, Mole [1993] reported that tannins were detected in only 6% of plants from the Acanthaceae family, which includes black mangroves. A molecular analysis also failed to detect tannins in black mangrove leaves [*Hernes and Hedges*, 2004]. Cordgrass, like most other monocots, also lacks tannins, so cypress needles are the only tannin-containing tissue analyzed in the present study [*Mole*, 1993; *Hernes and Hedges*, 2004]. As cypress needle Hyp was the most reactive of the three tissues, it is unlikely that complexation with tannins contributed significantly to the preservation of HRGP.

1.4.1.2. Physical protection from cell wall matrix

There is abundant evidence that association with an organic matrix such as the cell membrane or organelles can slow the degradation of otherwise labile proteins in marine environments [*Knicker and Hatcher*, 1997; *Nagata et al*., 1998; *Borch and*

Kirchman, 1999; *Moore et al*., 2012]. Therefore it is possible that association with the plant cell wall aids the preservation of HRGPs.

The physicochemical associations between HRGPs and other components of the plant cell wall are not well known. It was initially thought that HRGP forms an independent network in the cell wall, strengthened and made insoluble by isodityrosine (IDT) intramolecular cross-links [*Fry*, 1982; *Cooper and Varner*, 1984] and pulcherosine (tri-tyrosine) and di-IDT (tetra-tyrosine) linkages between HRGP monomers [*Brady et al*., 1996; *Held et al*., 2004]. This network was thought to form a net, weaving together cellulose microfibrils and increasing the physical strength of the cell wall [*Wilson and Fry*, 1986]. In this model, HRGPs do not form covalent bonds with other cell wall components, but may be protected by intimate physical association with the cell wall matrix. In addition, the basic AAs in HRGPs likely form ionic bonds with the negatively charged uronic acids in pectin [*Smith et al*., 1986], which may give the complex additional protection from microbial decomposition. However, more recent evidence suggests that HRGPs form a covalent bond with pectin in cultured cotton cells [*Qi et al*., 1995] and in sugar beet [*Nunez et al*., 2009]. The precise nature of the linkage is unclear, but it likely increases the resistance of associated HRGP to microbial degradation.

Whatever the linkage between HRGPs and pectin, it alone cannot explain the difference in reactivity between mangrove HRGP and HRGP from the other two plant tissues. Current models indicate that dicot and gymnosperm primary cell walls are very similar, with the only major difference being greater glucomannans in gymnosperm walls [*Popper*, 2008; *Sarkar et al.*, 2009]. Thus, HRGP from mangrove, a dicot, and HRGP from cypress, a gymnosperm, exist in a very similar physical environment, yet mangrove

HRGP is much more resistant to decomposition than cypress HRGP. This shows that while physical protection within the cell wall matrix may play a role in the protection of HRGP, it cannot explain the large difference in reactivity between mangrove and cypress HRGPs.

In addition, Hyp in mangrove leaves was less reactive than any of the cell wall components that may be associated with it. Lignin is generally less reactive than the polysaccharide components of cell walls [*Benner et al*., 1984; *Benner and Hodson*, 1985; *Stout et al*., 1988], yet Hyp was less reactive than lignin phenols in decomposing mangrove leaves. If the cell wall matrix is responsible for the protection of HRGP from microbial attack, the reactivity of HRGP should be similar to the wall components with which it is associated. This was observed for the cordgrass and cypress needles, where HRGP and lignin phenols have similar reactivity, but not the mangrove leaves. Again, it is likely that the organic matrix of the cell wall slows decomposition of HRGP in all three tissues, but it cannot explain the recalcitrance of HRGP in mangrove leaves relative to the other tissues.

1.4.1.3. Protection due to glycosylation

A third hypothesis explaining the preservation of HRGP is that glycosylation inhibits microbial decomposition of the peptide portion of the molecule. Kiel and Kirchman [1993] showed that marine microbes distinguish between glycosylated and nonglycosylated protein, and that the turnover time of the glycosylated protein was 34-202 times longer than that of unmodified protein. In addition, glycoproteins account for a major fraction of protein in marine dissolved organic matter (DOM) [*Yamada and Tanoue*, 2003], which is considered to be highly degraded (e.g. [*Kaiser and Benner*,

2009]). Together, these findings suggest that the glycosylation of proteins may decrease their reactivity and contribute to their survival in the environment.

Previous research on the structure of HRGPs supports the hypothesis that glycosylation contributes to their resistance to decomposition. The arabinosides bound to Hyp contribute to the overall stability of the molecule and lock it into an extended polyproline-II conformation [*Vanholst and Varner*, 1984; *Stafstrom and Staehelin*, 1986b]. The arabinosides appear to be very effective at protecting HRGP from degradation by proteases. Digestion with trypsin released only 5% of the Hyp in a cultured cotton cell wall, but this increases to 50% after the selective removal of arabinosides [*Qi et al*., 1995]. The hydrolysis of HRGP by pronase, a commercially available protease mix, was also more efficient after the removal of sugars [*Esquerre-Tugaye and Lamport*, 1979].

Hyp from dicots have the highest degree of arabinosylation (on average, 3.1 arabinose residues per Hyp). HRGPs from mangrove leaves, a dicot, were more resistant to decomposition than HRGPs from the other two plant types. Hyp from monocot cell walls was much less glycosylated and was more reactive. This is consistent with the protection of HRGPs by glycosylation. However, Hyp in gymnosperm cell walls has an average arabinoside length of 2.4. Gymnosperm HRGPs are only slightly less glycosylated than dicot HRGPs, but were more reactive than HRGPs in both monocots and dicots. Thus it appears that the extent of glycosylation is not, by itself, a good predictor of the reactivity of HRGP, which casts doubt on the hypothesis that glycosylation is solely responsible for its resistance to decomposition.

1.4.1.4. Protection due to protein-protein cross links

Dicot HRGPs contain extensive protein-protein cross links, both within and between peptide chains. The cross linking of dicot HRGPs is different from the cross linking of monocot and gymnosperm HRGPs, giving it the potential to further explain the difference in reactivity between the mangrove leaves and the other tissues.

Both intramolecular and intermolecular linkages involve tyrosine residues. Intramolecular IDT linkages arise from the formation of a diphenyl ether bond between two tyrosine residues in the repeated amino acid sequence Tyr-Lys-Tyr [*Epstein and Lamport*, 1984; *Stafstrom and Staehelin*, 1986a]. This cross link forms a kink in the otherwise rod-shaped HRGP molecule [*Stafstrom and Staehelin*, 1986a]. Pulcherosine (tri-tyrosine) and di-IDT (tetra-tyrosine) linkages cross link HRGP polypeptides [*Brady et al*., 1996; *Held et al*., 2004]. Like the IDT linkage, pulcherosine and di-IDT cross links involve highly stable diphenyl ether bonds. These linkages are very common in HRGPs; solid-state ^{13}C-NMR analyses of cotton cell walls indicate that 25% of the tyrosine residues are in the form of IDT [*Cegelski et al*., 2010]. However, it appears that IDT is specific to dicots. Although it appears to be ubiquitous among dicots, it is absent from the cell walls of maize, a monocot [*Kieliszewski and Lamport*, 1994] and Douglas Fir, a gymnosperm [*Kieliszewski et al*., 1992a].

The intermolecular tyrosine cross linking of HRGP is performed enzymatically by extensin peroxidase [*Everdeen et al*., 1988]. Schnabelrauch et al. [1996] proposed two conditions for successful cross linking: presence of the Val-Tyr-Lys AA sequence and a high level of glycosylation. Monocot HRGP lacks the Val-Tyr-Lys motif [*Kieliszewski et al.*, 1990] and was not cross linked by extensin peroxidase. While Douglas Fir HRGP

contains the Val-Tyr-Lys motif, the isolated HRGP monomers are lightly glycosylated [*Kieliszewski et al*., 1992a] and are also not cross linked by extensin peroxidase. This shows that there is a clear difference between the structures of dicot HRGPs and monocot and gymnosperm HRGPs. Dicot HRGP is extensively cross linked by IDT, pulcherosine, and di-IDT, while monocot and gymnosperm HRGPs are not. Further, these cross links involve diphenyl ether and biphenyl linkages, which are stable and difficult to degrade. Thus, this structural difference among plant tissues provides a likely mechanism contributing to the selective preservation of mangrove HRGP vs. cordgrass and cypress HRGP.

In summary, association with other components of the primary cell wall, including covalent or ionic bonds with pectin, likely contributes to the protection of HRGP from microbial attack in all three tissues. However, the cell walls of dicot angiosperms and gymnosperms are very similar in structure, so HRGP from mangrove leaves and cypress needles exists in similar physical environments. It appears that physical protection cannot explain the large difference in reactivity between mangrove HRGP and HRGP from cypress needles. Therefore, the difference in reactivity is likely caused by a difference between the structure of HRGP in mangrove leaves and in the other tissues. Differences in glycosylation is a tempting hypothesis, as dicot HRGP is the most heavily arabinosylated and glycosylation has been proposed as a mechanism for the production of recalcitrant OM in the ocean. However, gymnosperm HRGP is only slightly less glycosylated than dicot HRGP. Thus, differences in protein-protein cross linking between the tissue types most likely account for differences in HRGP reactivity. Dicot HRGP contains many IDT, pulcherosine, and di-IDT linkages between

polypeptides, which appear to be absent from monocotyledon and gymnosperm HRGP. These diphenyl ether linkages are very difficult to break down and may be responsible for the recalcitrance of mangrove HRGP.

1.4.2. Biogeochemical applications

Hyp has the potential to be a useful biogeochemical indicator in soil because it is restricted to only two major biochemical sources, HRGPs and collagen. Like HRGP, collagen is a rigid, Hyp-rich structural protein. It is the principle protein in animal connective tissue and has been found in every animal phylum [*Adams*, 1978]. It seems to have good preservation potential, as the isotopes of preserved collagen are commonly used in paleodietary studies [*Deniro,* 1985]. Fortunately, the occurrence of collagen is unlikely to affect the usefulness of Hyp as a biogeochemical indicator in most environments. Macrofaunal biomass and remains are likely minor components of soil OM (SOM), DOM, or sedimentary OM compared with detritus from plants, plankton and microbes. In addition, collagen contains the uncommon AA, Hly [*Szpak*, 2011], which can be measured in routine AA analyses, including the method used herein, and can be used to estimate collagen contribution to the measured Hyp. Hly was not detected in any of the samples in this study, confirming the absence of significant amounts of collagen.

The reactivity of Hyp was similar to the reactivity of the bulk plant N in cordgrass and cypress needles. This is consistent with results from Nguyen and Harvey [2003], who found that during the decomposition of the green alga *Botryococcus braunii,* Hyp was remineralized at a rate similar to other algal AAs. These results indicate that the N-normalized Hyp yield can be used as a quantitative tracer of plant N in systems with plant communities dominated by monocots, gymnosperms, or both. The accuracy of this

application was tested by comparing it with two independent methods for estimating the amount of plant-derived N in detritus, the plant reactivity method and the N isotope method. Results from the Hyp method agreed with the other two methods for cordgrass. For cypress needles, the Hyp method agreed with the plant reactivity method throughout the study and converged with the N isotope method after the 4 yrs. The agreement among these independent methods increases confidence in their accuracy, but of these approaches only the Hyp method can be readily applied to field studies.

Hyp in mangrove leaves was more resistant to decomposition than bulk plant N, so substantial litter input from dicots to soil could lead to overestimation of plant-derived N using the Hyp method. To evaluate the sensitivity of the tracer to changes in dicot input and to illustrate a system where Hyp could potentially be applied, we calculated the proportion (%) of plant-derived N in a mixture of gymnosperms, dicots and monocots representative of a mature black spruce stand in a boreal forest. The contribution of each plant group to the total net primary production (70% from gymnosperms, 27% from dicots and 3% from monocots; [*Mack et al*., 2008]) was assumed to reflect their contributions to the litter. The reactivity of Hyp and N in cypress needles, mangrove leaves and cordgrass as determined by this study was assumed to be representative of their behavior in gymnosperms, dicots and monocots, respectively. The N-normalized Hyp yield of this example mixture at time *t* during 4 yrs of decomposition was modeled using the equation:

$$\text{Hyp/N} = \frac{\sum_{i=d,m,g}\left[f_i \times (\%\text{Hyp remaining})_i \times (\text{Hyp/C})_{\text{plant},i}\right]}{\sum_{i=d,m,g}\left[f_i \times (\%\text{N remaining})_i \times (\text{N/C})_{\text{plant},i}\right]} \quad (1.8)$$

where f_i is the fraction of the litter from each plant type (dicots, monocots, and gymnosperms), and $Hyp/C_{plant,i}$ and $N/C_{plant,i}$ are the C-normalized Hyp yield and N:C weight ratio in senescent mangrove leaves, cordgrass, or cypress needles. %Hyp and %N remaining at time *t* were calculated using the yield of Hyp and N for each plant type as measured in this study.

The proportion (%) of plant-derived N in the model mixture was calculated using Eq. 1.5. To illustrate the sensitivity of the method to changes in the contribution of dicots to the mixture, the results were compared to the proportion (%) of plant-derived N as calculated using the Hyp method with cypress needles.

The calculations indicate the Hyp method has a relatively low sensitivity to change in dicot input. The Hyp method using cypress needles indicated 36% of the N present after 4 yrs of decomposition was plant-derived, while increasing the proportion of dicot input to 27% increased the estimate of plant-derived N to 49% (Fig. 1.8). The calculation with 0% dicot input is assumed to be an accurate estimate of the plant-derived N because the Hyp method agreed with the other two methods for calculating the proportion of plant-derived N in cypress needles after 4 yrs. Therefore, increasing the dicot input from 0 to 27% resulted in overestimation of the plant-derived N by 13%. This demonstrates the applicability of the Hyp method and the importance of estimating dicot inputs to the system being studied when applying this method.

The mixing model suggests that Hyp can be a good tracer of plant-derived N in boreal forest soils. This would be an important application because these ecosystems are globally important and contain as much as 550 Pg C, about half of the total C stored in forest ecosystems [*Larsen*, 1980; *Dixon et al.*, 1994]. Further research should focus on

the development of this tracer in boreal forest soils and in other ecosystems with known inputs of monocot, dicot and gymnosperm tissues. In addition, the distribution and reactivity of Hyp in different plant tissues (roots, shoots, and leaves) should be investigated. While we have demonstrated that the reactivity of Hyp in cordgrass and cypress needles is similar to that of bulk plant N, further studies are needed to fully determine the potential of Hyp as a quantitative tracer of plant-derived N in biogeochemical studies.

Table 1.1 Occurrence of Hyp in varying types of organisms (+, presence; -, absence).

Organism	Hydroxyproline	Reference
Angiosperms		
Monocots	+	e.g. Kieliszewski and Lamport 1987
Dicots	+	e.g. Stuart and Varner 1980
Gymnosperms	+	Kieliszewski et al. 1992a
Ferns	+	Lamport 1971
Bryophytes	+	Lamport 1971
Horsetails	+	Lamport 1971
Liverworts	+	Lamport 1971
Green algae	All but *Nitella*	Gotelli and Cleland 1968
Diatoms	+	Gotelli and Cleland 1968
Oomycetes	+	Crook and Johnston 1962
Fungi	-	Crook and Johnston 1962; this study
Bacteria	-	This study
Archaea	?	

Table 1.2 C and N remaining (%), C:N ratio, stable N isotopic composition, yield of major biochemical classes, and yield and mol% of Hyp during decomposition (THAA, total hydrolysable amino acids; THNS, total hydrolysable neutral sugars; nd, not determined).

Sample	%C remaining	%N remaining	C:N (molar)	$\delta^{15}N$ (‰)	THAA (%C)	THNS (%C)	THAS (%C)	Lignin (%C)	Hyp (nmol mgC^{-1})	Mol% Hyp
Mangrove Leaves										
Green	-	-	25.0	nd	7.8	15.8	nd	3.0	17.5	1.3
Senescent	100	100	60.6	6.4	2.5	18.0	0.05	2.5	17.2	3.8
42 days	72.6	81.7	54.0	nd	2.9	14.7	0.03	2.7	21.4	4.0
189 days	42.5	76.1	33.9	5.7	6.6	10.3	0.09	3.2	30.0	2.6
1.0 yr	19.8	56.5	21.3	6.1	9.6	10.7	0.34	3.5	45.3	2.6
1.8 yr	8.9	34.4	15.7	7.4	11.9	6.6	0.51	3.8	62.9	2.9
3.0 yr	3.4	15.0	13.6	8.8	12.7	7.7	0.89	4.6	71.6	3.0
4.0 yr	2.5	10.8	14.0	8.7	13.3	7.2	0.83	3.6	79.8	3.1
Smooth Cordgrass										
Green	-	-	41.6	nd	4.5	47.0	nd	4.5	7.6	1.2
Senescent	100	100	62.1	1.2	2.5	49.7	0.04	5.3	7.4	1.7
42 days	89.3	63.8	87.0	-	2.0	42.6	0.04	6.0	7.2	2.0
189 days	79.2	64.6	76.2	3.8	2.5	43.8	0.05	6.1	6.7	1.5
1.0 yr	41.9	52.7	49.1	4.0	3.9	35.2	0.23	7.0	6.8	1.0
1.8 yr	28.9	44.7	40.9	4.9	4.4	56.1	0.24	7.9	8.1	1.0
3.0 yr	13.4	31.2	28.0	5.8	6.8	44.7	0.60	10.8	10.1	0.8
4.0 yr	7.0	25.9	16.8	6.1	9.6	14.5	0.86	9.2	14.8	0.8
Cypress Needles										
Senescent	100	100	110	5.0	2.0	14.8	nd	2.2	11.8	3.4

42 days	83.2	90.4	102	nd	2.3	16.9	nd	1.9	10.8	2.8
189 days	54.4	107.2	56.1	4.7	3.7	11.7	nd	2.3	13.4	2.0
1.0 yr	38.9	105.7	40.7	4.3	5.0	7.0	nd	2.7	15.4	1.7
1.8 yr	24.4	64.1	42.1	5.0	4.3	3.6	nd	2.5	16.8	2.1
3.0 yr	15.6	47.4	36.3	6.1	3.7	3.0	nd	2.4	12.0	1.8
4.0 yr	12.4	34.5	39.8	7.6	3.5	2.9	nd	1.8	11.8	1.8

Table 1.3 AA composition (mol%) of Hyp-rich glycoproteins.

	Ala	Gly	Val	Leu	Ile	Thr	Ser	Pro	Asp	Met	Hyp	Glu	Phe	Lys	His	Tyr	Arg
Dicotyledons																	
Soybean 33kD RPRP[a]	0.0	0.0	17.3	0.0	1.1	0.4	0.0	21.5	1.2	0.0	20.0	8.9	0.0	17.3	0.0	11.5	0.0
Soybean seed coat cell wall HRGPb	1.9	4.0	2.5	1.3	0.9	1.3	8.2	9.9	2.1	2.2	36.2	2.4	0.5	10.8	8.8	8.3	1.0
Tomato extensin P1[c]	3.2	1.6	5.0	0.8	1.8	7.2	9.8	8.3	1.8	0.0	33.5	1.9	1.3	10.5	7.1	6.3	1.2
Tomato extensin A[d]	3.5	0.8	9.6	0.4	0.4	5.3	8.0	10.8	1.0	0.0	34.3	1.1	0.0	10.0	5.5	7.5	0.1
Tomato extensin B[d]	1.8	1.0	9.1	0.6	0.4	6.1	7.8	7.4	1.9	0.0	34.6	1.1	0.0	10.4	7.7	8.6	0.6
Carrot disk HRGP[e]	0.6	0.7	3.0	0.3	0.3	1.1	12.8	1.1	0.4	0.0	50.8	0.4	0.0	6.9	11.4	10.1	0.2
Carrot root HRGP[f]	0.4	0.4	5.9	0.3	0.3	1.2	14.0	0.9	0.3	0.0	45.5	0.3	0.0	6.5	11.8	11.0	0.0
Sugar beet extensin P1[g]	1.5	1.4	10.8	0.6	0.5	6.7	9.6	6.1	0.6	0.3	33.8	3.4	0.0	9.6	5.6	9.4	0.1
Potato extensin[h]	1.2	0.5	10.1	0.3	0.6	6.2	2.0	20.0	1.3	0.0	30.0	1.3	0.2	11.5	8.8	5.6	0.5
Potato bacterial agglutinin[i]	0.9	1.1	3.8	0.2	0.3	3.2	9.4	9.2	0.7	0.0	41.7	1.1	0.1	15.9	5.1	6.2	0.2
Mean Dicot	1.5	1.1	7.7	0.5	0.7	3.9	8.2	9.5	1.1	0.3	36.0	2.2	0.2	10.9	7.2	8.4	0.4
Monocotyledons																	
Maize THRGP[j]	1.7	2.4	0.7	0.2	0.1	25.3	7.3	14.5	0.7	0.0	24.8	2.3	0.1	13.5	2.4	3.9	0.1
Maize PC1[k]	5.2	7.1	2.7	1.0	0.4	17.5	5.5	13.5	2.4	0.0	21.9	2.5	0.1	11.3	3.6	4.6	0.7
Maize HHRGP[l]	13.2	5.3	1.1	1.4	0.8	2.7	11.1	4.9	1.0	0.2	34.7	3.9	3.4	1.9	12.0	3.9	2.1
Mean Monocot	6.7	4.9	1.5	0.9	0.4	15.2	8.0	11.0	1.4	0.1	27.1	2.9	1.2	8.9	6.0	4.1	1.0
Gymnosperms																	
D. Fir extensin PHRGP[m]	0.0	0.6	17.3	0.0	8.9	1.5	2.5	21.3	0.0	0.0	28.7	0.0	0.0	11.0	1.2	4.9	1.9

D. Fir extensin P2[m]	4.1	2.0	6.5	1.8	0.9	4.5	6.8	14.2	0.0	0.0	29.2	2.9	0.7	14.9	6.0	4.6	0.6
Mean Gymnosperm	2.1	1.3	11.9	0.9	4.9	3.0	4.7	17.8	0.0	0.0	29.0	1.5	0.4	13.0	3.6	4.8	1.3

[a]Datta et al. 1989; [b]Cassab et al. 1985; [c]Smith et al. 1984; [d]Brownleader and Ley 1993; [e]Stuart and Varner 1980; [f]Van Holst and Varner 1984;[g]Li et al. 1990; [h]Dey et al. 1997; [i]Leach et al. 1982; [j]Kieliszewski and Lamport 1987; [k]Hood et al. 1988;[l]Kieliszewski et al. 1992b; [m]Kieliszewski et al. 1992a

Table 1.4 Distribution of hydroxyproline arabinoside lengths in cell walls of several plant species.

	Hydroxyproline Arabinosides (% total Hyp)					Arabinose	
Species	Hyp-Ara_4	Hyp-Ara_3	Hyp-Ara_2	Hyp-Ara	Hyp	per Hyp	Reference
Gymnosperms							
Ginko biloba	33	44	6	4	13	2.8	Lamport and Miller, 1971
Cupressus sp.	26	34	8	6	26	2.3	Lamport and Miller, 1971
Ephedra sp.	27	37	4	6	26	2.3	Lamport and Miller, 1971
Pseudotsuga menziesii	20	45	6	6	10	2.3	Kieliszewski et al., 1992a
Mean gymnosperm	27	40	6	6	19	2.4	
Monocotyledons							
Zea mays	4	13	2	15	66	0.7	Lamport and Miller, 1971
Zea mays	20	41	6	9	24	2.2	Kieliszewski and Lamport, 1987
Avena sativa	6	11	3	5	71	0.7	Lamport and Miller, 1971
Iris kaempferi	10	11	3	5	73	0.8	Lamport and Miller, 1971
Allium porrum	6	13	3	5	73	0.7	Lamport and Miller, 1971
Mean monocot	9	18	3	8	61	1.0	
Dicotyledons							
Acer pseudoplatanus	75	17	3	2	3	3.6	Lamport and Miller, 1971
Gossypium hisutum	48	31	4	5	12	3.0	Qi et al., 1995
Lycopersicon esculentum	52	28	4	6	10	3.1	Lamport and Miller, 1971
Lycopersicon esculentum	49	28	9	10	5	3.0	Smith et al., 1984
Convolvulus arvensis	63	22	6	4	5	3.3	Lamport and Miller, 1971
Vicia tetrasperma	52	31	5	4	8	3.2	Lamport and Miller, 1971
Pisum sativum	33	41	7	6	13	2.8	Lamport and Miller, 1971
Mean dicot	53	28	5	5	8	3.1	

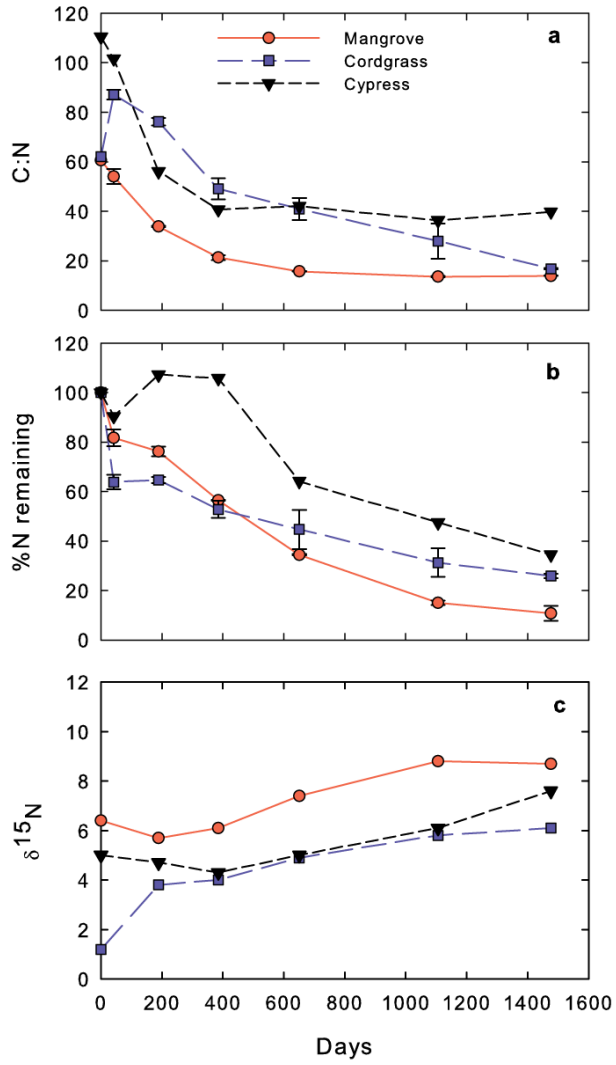

Figure 1.1 C:N ratio (a), %N remaining (b) and N isotope composition (c) during decomposition. Error bars represent deviation from replicate litter bags.

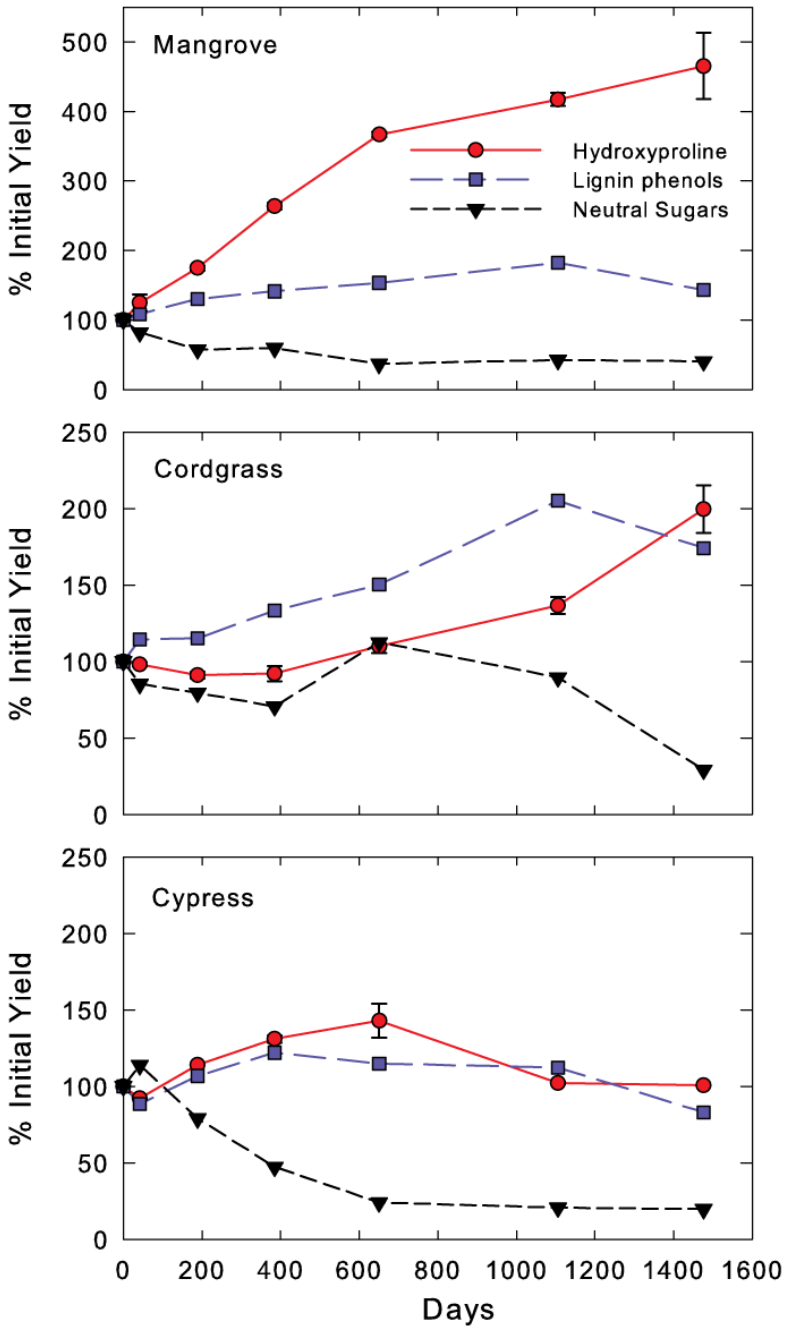

Figure 1.2 Yield of Hyp, lignin phenols and hydrolysable neutral sugars in detritus of decaying mangrove leaves, cordgrass and cypress needles, normalized to yield from their respective senescent tissues. Error bars show range of Hyp yield for duplicate litter bags.

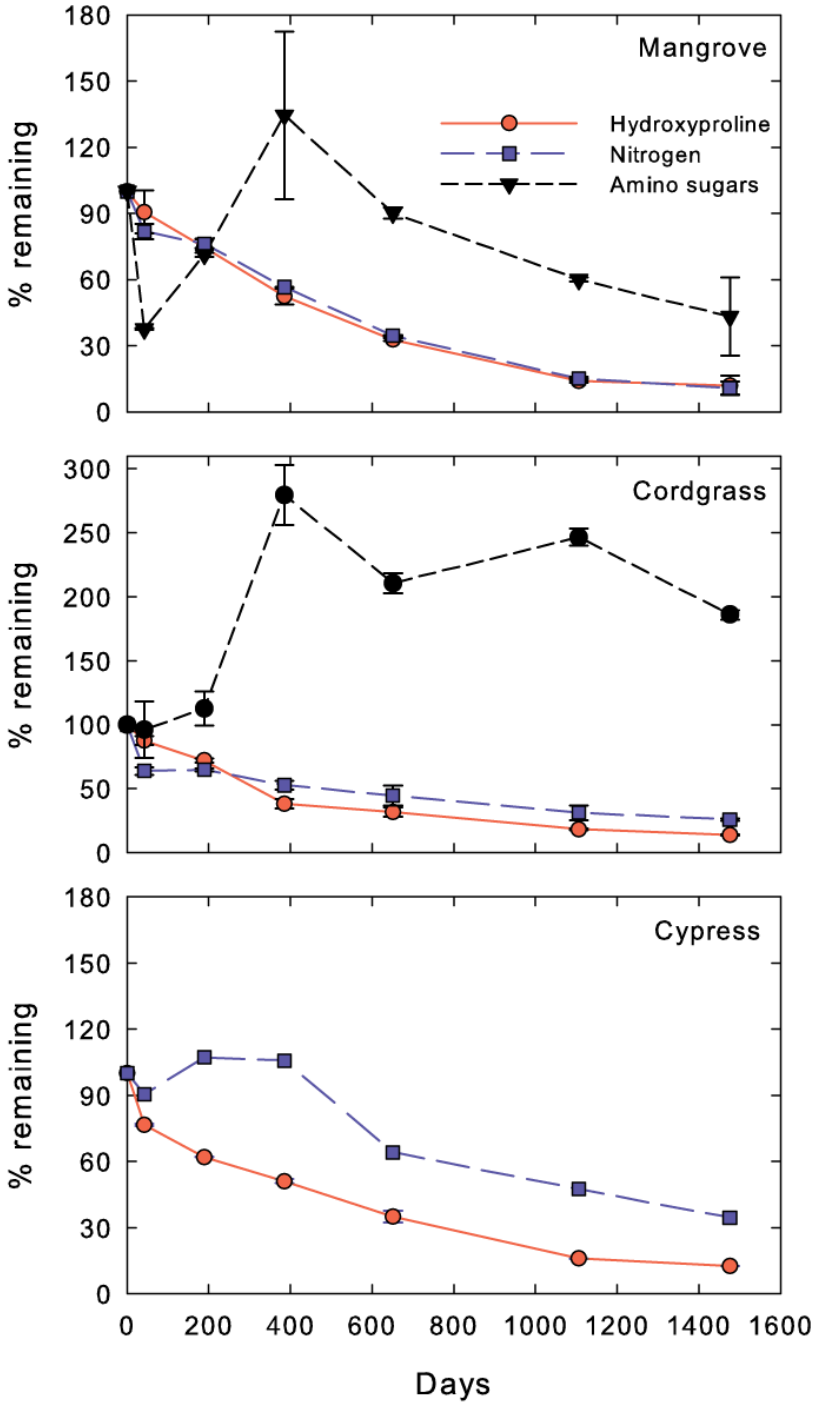

Figure 1.3 Proportion (%) of initial Hyp, N and amino sugars remaining during decomposition. Error bars represent deviation from replicate litter bags.

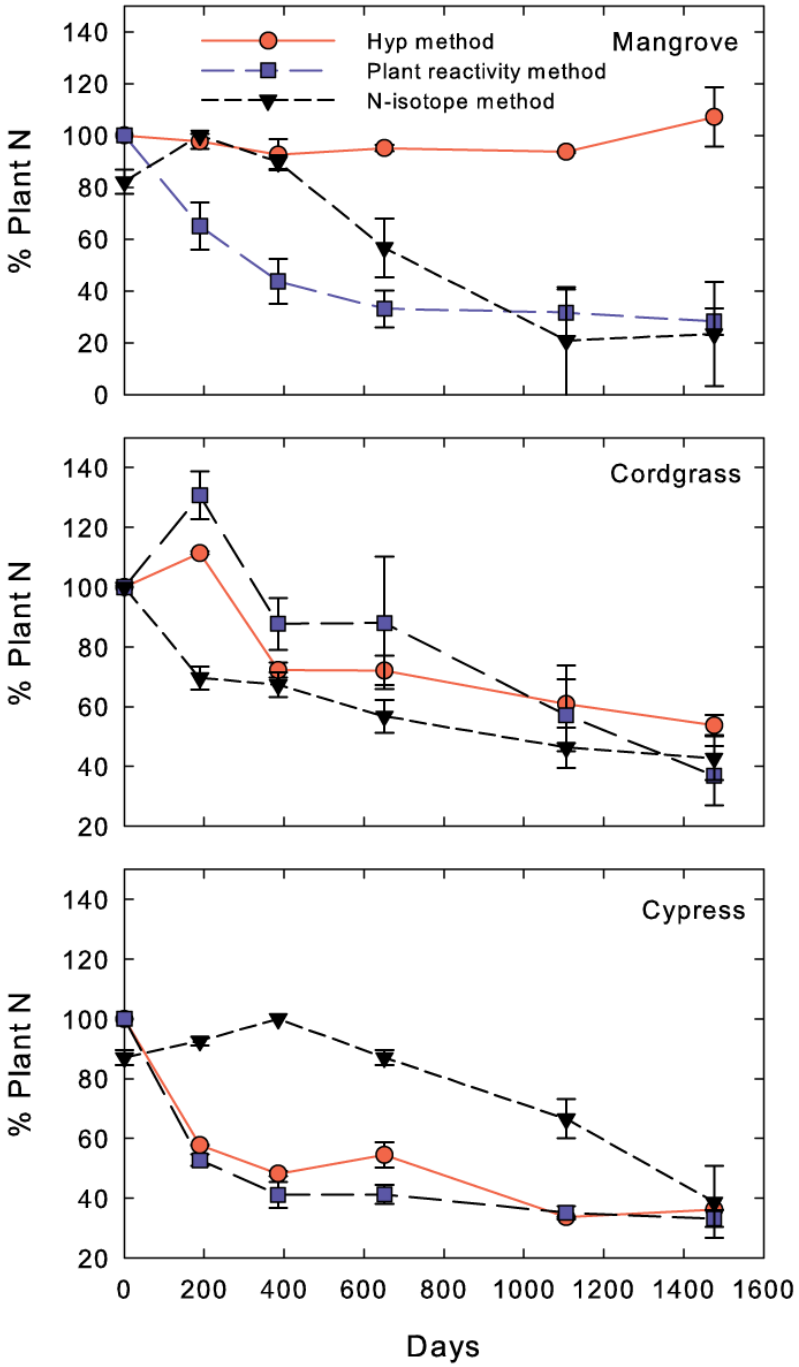

Figure 1.4 N derived from senescent plant tissue (% Plant N) during decomposition, calculated using the N-normalized Hyp yield [Eq. (5)), the ‘‘Plant reactivity’’ method (Eqs. 1.2 and 1.3) and N isotopes (Eq. 1.4). Error bars represent deviation from replicate litter bags for the Hyp method, or range derived from different assumptions for the plant reactivity and N isotope methods (Section 1.2.4).

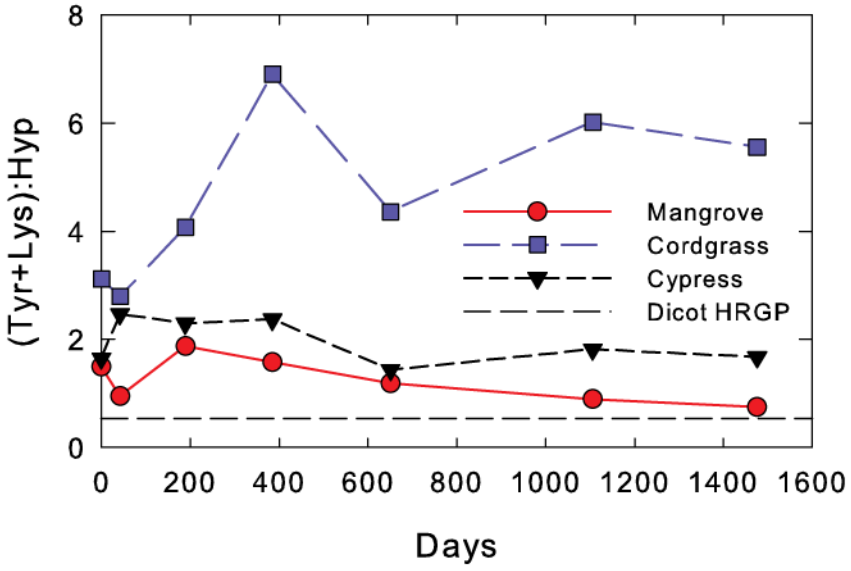

Figure 1.5 Ratio of mol% (lysine + tyrosine) to mol% Hyp in detrital samples during decomposition. The dashed line at y = 0.54 shows average ratio in dicot Hyp-rich glycoproteins (Table 1.3).

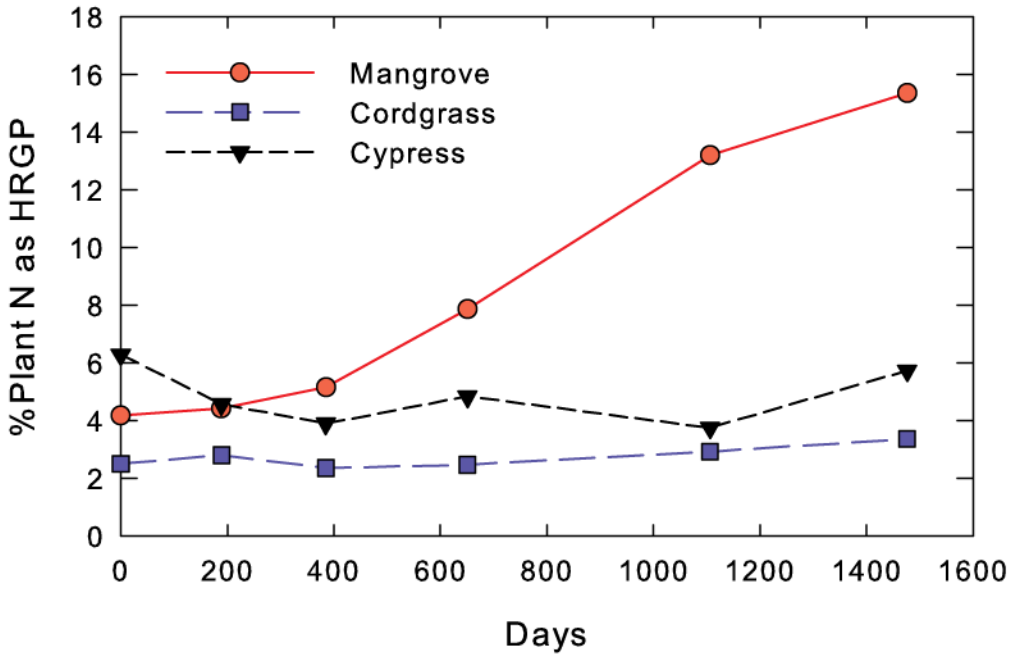

Figure 1.6 Plant N (%) as HRGPs in mangrove leaves, cordgrass and cypress needles during decomposition. Plant N was calculated as the product of wt.% N and% plant N and HRGP N was calculated using the Hyp yield for each detrital sample (Table 1.1) and the mean AA composition of HRGPs from each taxonomic grouping (Table 1.3), assuming that all Hyp was derived from HRGPs.

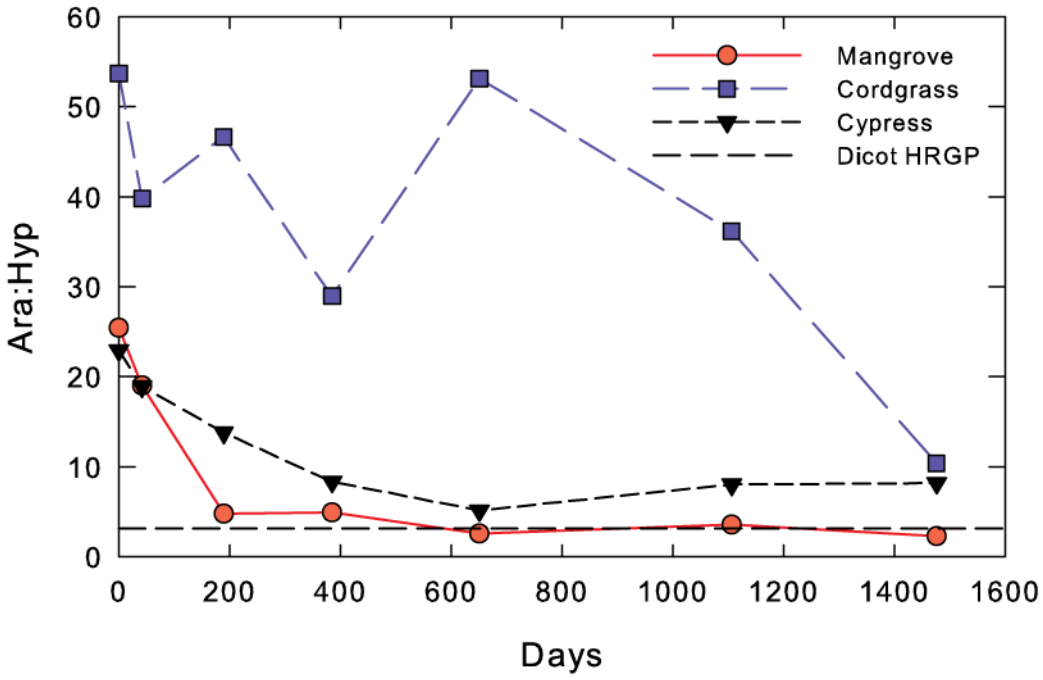

Figure 1.7 Arabinose: Hyp ratio in decaying mangrove leaves, cordgrass and cypress needles. Dashed line at Ara:Hyp = 3.1 represents mean ratio in dicot HRGP (Table 1.4).

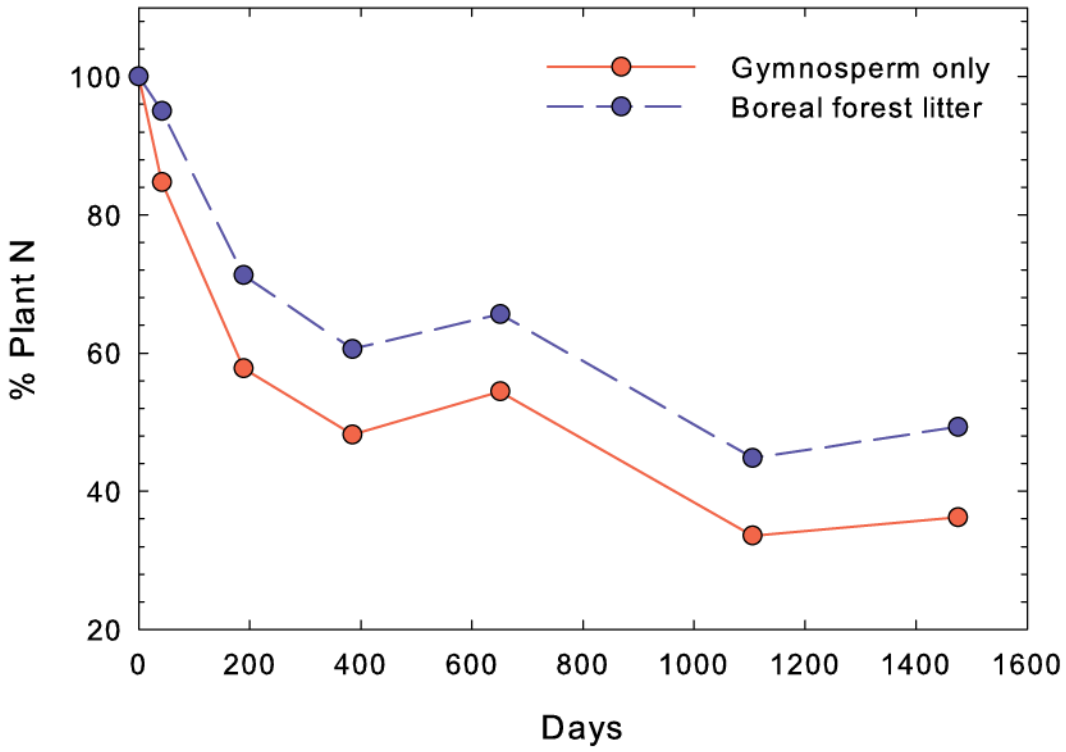

Figure 1.8 Plant-derived N (%) calculated using the Hyp method in cypress needles (solid red line) and in a model mixture of gymnosperms, dicots and monocots representative of a black spruce stand in a boreal forest (70% gymnosperm, 27% dicot and 3% monocot; dashed blue line). The % plant N in the model mixture was calculated assuming that the reactivity of Hyp and N in cypress needles, mangrove leaves and cordgrass was representative of their behavior in gymnosperms, dicots and monocots, respectively (Section 1.4.2).

CHAPTER 2

BIOCHEMICAL EVIDENCE FOR MINIMAL VEGETATION CHANGE IN PEATLANDS OF THE WEST SIBERIAN LOWLAND DURING THE MEDIEVAL CLIMATE ANOMALY AND LITTLE ICE AGE[2]

2.1. Introduction

The climate of the last millennium was dominated by two periods of sustained temperature anomalies: the relatively warm Medieval Climate Anomaly (MCA; defined here as 950-1250 C.E. after Mann et al. [2009]) was followed by the Little Ice Age (LIA; 1400-1700 C.E.). These events were globally widespread, but it is now apparent that the MCA and LIA varied greatly in both timing and magnitude among regions [*Osborn and Briffa*, 2006; *Mann et al.*, 2009; *Guiot et al.*, 2010]. There was cooling associated with LIA on every continent, but the pattern of climate change within continents was variable and some regions did not experience change at all [*PAGES 2k Consortium*, 2013]. Identifying patterns of past climate change and the processes that drive them is important for predicting the spatial distribution of future climate change.

It is difficult to evaluate the spatial heterogeneity of the MCA and LIA because quantitative, high-resolution paleotemperature proxies are limited both in number and spatial coverage. Proxy networks calibrated using the modern instrumental temperature

[2] Philben, M., K. Kaiser, and R. Benner (2014a), Biochemical evidence for minimal vegetation change in peatlands of the West Siberian Lowland during the medieval climate anomaly and little ice age, *Journal of Geophysical Research: Biogeosciences*.

records can be used to interpolate between individual proxy records (e.g. [*Mann et al.*, 1998]), but direct evidence of climate change is lacking in many regions, particularly the subarctic. Peatlands have the potential to fill some of these gaps and verify the spatial patterns of climate change predicted by instrumental calibrations of other proxies. Peatlands are useful climate archives because they are isolated from the local groundwater, so the water table level depends on the balance between precipitation and evaporation. The surface vegetation is in turn controlled by water table depth, as *Sphagnum* mosses generally prefer wetter conditions while vascular plants prefer drier conditions [*Valiranta et al.*, 2007]. This makes vegetation a useful, if qualitative, paleoclimate proxy. Peat climate archives covering the last millennium are generally consistent with other proxies, and LIA cooling was coincident with wet-shifts in peatland vegetation across Europe and the UK [*Barber et al.*, 2000; *Mauquoy et al.*, 2002].

The West Siberian Lowland (WSL) contains the world's largest peatland complex and is located in a region with few other climate proxy records [*Gorham*, 1991]. Tree-ring records from the Yamal peninsula, the northern boundary of the WSL, indicate a warm MCA and cool LIA [*Briffa*, 2000; *Osborn and Briffa*, 2006]. There are no quantitative proxy records from the subarctic southern WSL, but climate models and proxy interpolations indicate that these events were less severe in the south than in the arctic [*Mann et al.*, 2009]. The peat vegetation record provides an opportunity to independently test this prediction. To date several studies have examined WSL vegetation development over the Holocene [*Peteet et al.*, 1998; *Pitkanen et al.*, 2002; *Kremenetski et al.*, 2003], but none have focused on the last millennium with sufficient resolution to identify effects of MCA or LIA climate change. In this study we analyze vegetation

change in the WSL over the last 2000 years to evaluate the magnitude of MCA and LIA climate change in this important region.

Macrofossil analysis is the most commonly employed technique for evaluating peatland paleovegetation. Unlike pollen analysis, which reveals regional vegetation trends, macrofossils show the volumetric contribution of each plant species to the peat matrix in a particular core. Macrofossils are relatively simple to interpret and can characterize the vegetation community at species or genera level. However this approach is limited in peats where decomposition and humification have destroyed the physical structure of the plant remains. In highly decomposed peats, as little as 30% of the matrix can be identified as plant remains [*Comont et al*., 2006; *Swindles et al*., 2007; *Delarue et al*., 2011]. The abundance of unidentified organic material and the likelihood of selective preservation of some plant remains complicate the quantitative application of this technique. In addition, macrofossil analyses result in a volumetric rather than mass-based vegetation reconstruction. There are likely significant differences between the two because *Sphagnum* mosses are typically less dense than vascular plant tissues. This can be problematic for quantitative applications such as modeling peat accumulation, which typically operate in units of mass or carbon [e.g. *Frolking et al*., 2010].

Paleovegetation reconstructions based on biochemical tracers characterize all peat C, regardless of diagenetic alteration and preservation of the physical structure. Several types of biomarkers, including alkanes [*Baas et al*., 2000; *Pancost et al*., 2002, 2003], alkanones [*Nichols and Huang*, 2007], sphagnum acid [*McClymont, et al*., 2011], and sterols [*Ronkainen et al*., 2013] have been explored for the potential to reconstruct paleovegetation in peats with poorly preserved macrofossils. Of these, *n*-alkanes are the

most widely applied, as Nichols and Huang [2006] developed a mixing model to quantitatively estimate the contributions of *Sphagnum* and vascular plants to the peat based on the C23:C29 alkane ratio. Alkanes are very resistant to decomposition, and this ratio is assumed to remain constant with diagenesis. This approach for reconstructing the vegetation community at the time of peat formation has been shown to correlate with other proxies for paleoclimate and surface wetness [*Zhou et al*., 2005; *Nichols et al.*, 2006; *Zhou et al*., 2010]. However, due to their recalcitrance, alkane-based reconstructions do not account for differences in reactivity among plant types. Selective decomposition of plant tissues can generate substantial differences between the original plant community and that preserved in peats. The Holocene Peat Model predicted that vascular plants account for 65% of net primary production but only 35% of contemporary peat mass in a simulated bog [*Frolking et al*., 2010]. This makes alkane-based reconstructions useful for paleoenvironmental reconstruction but demonstrates the limitations of the approach for characterizing sources of C in contemporary peat.

We have developed a quantitative approach to estimate *Sphagnum* and vascular plant contributions to the peat C using hydrolysable neutral sugars and lignin phenols. Neutral sugars are useful because different plant types synthesize different suites of hemicelluloses, so their biomass is composed of different sugars [*Carpita*, 1996]. Lignin is synthesized only by vascular plants, so its yield in peat is proportional to the contribution of vascular plants. Both neutral sugars and lignin phenols have been used as indicators of peat paleovegetation and these biochemical reconstructions appear to agree with macrofossil-based reconstructions, but these studies were qualitative in nature [*Bourdon et al.*, 2000; *Williams and Yavitt*, 2003; *Tareq et al.*, 2004; *Comont et al*., 2006;

Delarue et al., 2011]. We have developed a set of mixing models using modern peat-forming vegetation as end members to quantitatively estimate the contributions of *Sphagnum* and vascular plants to peat.

We hypothesized the plant community would respond to climate change over the last 2000 years, particularly the Medieval Climate Anomaly and the Little Ice Age. Specifically, we predicted warm and dry conditions during the Medieval Climate Anomaly to favor vascular plants and cool and wet conditions during the Little Ice Age to favor *Sphagnum*. In the northern cores we expected colder climate to be associated with dry-adapted plant assemblages due to soil-heaving associated with permafrost development. Our results supported the latter hypothesis, as lichens were present in the northern cores following the Medieval Climate Anomaly in the northern cores. However, the plant community in the southern cores did not have a consistent response to either climate anomaly. This indicates climate change during the Medieval Climate Anomaly and Little Ice Age was not sufficient to drive vegetation change at these sites in southern West Siberian Lowland.

2.2. Materials and Methods

2.2.1 Study sites and sampling

This study uses a subset of a large network of peat cores collected from the West Siberian Lowland between 1999 and 2001 [*Smith et al*., 2004, 2012; *Beilman et al*., 2009]. The four cores selected for analysis spanned a latitudinal gradient (56-66 °N) from non-permafrost peatlands in the boreal forest regions in the south to open tundra permafrost peatlands in the north (Fig. 2.1). Cores were extracted with a 5-cm rotating sleeve side-cut Russian corer (non-permafrost sites) or a modified Cold Regions

Research and Engineering Lab (CRREL) corer (permafrost sites). Subsamples (1 cm-thick) were collected every 2-6 cm (southern cores) or every 1-2 cm (northern cores). The cores SIB04 (56.8°N 78.7°E) and SIB06 (58.4°N 83.4 °E) were collected from non-permafrost bogs with high apparent accumulation rates (44 and 28 g C m^2 a^{-1}, respectively) over the last 2000 years [*Beilman et al.*, 2009]. The cores G-137 (63.7°N 75.8°E) and E-113 (66.4°N 79.3°E) were collected from permafrost peat plateau sites with present thaw depths of 50 and 17 cm, respectively [*Smith et al.*, 2012]. Apparent carbon accumulation rates of these two sites ranged from 10-15 g C m^2 a^{-1} over the last 2000 years. *Sphagnum fuscum* dominates the surface vegetation at all 4 sites, with *Pinus sylvestris* (SIB04) and *Eriophorum* sp. (SIB06) also prominent at the southern sites and lichens common at the northern sites [*Smith et al.*, 2012]. Age models were developed based on linear interpolation between three or four radiocarbon dates targeting the last 2000 years in each core (Table 1; [*Beilman et al.*, 2009]). Additional details about the cores and coring sites can be found in Beilman et al. [2009] and Smith et al. [2004; 2012].

Samples of fresh peatland and boreal forest vegetation were also analyzed to identify the chemical signature of peat-forming plants. Unfortunately, no fresh vegetation was available from the coring sites. Instead, representative vegetation was collected from similar environments, including bogs in James Bay Lowland, QC, Canada; tundra near Toolik Lake, Alaska, USA; and a boreal forest in Codroy Valley, NL, Canada. The lignin phenol composition of these plants was supplemented with previously published results for peat-forming vegetation [*Williams et al.*, 1998].

2.2.2. Chemical analyses

Frozen slices of peat (1 cm) were thawed and dried in a Savant SpeedVac vacuum centrifuge at 40 °C. Dry peat material was ground in a Wiley mill to pass a 40-mesh filter. Carbon content was measured after combustion at 980 °C using a Costech ECS 4010 elemental analyzer. The analytical precision for duplicate analyses was ±0.7 %.

Neutral sugars were analyzed according to Skoog and Benner [1997] with modifications. About 5 mg of dry peat was weighed into 2 mL muffled glass ampules and immersed in 12 mol L^{-1} sulfuric acid for 2 hours at room temperature. After addition of 1.8 mL of ultrapure water, the ampules were flame-sealed and heated to 100 °C in a water bath for 3 hours. The hydrolysis was terminated in an ice bath. Ampules were cracked open, and deoxyribose was added as an internal standard. About 400 µL of sample hydrolysate were immediately neutralized with 2 mL self-absorbed ion retardation resin (Biorad AG11 A8, [*Kaiser and Benner*, 2000]). Residual particles in the hydrolysate were trapped at the surface of the neutralization resin.

Before chromatography, ~2 mL of sample was deionized with a mixture of cation and anion exchange resins (Biorad AG50 and AG2). Neutral sugars were separated isocratically with 25 mmol L^{-1} NaOH on a PA1 column in a Dionex 500 system with a pulsed amperiometric detector (PAD). Detector settings were analogous to Skoog and Benner [1997]. Method blanks were run after every 12th sample. Seven sugars were measured: fucose (Fuc), rhamnose (Rha), arabinose (Ara), galactose (Gal), glucose (Glc), mannose (Man), and xylose (Xyl). The analytical precision of duplicate analyses performed on different days was ±2% for glucose and ± 4% for all other sugars.

Concentrations of phenols were determined by GC-MS following CuO oxidation [*Kaiser and Benner*, 2012]. Dry peat samples (10-15 mg) were reacted with 330 mg CuO, 106 mg of $Fe(NH_4)_2(SO4)_2 \cdot 6H_2O$ and 2.5 mL of 2 mol L^{-1} NaOH in Monel reaction vessels. Vessels were kept in argon-filled containers to exclude molecular oxygen. After oxidation, vessels were uncapped and a mixture of trans-cinnamic acid and ethyl-vanillin was added as internal standards. Samples were purified by solid phase extraction (SPE) using Oasis HLB cartridges and a vacuum manifold. After SPE, samples were gently dried under a stream of argon and redissolved in 200 µL of dry pyridine. Samples were stored at -20 ºC until analysis.

Gas chromatography was carried out using an Agilent 7890 system connected to an Agilent 5975C triple axis mass detector with electron impact ionization. Samples were derivatized with BSTFA/TMCS before analysis. Typically, 15 µL of sample were reacted with 15 µL of BSTFA/TMCS reagent at 75 °C for 15 min. Mass spectrometer settings are described in detail by Kaiser and Benner [2012]. Analyzed phenols included *p*-hydroxy (P) phenols (*p*-hydroxybenzaldehyde (PAL), *p*-hydroxyacetophenone (PON), *p*-hydroxybenzoic acid (PAD)); vanillyl (V) phenols (vanillin (VAL), acetovanillone (VON), vanillic acid (VAD)); syringyl (S) phenols (syringaldehyde (SAL), acetosyringone (SON), syringic acid (SAD)); cinnamyl (C) phenols (cinnamic acid (CAD) and ferulic acid (FAD)) and 3,5-dihydroxy-benzoic acid. The analytical precision of duplicate analysis was ±4 %.

2.2.3 Vegetation reconstruction

The paleovegetation at each of the four sites was reconstructed using two independent methods: (1) neutral sugar compositions of peat forming plants and lichens;

and (2) lignin phenols as indicators of vascular plant remains (Table 2.2). The carbohydrate approach uses previously identified differences in the ratios of neutral sugars between *Sphagnum* mosses, vascular plants, and lichens [*Comont et al.*, 2006; *Jia et al.*, 2008; *Delarue et al.*, 2011]. *Sphagnum* was identified by the carbohydrate *Sphagnum* index (SI_{Carb}), defined as the molar ratio of the sugars:

$$\text{Carbohydrate } \textit{Sphagnum} \text{ index} = \frac{\text{Rhamnose}}{\text{Mannose} + \text{Xylose}} \tag{2.1}$$

To quantitatively estimate the fraction of peat derived from *Sphagnum* litter, we calculated the mean C-normalized neutral sugar yields for *Sphagnum* and peat-forming vascular plants (Table 2.3) and used these as end members in a nonlinear mixing model. The yield of each neutral sugar and resulting carbohydrate *Sphagnum* index in a theoretical mixture of *Sphagnum* and vascular plants was calculated and fit to a 3rd degree polynomial using MATLAB. This regression results in an equation for calculating the contribution of *Sphagnum* to the peat C using the carbohydrate *Sphagnum* index as an independent variable (Fig. 2.2).

Lichens were identified by their abundance of Man and Gal [*Jia et al.*, 2008]. We used the molar ratio:

Carbohydrate lichen index =(Mannose+Galactose)/(Rhamnose+Arabinose+Xylose) (2.2)

to differentiate lichen from *Sphagnum* and vascular plant contributions. Lichen neutral sugar concentrations reported by Jia et al. [2008] were converted to C-normalized yields assuming 44 %C, the mean C content of the other analyzed vegetation. As for the *Sphagnum* index, a theoretical mixing curve between lichens and a 50/50 mixture of *Sphagnum* and vascular plants was calculated using the neutral sugar yields in fresh plant and lichen tissues as end-members and was fit to a 3rd order polynomial to generate an

equation for lichen input to the peat (Table 2.2). After the *Sphagnum* and lichen contributions were calculated independently using their respective carbohydrate indices, the vascular plant contribution was calculated by difference.

An independent proxy for paleovegetation, lignin phenols (nmol V+S phenols mg C^{-1}; VPI_{Phenol}) was used to estimate vascular plant contributions to the peat C according to the equation:

$$fVascular = (VPI_{Phenol})_{Peat}/(VPI_{Phenol})_{Plant} \quad (2.3)$$

where $(VPI_{Phenol})_{Plant}$ is the mean phenol vascular plant index in modern peat-forming vascular plants (Table 2.4). Unlike the carbohydrate method, the phenol method directly estimates the vascular plant rather than *Sphagnum* contribution. *Sphagnum* and lichens cannot be differentiated and the total *Sphagnum* + lichen contribution was calculated by difference.

In addition to the quantitative reconstruction of *Sphagnum* vs. vascular plant contributions to the peat, we applied several qualitative indicators to provide insights about the composition of the vascular plant community. The ratio of syringyl to vanillyl phenols (S:V) is an indicator of the relative proportions of angiosperms (enclosed seeds) and gymnosperms (naked seeds), as angiosperms produce both S and V phenols while gymnosperms produce only V phenols. The Cyperaceae Index (CI_{Carb}), the molar ratio of the neutral sugars (Arabinose+Xylose)/(Rhamnose+Mannose+Galactose), is indicative of sedges (monocotyledons in family Cyperaceae, e.g. *Carex* and *Eriophorum*; *Jia* et al., 2008). This is likely due to the abundance of arabinoxylan hemicelluloses in the cell walls of monocotyledons [*Carpita*, 1996; *Buranov and Mazza*, 2008]. Cell wall

arabinoxylans are ester-bonded to ferulic acid (CI_{Phenol}, [*Carpita*, 1996; *Buranov and Mazza*, 2008]) making this phenol another useful indicator of monocot remains.

The *p*-hydroxyacetophenone (PON) yield of the peat was also evaluated as an indicator of *Sphagnum* remains because *Sphagnum* is highly enriched in PON relative to vascular plants (Table 2.4). Vascular plants also contain small amounts of PON, so a third mixing model was tested to simulate the PON yield in a mixture of *Sphagnum* and vascular plant litter. We found that this method agreed with the other two methods in the southern cores (SIB04 and SIB06) but not in the more highly decomposed northern cores (G-137 and E-113; Fig. A1-A3). We concluded that the presence of PON reservoirs of different reactivities in both *Sphagnum* and vascular plant tissues made the PON method more sensitive to diagenetic alteration and, therefore, was a less reliable indicator of paleovegetation than the other two indices (see section 2.4.1.2). It was not used in the quantitative reconstruction of paleovegetation.

2.3. Results

2.3.1. Neutral sugar and phenol yields in peat-forming vegetation

Neutral sugars constituted a large fraction of all plants analyzed, accounting for 22-40% of the total C (Table 2.3). Glucose was the most abundant neutral sugar in all of the plants analyzed, ranging from 45-65 mol% of the total neutral sugars. The *Sphagnum* mosses analyzed are characterized by a high rhamnose yield (5.7-6.8 mol%) compared to vascular plants (0.4-2.3 mol%). Galactose and mannose were also, on average, more abundant in *Sphagnum* than in vascular plants (Table 2.3), but their yields in vascular plants were variable and in some cases higher than in *Sphagnum*. Most vascular plants had a higher xylose yield than *Sphagnum*, with the exception of *Abies balsamea* needles

(Table 2.3). As all *Sphagnum* species analyzed were rich in rhamnose and vascular plants were rhamnose-poor but comparatively rich in mannose, xylose or both, the carbohydrate *Sphagnum* index was used to differentiate *Sphagnum* from vascular plant sources. The carbohydrate *Sphagnum* index ranged from 0.35-0.50 in *Sphagnum*, but was <0.12 in all vascular plants analyzed. Jia et al. [2008] analyzed neutral sugars in 7 lichen species and found mannose and galactose (67±10 mol % s.d.) were the dominant sugars. The carbohydrate lichen index in these lichens was 20 ±10 but was <1.15 in *Sphagnum* and <0.95 in vascular plants.

The eleven *p*-hydroxy (P), vanillyl (V), syringyl (S) and cinnamyl (C) phenols accounted for 3.9 ± 1.6 % s.d. of the carbon in vascular plants and 2.1 ± 0.3 % C in *Sphagnum*. The phenol content of *Sphagnum* was dominated by *p*-hydroxy phenols, especially *p*-hydroxyacetophenone, which had a yield of 109 ± 14 nmol mg C^{-1} (Table 2.4). Small amounts of vanillyl and syringyl phenols were also detected in *Sphagnum*, likely due to minor contamination with vascular plant fragments in field samples of *Sphagnum*. Vascular plants had substantial yields of vanillyl phenols, and all but *Picea* and *Abies balsamea* contained significant amounts of syringyl phenols (Table 2.4). The sum of vanillyl and syringyl phenols (VPI_{Phenol}) in vascular plants was 220 ± 128 nmol mg C^{-1}.

2.3.2 Vegetation indices in peat cores

The carbohydrate *Sphagnum* index (SI_{Carb}) ranged from a minimum of 0.05 to a maximum of 0.48 in the peat cores (Fig. 2.3). SI_{Carb} was generally higher in SIB04 than in SIB06. While neither core showed a strong depth trend, SI_{Carb} varied dramatically between adjacent samples representing timescales of <50 years, indicating rapid

vegetation change at these sites. These changes appeared to be cyclical, as SI_{Carb} declined repeatedly in SIB04 and SIB06, with an average periodicity of 240 and 420 years, respectively. SI_{Carb} declined at the onset of the Little Ice Age at SIB06 but there was no apparent correlation between either climate event and SI_{Carb} at SIB04. At G-137, SI_{Carb} was very low between 1-12 cm (50-450 cal. BP) but increased to near the range of SI_{Carb} values in fresh *Sphagnum* then gradually declined with depth. Like the southern cores, E-113 did not display any apparent depth trend and indicated relatively rapid shifts in the dominant vegetation (Fig. 2.3).

The depth profile for the phenol vascular plant index (VPI_{Phenol}) in the southern cores largely appeared to be a mirror image of the profile for SI_{Carb} (Fig. 2.3). In both SIB04 and SIB06, many negative peaks in SI_{Carb} were coincident with positive peaks in VPI_{Phenol} and vice versa. The similarity between the profiles of SI_{Carb} and VPI_{Phenol} was less apparent in the northern cores due to the absence of abrupt changes in the indices. Both indices were generally intermediate compared with values in the southern cores. At G-137, VPI_{Phenol} was low in peat deposited in the last 550 years despite low SI_{Carb}, likely due to the presence of lichens.

The carbohydrate lichen index (LI_{Carb}) was <1.2 and within the range of fresh *Sphagnum* and vascular plants throughout SIB04 and SIB06 (Fig. 2.3). In the northern cores, however, LI_{Carb} indicated significant post-LIA lichen contributions. At G-137, LI_{Carb} in the peat was in the range of LI_{Carb} in fresh lichens between 1-12 cm (50-450 cal. BP), indicating a substantial lichen input to the peat. Smaller peaks in LI_{Carb} were visible at the surface and at 31 cm (~2130 cal. BP) in G-137 and at 23 cm (~750 cal. BP) in E-

113 (Fig. 2.3). These peaks coincided with low values for SI_{Carb} and VPI_{Phenol}. LI_{Carb} indicated that there was no significant lichen contribution to the peat at other depths.

2.3.3 Vegetation reconstruction

The carbohydrate *Sphagnum* index, the phenol vascular plant index, and the carbohydrate lichen index were used to quantitatively estimate the contribution of *Sphagnum*, vascular plants, and lichens to the peat using the equations presented in Table 2.2. This resulted in two independent estimates of the paleovegetation: (1) the carbohydrate *Sphagnum* and lichen indices were used to calculate the *Sphagnum* and lichen contribution, respectively, and vascular plants were calculated by difference (Fig. 2.4a); and (2) the phenol vascular plant index was used to estimate the vascular plant abundance while *Sphagnum* plus lichens (which could not be resolved using phenols) were calculated by difference (Fig. 2.4b). The two approaches revealed largely the same trends in vegetation, but differed somewhat on the magnitude of vegetation change in the peatlands (Fig. 2.4). For example, at SIB04 both methods agreed that the core was generally dominated by *Sphagnum* but quickly and transiently shifted to vascular plant dominance every 50-300 years. However, the carbohydrate *Sphagnum* index indicated that during vascular plant invasions, vascular plants accounted for about 20% of the peat C, and during periods of *Sphagnum* dominance they are absent entirely, while the phenol vascular plant index indicated that vascular plants typically contributed about 20% to the peat C, increasing to >40% of the C during peaks in vascular plant abundance.

This pattern was also apparent in the other three cores, as the two methods displayed the same patterns of vegetation change but the phenol vascular plant index generally indicated a higher vascular plant input (Fig. 2.4). In G-137, carbohydrate

indices indicated that lichens accounted for 80-100% of the peat in the last 500 years, and 25% at 31 cm (2130 cal. BP). Both neutral sugars and phenols indicated that vascular plants made up <50% of the peat throughout the core. Vascular plant remains also accounted for less than half of the peat C in E-113 according to both tracers. The carbohydrate lichen index indicated that the surface peat (0-25 cal. BP) was 20-30% lichens and peat at 23 cm (750 cal. BP) was 55% lichens.

2.3.4 Error analysis

The two vegetation indices generally agreed concerning the contributions of *Sphagnum* and vascular plants in the peat. Of the 143 total depths analyzed for both carbohydrates and phenols, the two estimates of % *Sphagnum* were within 20% of one another in 95 (66%) of the samples (Fig. 2.5). This number did not include samples in which the carbohydrate lichen index suggested a lichen contribution, as these samples had low carbohydrate *Sphagnum* index but also lacked vanillyl and syringyl phenols. The agreement was strongest in E-113, where 73% of the 26 samples agreed within 20% and weakest in G-137, where 55% of the samples agreed.

The carbohydrate indices tended to indicate a higher % *Sphagnum* and lower % vascular plants than the phenol vascular plant index (Fig. 2.6). Overall, the % *Sphagnum* was higher using the carbohydrate Sphagnum index in 75% of the samples and in 92% (44 of 48) of the samples where the difference between the methods was greater than 20%. This was especially evident in SIB04, where the carbohydrate-based estimate of % *Sphagnum* was larger in 92% of the samples (Fig. 2.6).

2.3.5 Composition of vascular plant community

At SIB04, peaks in vascular plant input to the peat at 162, 224, and 230 cm (1210, 1680, and 1730 cal. BP) were associated with elevated ratios of syringyl to vanillyl phenols (S:V; Fig. 2.7a), suggesting that during these intervals, the vascular plant community was primarily angiosperms. However, the S:V ratio remained low during vascular plant invasions at 80 and 136 cm (580 and 1010 cal. BP), indicating gymnosperm dominance. The carbohydrate Cyperceae index (CI_{Carb}) was low (<1) throughout the core and phenol Cyperceae index (CI_{Phenol}) was low other than at the surface and at 82 cm (600 cal. BP). This indicates that among angiosperms, dicotyledons (e.g. Ericaceae) were more prevalent than sedges. Several depths in SIB06 with significant vascular plant input, including 36, 84, 158, and 178 cm (40, 510, 1510, and 1780 cal. BP), had higher values for both Cyperceae indices, indicating a larger contribution of sedges at SIB06 than at SIB04 throughout the last 2000 years (Fig. 2.7).

In the northern cores, S:V was <0.5 throughout both cores except at the surface of G-137 and at 21 cm (660 cal. BP) in E-113. CI_{Carb} was also low (<1) throughout both cores but generally increased with depth in E-113. CI_{Phenol} was <10 throughout G-137 but increased to 27 at 43 cm (1650 cal. BP) in E-113. These indicators indicate that gymnosperms or dicotyledons might have been the dominant vascular plants at the northern cores other than at the bottom of E-113, where there appeared to be some sedge input. However, the interpretation of these indicators is complicated by variability in the source vegetation and sensitivity to diagenetic alteration (see section 2.4.1.2).

2.4. Discussion

2.4.1 Evaluation of methods

2.4.1.1 Development of vegetation indices

Both neutral sugars and plant phenols have been used previously to qualitatively evaluate changes in peatland paleovegetation. Comont et al. [2006] identified rhamnose, galactose, and mannose as indicators for moss remains, while Jia et al. [2008] proposed the indices mol % (Fucose+Rhamnose) and [(Mannose+Galactose):(Xylose+Arabinose)] as indicators of *Sphagnum* and lichen remains, respectively. The molar ratio [(Arabinose+Xylose):(Rhamnose+Galactose+Mannose)] is indicative of Cyperaceae remains [*Delarue et al.,* 2011]. Each of these indicators has been shown to qualitatively correlate with the remains of their respective plant tissues in peat cores, but have not been applied quantitatively [*Bourdon et al.,* 2000; *Comont et al.*, 2006; *Jia et al.*, 2008].

We developed modified versions of these indices using the neutral sugar compositions of peat-forming plants from a variety of boreal forest and peatland ecosystems. Unlike the Jia et al. [2008] index, the index we introduce (the carbohydrate *Sphagnum* index) does not include fucose. While mol % fucose is higher on average in *Sphagnum* than in vascular plants, the difference between *Sphagnum* and vascular plants is small and the yield in vascular plants is highly variable. In addition, fungi collected from a Canadian boreal forest were found to be rich in fucose (12 ±7 mol %; data not shown). Although fungal activity is generally lower than bacterial activity in peatlands, fungi can be important decomposers, especially under dryer conditions [*Jaatinen et al.,* 2008]. This could confound the interpretation of fucose data. In contrast, mol % rhamnose was on average 4.5 times higher in *Sphagnum* than in vascular plants, likely

due to the abundance of rhamnogalacturonans in *Sphagnum* cell walls [*Ballance et al.*, 2007]. Mannose and xylose were included in the denominator of the carbohydrate *Sphagnum* index because they are the most abundant sugars in lichen and vascular plant tissues, respectively. This allows the carbohydrate *Sphagnum* index to effectively distinguish *Sphagnum* from both lichens and vascular plants. While galactose was also abundant in both lichens and vascular plants, it was not included in the carbohydrate *Sphagnum* index because its yield was variable among vascular plants as the average mol % Gal was 2.3 times higher in dicots than in monocots. Similarly, we modified the lichen index proposed by Jia et al. [2008] ((Mannose+Galactose):(Xylose+Arabinose)) by adding rhamnose to the denominator of the carbohydrate lichen index to more effectively separate lichens from *Sphagnum*. The sugars used in the carbohydrate Cyperceae index were the same as those proposed by Delarue et al. [2011], but this index was not applied quantitatively because it is very sensitive to diagenesis (see section 2.4.1.2).

The vanillyl (V) and syringyl (S) phenols are exclusively indicative of lignin, which is synthesized by all vascular plants [*Sarkanen and Ludwig,* 1971]. The *p*-hydroxy (P) phenols can also be components of lignin, but there are non-lignin sources of these phenols as well [*Opsahl and Benner,* 1995]. The ratio of P to lignin (V and S) phenols has been used to identify the relative contributions of *Sphagnum* and vascular plants to peat [*Williams et al.*, 1998; *Williams and Yavitt*, 2003], as *Sphagnum* is rich in P phenols but lack V and S phenols and true lignin [*Williams et al.*, 1998; *Wilson et al.*, 1989]. The source specificity of V and S phenols facilitates their use as quantitative tracers of vascular plant material in peats. Assuming V and S phenols represent a constant fraction of vascular plant C and that this fraction does not change appreciably with diagenesis, the

yield of these phenols in peats is directly proportional to the fractional contribution of vascular plants to the peats as shown in Figure 2.2. Minor amounts of V and S phenols were measured in field-collected *Sphagnum*, but these were likely due to contamination from vascular plant debris so the *Sphagnum* end-member in our mixing model does not contain V or S phenols.

2.4.1.2 Analysis of error

The two indices generally produced similar results, and the difference in % *Sphagnum* between the two methods was <20% in 66% of samples. These indices are independent, so this agreement increases confidence in the accuracy of these results. The differences between the two methods are likely caused by either alteration of the indices during diagenesis or by variations in the indices of the fresh plant end members.

The carbohydrate *Sphagnum* index is relatively uniform among the *Sphagnum* species and vascular plants analyzed and presented in Table 2.3, and there is a three-fold difference between the two plant types. This makes the neutral sugar-based reconstruction relatively robust to changes in the composition of the vascular plant community. The phenol vascular plant index (VPI_{Phenol}) was more variable among vascular plants, and *Ledum* leaves had a particularly low VPI_{Phenol} (24-53 nmol mg C^{-1}) compared to other vascular plants. A *Ledum*-dominated plant community would produce peat with a lower VPI_{Phenol} than other plants, which would bias the quantitative vegetation reconstruction. However, *Ledum* stems had a VPI_{Phenol} of 458 nmol mg C^{-1}, approximately double the average of all vascular plants, potentially compensating for the low yield in leaves. The index is relatively constant in other vascular plant species, so

changes in the vascular plant community likely have a minor effect on the results of the vegetation reconstruction.

Neutral sugars are the building blocks of structural polysaccharides in plants, and they account for a large fraction of the C in vegetation and peat. They are more reactive than lignin during early diagenesis of plant litter and their C-normalized yields decline with decomposition [*Opsahl and Benner*, 1995, 1999]. Using ratios of sugars as indicators of source vegetation avoids some problems associated with diagenesis, because ratios are independent of the total yield of neutral sugars. However, neutral sugars are not uniformly distributed among plant polysaccharides, which could make these ratios sensitive to diagenetic alteration. Although the relative bioreactivity of neutral sugars has not been evaluated in peatlands, studies in other ecosystems consistently indicate the mol% rhamnose increases and the mol% xylose decreases during decomposition. The mol % rhamnose increased by a factor of 2-5 during a 4-year decomposition study of vascular plant detritus [*Opsahl and Benner*, 1999]. In addition, the mol % rhamnose is greater in soil organic matter than fresh plant material [*Derrien et al*., 2007]. Mol % rhamnose was also higher in more decomposed organic matter in the Amazon basin [*Hedges et al*., 1994]. This implies that rhamnose is selectively preserved compared to other sugars, has a substantial microbial source, or both. In contrast, xylose is more reactive than other sugars and the mol% xylose tends to decrease with decomposition [*Opsahl and Benner*, 1999]. As decaying detritus tends to become enriched in rhamnose and depleted in xylose, the carbohydrate *Sphagnum* index can be expected to increase with diagenesis. In addition, vascular plant litter decomposes more rapidly than *Sphagnum* litter [*Moore et al.*, 2007; *Bragazza et al.*, 2009]. Carbohydrates comprise a

large fraction of *Sphagnum* C, so *Sphagnum*-derived neutral sugars are likely less reactive than those in vascular plants. Furthermore, *Sphagnum* cell wall polysaccharides are very resistant to decomposition and contribute to the recalcitrance of bulk *Sphagnum* litter [*Hajek et al.*, 2011]. Therefore, it is likely that the carbohydrate *Sphagnum* index increases with decomposition as rhamnose and *Sphagnum*-derived sugars are selectively preserved and vascular plant-derived sugars are selectively decomposed. The neutral sugar based vegetation reconstruction likely overestimates *Sphagnum* contributions and underestimates vascular plant contributions.

The lignin component of vascular plant litter is more resistant to decomposition than bulk C under aerobic and anaerobic conditions [*Benner et al.*, 1984; *Benner et al.*, 1987; *Opsahl and Benner*, 1995]. The phenol vascular plant index is therefore expected to increase with diagenesis, implying that the phenol-based vegetation reconstruction is likely to overestimate vascular plant contributions and underestimate *Sphagnum* contributions. The phenol and neutral sugar-based reconstructions of paleovegetation tend to offset each other with regards to estimation of vascular plant and *Sphagnum* contributions. Therefore, the two methods should provide a range of values that encompasses the contributions of *Sphagnum* and vascular plant carbon in peats.

Independent biochemical indicators show that the northern cores are more extensively decomposed than the southern cores. The acid:aldehyde ratios of vanillyl and syringyl phenols were significantly higher in the two northern cores compared with the two southern cores (Chapter 3). These ratios increase with microbial decomposition of lignin [*Hedges et al.*, 1988; *Opsahl and Benner*, 1995], indicating that vascular plant material is more extensively decomposed in the northern cores than in the southern cores

despite forming under cooler conditions. Yields of hydroxyproline, an amino acid found in plant structural glycoproteins, were significantly higher in northern cores compared with southern cores (Chapter 3). Hydroxyproline-rich glycoproteins are not synthesized by microbes and are generally less reactive than bulk plant carbon (Chapter 1), so elevated yields supported the conclusion that the northern cores were more extensively decomposed than the southern cores.

The general agreement between the results of the carbohydrate and phenol-based reconstructions indicates these independent indicators provide fairly representative reconstructions of paleovegetation. The estimate of % *Sphagnum* using the carbohydrate *Sphagnum* index was higher than the estimate using the phenol vascular plant index in 75% of the samples and 90% of the samples where the difference between the two was greater than 20% (Fig. 2.6), consistent with an overestimation of % *Sphagnum* using the carbohydrate method compared to the lignin phenol method. However, the differences between the two methods were similar for the northern and southern cores despite more extensive decomposition of the northern peats. The average difference in % *Sphagnum* calculated using the two methods was 21 and 13% in SIB04 and SIB06, respectively, compared to 18 and 16% in G-137 and E-113. This indicates diagenetic effects on vegetation reconstruction were relatively minor in peats with quite variable extents of alteration and decomposition.

The carbohydrate Cyperceae index (CI_{Carb}) was used qualitatively to identify peat with sedge inputs, but was not applied quantitatively because it is very sensitive to diagenetic alteration. The index declined from 15.9 to 3.2 in smooth cordgrass, a monocot, over the course of a 4-year decomposition study (recalculated from [*Opsahl*

and Benner, 1999]). If a mixing model was developed to estimate Cyperaceae contributions to the peat it would likely underestimate this fraction, especially in highly decomposed peats. The low values of CI_{Carb} throughout both northern cores could be due to diagenetic alteration rather than the lack of sedge remains. Therefore, only the carbohydrate *Sphagnum* and lichen indices and the phenol vascular plant index were used quantitatively, while CI_{Carb} was used to qualitatively infer changes in the composition of the vascular plant community.

Like the carbohydrate Cyperceae index, *p*-hydroxyacetophenone (PON) offered potential as an indicator of *Sphagnum* remains but was ultimately excluded due to its sensitivity to diagenesis. There are likely two major reservoirs of PON in peat, one derived from *Sphagnum* cell walls [*Rasmussen et al.*, 1995] and another associated with lignin in vascular plants. These reservoirs seem to have different reactivities, as PON often underestimated *Sphagnum* inputs compared to neutral sugar and lignin phenol indices in peat samples with >50% *Sphagnum*, but overestimated the % *Sphagnum* in vascular plant-dominated samples (Fig. A3). These differences are most pronounced in the two more highly decomposed northern cores. In addition, PON yields indicated declining *Sphagnum* contributions in G-137 and E-113 with depth, a trend that is not apparent from the other indices. This indicates PON is preferentially removed in more decomposed peats. Although PON yields are very different between *Sphagnum* and vascular plants, PON is not a reliable tracer of *Sphagnum* contributions in peats due to its inconsistent pattern of alteration during diagenesis.

2.4.2 Paleovegetation in the West Siberian Lowland over the last 2000 years

The northern cores (G-137 and E-113) were collected near the Yamal Peninsula, where tree-ring evidence indicates a warm Medieval Warm Period (MCA) and cool Little Ice Age (LIA) [*Briffa*, 2000; *Osborn and Briffa*, 2006]. These cores appear to record opposite trends. Both cores are generally *Sphagnum*-dominated, but E-113 shows a lichen invasion ~750 cal. BP, between the MCA and LIA, while G-137 was lichen-dominated from the peak of the LIA to present. Lichens thrive in dry conditions, but developed at these sites during periods of supposedly cool and wet conditions. This apparent contradiction may be explained by the development of permafrost. Permafrost causes heaving of the soil, which raises the peat surface relative to the water table and creates locally drier conditions [*Zoltai*, 1993; *Sannel and Kuhry*, 2008]. Surface peat (upper 30 cm) had lower average water content in permafrost vs. non-permafrost cores both among the four cores analyzed (87.5 vs. 91.0%) and across the West Siberian Lowland (81.6 vs. 92.0%; *Smith et al.*, 2012). Climate cooling associated with the transition from the MCA to the LIA could have triggered the expansion of permafrost at these sites, creating locally drier conditions even in a cooler and wetter climate.

Sphagnum remains dominate the southern cores (SIB04 and SIB06) throughout most of the past 2000 years, punctuated by repeated but short-lived vascular plant invasions. Vascular plant signals were often confined to single sample intervals, representing <100 years of accumulation. There are three commonly observed drivers of peatland vegetation change that may have triggered the oscillations observed in SIB04 and SIB06: burning of surface vegetation and the establishment of short-lived pioneer communities, rapid climate change causing water table fluctuations, and internal peat

dynamics and complex ecohydrological feedbacks driving vegetation succession independent of climate change. We evaluate the likelihood of each below.

The repeated burning of the peat surface has the potential to produce the observed pattern of vegetation change. Peat fires remove the surface vegetation, which is replaced by pioneer plant communities that are typically dominated by vascular plants [*Kuhry*, 1994; *Sillasoo et al.*, 2011]. However these communities are often short-lived and are replaced by the original vegetation within a few decades [*Kuhry*, 1994]. The fire return interval is variable among bogs, but is on the order of centuries. These features make peat fires a possible explanation for the observed invasions of vascular plants that occurred repeatedly every few centuries but lasted only decades.

However, there is no evidence in the cores themselves to suggest extensive burning. While a quantitative charcoal analysis was not conducted, there did not appear to be any significantly charred layers in these cores (D. Beilman and K. Willis, personal communication). In addition, the C content of the cores fell in a relatively narrow range from 42-48% in SIB04 and 36-51% in SIB06 and did not appear to be correlated with vegetation changes. Ash content was <6% in all but one sample in both SIB04 and SIB06 [*Smith et al*., 2012]. This indicates fires did not drive the observed vegetation change, as they would likely cause variations in the ash and C contents of the peat. This is consistent with previous research indicating that fire is relatively rare in West Siberian Lowland peatlands, particularly in the late Holocene [*Turunen et al*., 2001].

Climate change is a more likely driver of the observed vegetation patterns. The frequent shifts between *Sphagnum* and vascular plant dominance imply rapid changes in the position of the water table relative to the bog surface. Changes in temperature and

precipitation alter the moisture balance and water table level in peatlands, which in turn determine the composition of the plant community [*Barber et al.*, 1994; *Valiranta et al.*, 2007]. However, this explanation remains problematic because vegetation changes in the two cores display different periodicities despite their close proximity (approximately 330 km). SIB04 cycles between *Sphagnum* and vascular plants on average every 240 years, compared with approximately 420 years in SIB06. This is likely due to differences in microtopography between the sites. Vegetation at hummock microsites may be more sensitive to water table variations than lawns or hollows [*Loisel and Garneau*, 2010]. The carbohydrate and phenol Cyperceae indices were elevated during vascular plant invasions at SIB06 but not at SIB04, indicating sedges were an important part of the vascular plant community only at SIB06. It appears conditions were wetter at SIB06 than at SIB04, which was likely colonized by gymnosperms and herbaceous angiosperms during vascular plant invasions, characteristic of a relatively dry hummock environment. This could explain the more frequent vegetation changes observed in SIB04, as the hummock plant community was likely more sensitive to small changes in water table level than the *Sphagnum*/sedge community at SIB06.

The oscillation between *Sphagnum* and vascular plant dominance indicated a dynamic water table and plant community. However, the MCA and LIA did not produce a consistent vegetation change in the cores. SIB04 and SIB06 appeared to be *Sphagnum*-dominated during both events, indicating wet conditions. It is unlikely that this is due to chronological uncertainty because there do not appear to be any sustained shifts in vegetation in either core during the past 2000 years. This indicates that the two climate anomalies were not sufficient to cause significant vegetation change at SIB04 and SIB06.

There are two plausible explanations for this lack of response of the vegetation to climate change: either (1) climate change in the southern West Siberian Lowland was relatively mild; or (2) vegetation in West Siberian Lowland peatlands is insensitive to climate change due to internal ecohydrological feedbacks.

The lack of vegetation change in the southern cores during the MCA and LIA is consistent with the heterogeneity of climate change during these events. The MCA and LIA were widespread across the northern hemisphere [*Osborn and Briffa*, 2006; *Mann et al*., 2009], but the timing and magnitude of the MCA and LIA varied within Europe [*Guiot et al*., 2010] as well as between continents [PAGES 2k Consortium, 2013]. Climate models and calibrated proxy paleotemperature reconstructions indicate a significant difference between MCA and LIA temperatures in arctic Eurasia, near the sites of the northern cores, but a smaller difference at lower latitudes in the West Siberian Lowland [*Mann et al.*, 2009]. The lack of vegetation change is consistent with a mild MCA and LIA, given our limited data set.

In contrast, it is also possible that vegetation did not change during the MCA and LIA because it is relatively insensitive to climate change. Peatlands are not passive receptacles of climate conditions but complex living ecosystems. The response of the water table level to climate change is nonlinear due to ecohydrological feedbacks in the peat system. The water table depth is affected both by climatic water balance, which determines the rate of water storage in the peat, and by peat formation rate. These variables are closely linked, as moisture conditions affect primary production and rates of decomposition, the balance between which determines peat accumulation [*Belyea*, 2009]. A change in precipitation balance will either be amplified or dampened by feedbacks due

to the rate of peat growth, depending on the peat microform [*Belyea*, 2009]. In addition, bog water table can also vary independently of climate through processes internal to bog development [*Swindles et al*., 2012; *Loisel and Yu*, 2013]. It is clear that not all climate change causes a change in the position of the bog water table, and not all apparent changes in bog water table are necessarily driven by climate.

The lack of vegetation change in response to the MCA and LIA cannot therefore rule out significant climate change during these events. To be recorded in the bog vegetation record, climate must alter the water table level enough to significantly alter the competitive balance between *Sphagnum* and vascular plants. There appears to be a minimum threshold necessary to affect vegetation due to the complex feedbacks between water table level and peat growth [*Charman*, 2007], and the threshold is likely higher in the large bog complexes of the West Siberian Lowland than smaller bogs in United Kingdom and Western Europe. The lack of vegetation change at SIB04 and SIB06 indicates that this threshold was not met during the MCA and LIA at these sites. This suggests that the MCA and LIA were relatively mild at these sites in the West Siberian Lowland, but it is difficult to estimate the magnitude because the climate threshold for vegetation change in these bogs is unknown.

In addition, the lack of vegetation change at SIB04 and SIB06 is not necessarily representative of the entire southern West Siberian Lowland. While peatland vegetation records are generally reproducible given a sufficient sample size [*Barber et al*., 1998], they are variable enough that two cores should not be extrapolated to the entire region. Our results are consistent with model predictions of a mild Medieval Climate Anomaly

and Little Ice Age in the southern West Siberian Lowland, but further study is needed to determine the magnitude and spatial extent of the events.

Table 2.1 Locations and radiocarbon ages of the four peat cores

Core	Latitude	Longitude	Depth (cm)	Median calibrated 14C age (calendar years BP)[a]
SIB04	56°48'14"N	78°44'13"E	42-43	290
			258-259	1940
			284-285	2060
SIB06	58°26'09"N	83°26'03"E	24-25	29
			31-32	40
			179-180	1670
			189-190	2400
G-137	63°45'01"N	75°45'58"E	7-8	370
			15-16	520
			22-23	730
			60-61	5240
E-113	66°26'59"N	79°19'24"E	7-8	180
			15-16	390
			47-48	1885
			78-79	2400

[a]From Beilman et al. [2009].

Table 2.2 Summary of vegetation indices and equations for vegetation reconstruction.

Index name	Abbreviation	Definition	Equation
Quantitative indices			
Carbohydrate *Sphagnum* index	SI_{Carb}	Rha/(Man+Xyl)[a]	$fSphagnum=2.700(SI_{Carb})^3-4.589(SI_{Carb})^2+3.378(SI_{Carb})-0.2161$
Carbohydrate lichen index	LI_{Carb}	(Man+Gal)/(Xyl+Ara+Rha)[a]	$fLichens=0.00039(LI_{Carb})^3-0.014(LI_{Carb})^2+0.20(LI_{Carb})-0.085$
Phenol vascular plant index	VPI_{Phenol}	nmol V+S phenols mgC^{-1}	$fVascular=VPI_{Phenol}/220$[c]
Other indices			
Carbohydrate Cyperaceae index	CI_{Carb}	(Xyl+Ara)/(Man+Gal+Rha)[a,b]	-
Phenol Cyperaceae index	CI_{Phenol}	nmol FAD mgC^{-1}	-
Phenol *Sphagnum* index	SI_{phenol}	nmol PON mgC^{-1}	$fSphagnum=0.00994(SI_{PON})-0.0873$

[a]Molar ratios of sugars

[b]Jia et al. (2008)

[c]220 represents the mean VPI_{Phenol} in vascular plant sources (Table 2.4)

Table 2.3 Neutral sugar yields and vegetation indices in peat-forming vegetation.

	Source	n	Fuc	Rha	Ara	Gal	Glc	Man	Xyl	sum	Yield	SI_{Carb}	LI_{Carb}	CI_{Carb}
			nmol/mg C								(%OC)			
Bryophytes														
S. fuscum[a]	James Bay, QC, Canada	2	47	307	134	761	2806	266	474	4795	33.8	0.42	1.12	0.46
S. angustifolium[a]	James Bay, QC, Canada	2	47	367	138	850	3226	170	583	5382	37.9	0.49	0.94	0.52
S. magellanicum[a]	James Bay, QC, Canada	2	37	288	221	965	2698	237	580	5025	35.3	0.35	1.10	0.54
S. quinquefarium	Codroy Valley, NL, Canada	1	67	326	164	807	3145	316	490	5316	37.5	0.40	1.15	0.45
Vascular Plants														
Carex sp.[a]	James Bay, QC, Canada	2	44	138	732	559	2717	83	1760	6033	40.5	0.08	0.24	3.19
Carex sp.	Toolik Lake, Alaska	2	2	23	531	245	2864	24	1227	4916	33.3	0.02	0.15	6.03
Eriophorum vaginatum	Toolik Lake, Alaska	2	5	21	653	246	3178	22	1522	5647	38.1	0.01	0.12	7.53
Ledum palustre	Toolik Lake, Alaska	3	4	60	371	394	2122	27	487	3464	23.9	0.12	0.46	1.78
Abies balsamea needles	Codroy Valley, NL, Canada	3	23	49	358	261	2075	274	146	3186	22.4	0.12	0.97	0.86

[a]Field samples that may include traces of litter from other plants

Table 2.4 Phenol yields and VPI_{Phenol} in peat-forming vegetation.

	Source	n	PAL	PON	PAD	VAL	VON	VAD	SAL	SON	SAD	CAD	FAD	VPI_{Phenol}[a]	Yield
			(nmol/mgC)												(%OC)
Bryophytes															
S. fuscum[b]	James Bay, QC, Canada	2	46.0	114.8	54.5	4.2	0.8	1.0	3.2	0.5	0.5	4.1	1.2	10.3	2.3
S. angustifolium[b]	James Bay, QC, Canada	2	63.0	126.5	49.6	3.0	0.7	1.0	2.2	0.4	0.4	7.9	0.6	7.7	2.4
S. magellanicum[b]	James Bay, QC, Canada	2	42.0	101.1	48.3	12.1	5.1	3.5	4.9	0.7	0.8	5.9	2.6	27.1	2.2
S. quinquefarium	Codroy Valley, NL, Canada	1	32.8	95.1	37.2	10.6	2.5	3.2	1.5	0.3	0.3	3.4	0.6	18.4	1.7
Vascular Plants															
Carex sp.[b]	James Bay, QC, Canada	2	40.8	21.0	19.2	108.1	16.8	15.1	69.4	22.9	13.9	60.2	71.7	246.3	4.8
Carex sp.	Toolik Lake, Alaska	2	20.0	8.4	8.1	67.9	15.5	8.7	62.5	35.2	14.9	79.6	56.3	204.6	4.0
Eriophorum vaginatum	Toolik Lake, Alaska	2	11.7	2.1	3.8	51.3	7.7	7.7	67.1	44.4	15.8	77.2	75.1	194.0	4.0
Sedge Leaves[c]	Spring Pond Bog, NY, USA	1	27.8	9.1	11.3	99.3	21.4	18.8	115.8	0.0	20.7	151.3	118.3	275.9	6.2
Ledum palustre	Toolik Lake, Alaska	3	7.8	1.1	17.3	26.9	4.3	5.2	13.5	1.7	1.8	33.3	4.9	53.4	1.2
Ledum leaves[c]	Spring Pond Bog, NY, USA	1	4.1	1.9	6.7	6.5	1.4	1.5	4.9	8.7	0.5	102.8	4.0	23.6	1.5
Ledum stems[c]	Spring Pond Bog, NY, USA	1	10.5	9.3	4.8	104.7	15.6	14.5	293.1	1.6	28.4	50.4	21.1	457.9	5.5
Abies balsamea needles	Main Brook, NL, Canada	2	16.4	5.9	20.9	119.9	30.1	39.6	6.5	1.5	3.1	31.1	11.1	200.7	2.9
Picea wood[c]	Spring Pond Bog, NY, USA	1	36.9	8.4	16.6	271.4	33.9	48.4	0.0	0.0	0.0	4.0	19.3	353.7	4.2
Picea needles[c]	Spring Pond Bog, NY, USA	1	26.6	42.7	111.6	127.3	32.0	35.2	0.0	0.0	0.0	45.4	15.3	194.5	4.4

[a]nmol V+S phenols mg C^{-1} [b]Field samples that may include traces of litter from other plants [c]From [*Williams et al.*, 1998].

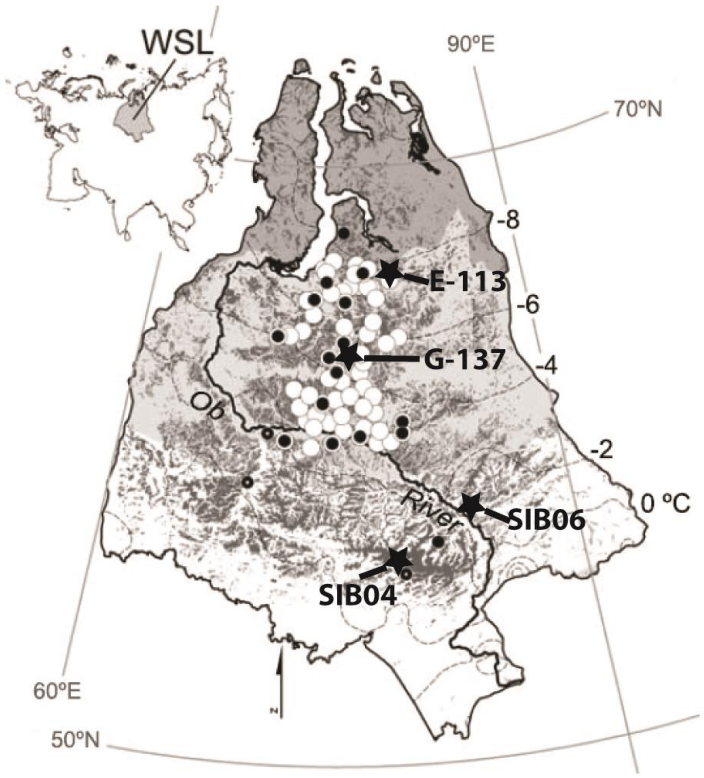

Figure 2.1 Location of the four cores used in this study (black stars) in comparison to the larger 77 core network used by Beilman et al. [2009]. Cores with only a basal radiocarbon age are indicated with a white circle. Cores with the 2 ka depth identified are indicated with black circles, and those with additional radiocarbon ages near the surface contain white dots. Modern mean annual air temperature isotherms are shown by dashed lines (1931–2000) (K. Matsuura and C. J. Willmott, Arctic Land- Surface Air Temperature: 1930–2000 Gridded Monthly Time Series, version 1.01, 2004, Center for Climate Research, University of Delaware, Newark; available at http://climate.geog.udel.edu/~climate/html_pages/archive.html). Modified from Beilman et al. [2009].

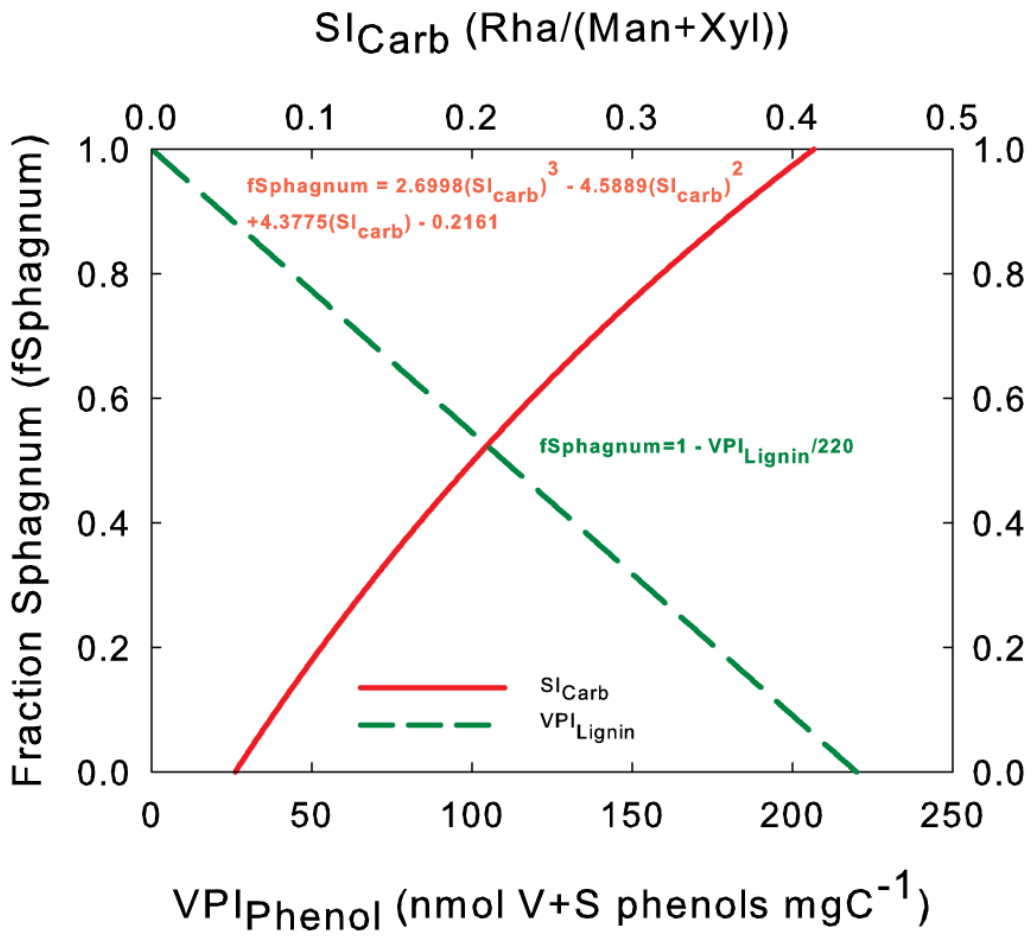

Figure 2.2 Carbohydrate Sphagnum index (SI_{carb}; solid red line) and phenol vascular plant index (VPI_{phenol}; dashed green line) in a modeled mixture of Sphagnum and vascular plants. The equations shown are derived from the regressions of the mixing curves. Neutral sugar and phenol yields in Sphagnum and vascular plant end-members were calculated as the average for each plant type from Tables 2.3 and 2.4. fSphagnum = fractional contribution of Sphagnum to the total C in the modeled mixture.

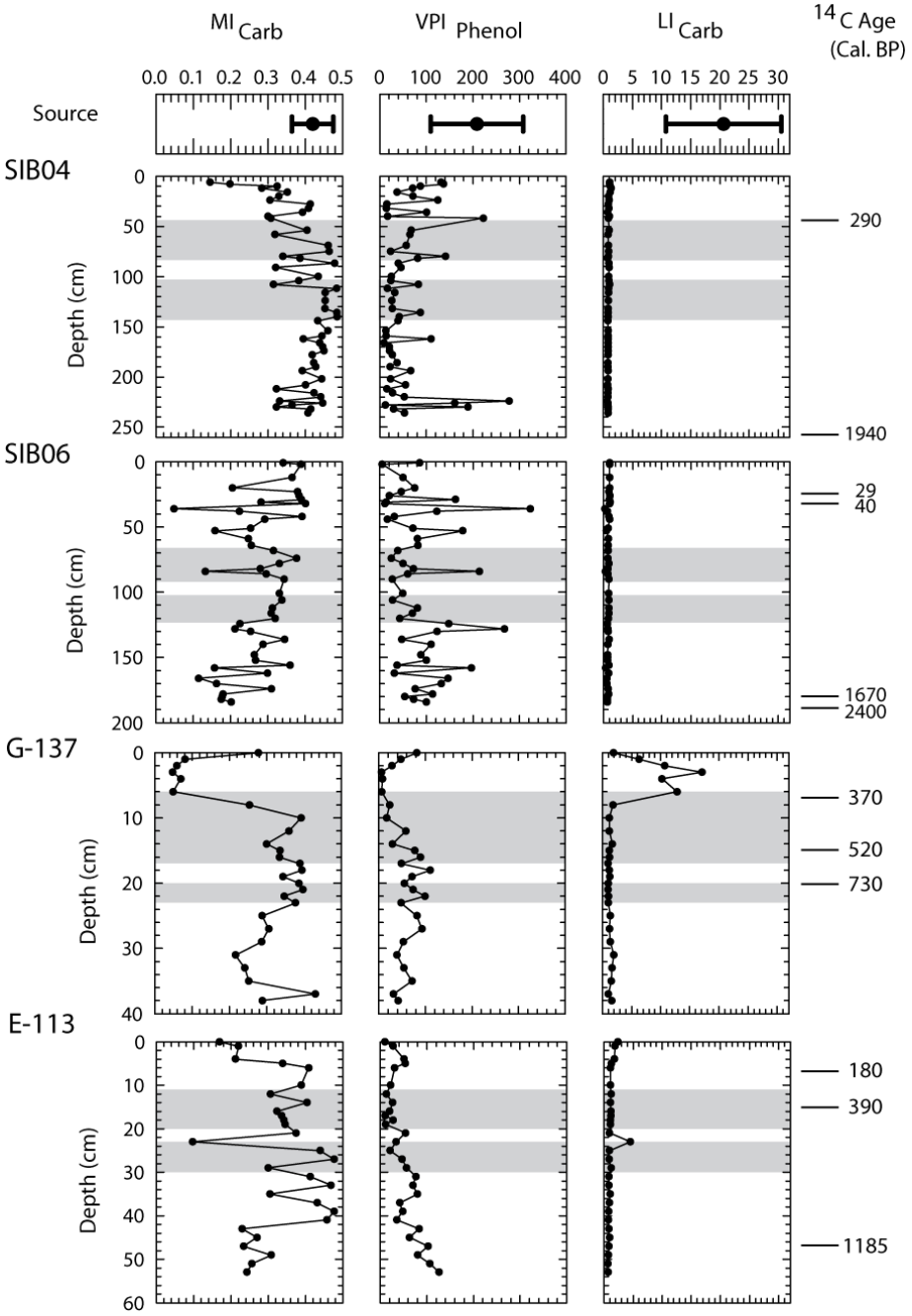

Figure 2.3 Profiles of the carbohydrate Sphagnum index (SIcarb), the phenol vascular plant index (VPIphenol), and the carbohydrate lichen index (LIcarb) in the four cores. The indices are defined in Table 2.2. Values (average ± standard deviation) of the indices in source vegetation (Sphagnum, vascular plants, and lichens) are shown at the top of their respective profiles. Median calibrated ^{14}C ages are from Table 2.1. Gray bars from 850–1050 to 300–600 cal years B.P. correspond to the Medieval Climate Anomaly and the Little Ice Age, respectively, based on linear interpolation between dated intervals.

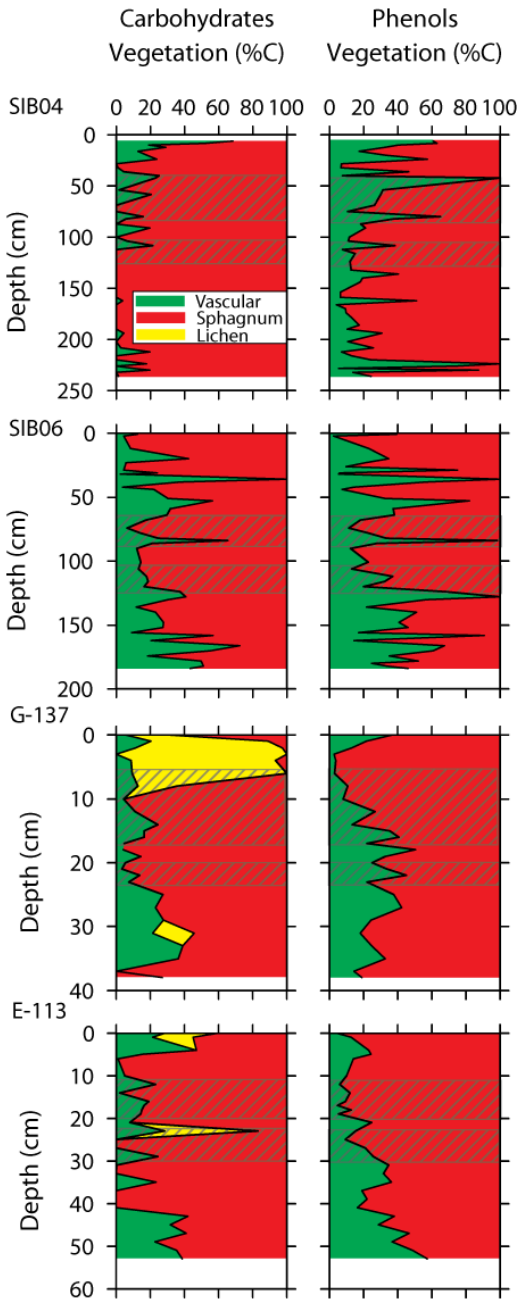

Figure 2.4 Vegetation reconstruction using (left) carbohydrates and (right) lignin phenols in the four cores. Diagonal bars indicate the positions of the Medieval Climate Anomaly and the Little Ice Age. For the neutral sugar-based reconstruction, % Sphagnum was calculated using SI_{carb}, % lichen was calculated using LI_{carb}, and % vascular plant was calculated by difference. For the phenol-based reconstruction, % vascular plant was calculated using VPI_{phenol}, and Sphagnum and lichens were calculated by difference. Sphagnum and lichens cannot be differentiated using the phenol method, so their sum is presented as % Sphagnum

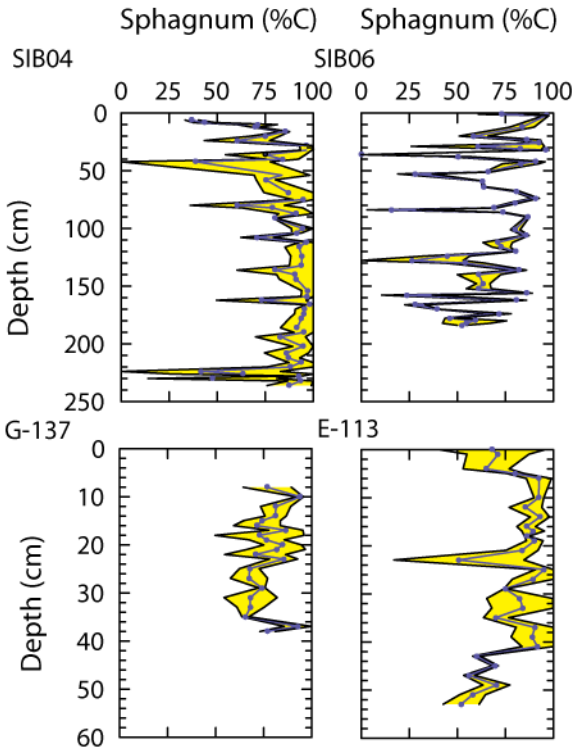

Figure 2.5 Average (line and dots) and range (yellow fill) of % C as *Sphagnum* in the four cores, calculated using SI_{Carb} and VPI_{Phenol}. The lichen-dominated upper 8 cm of G-137 is omitted.

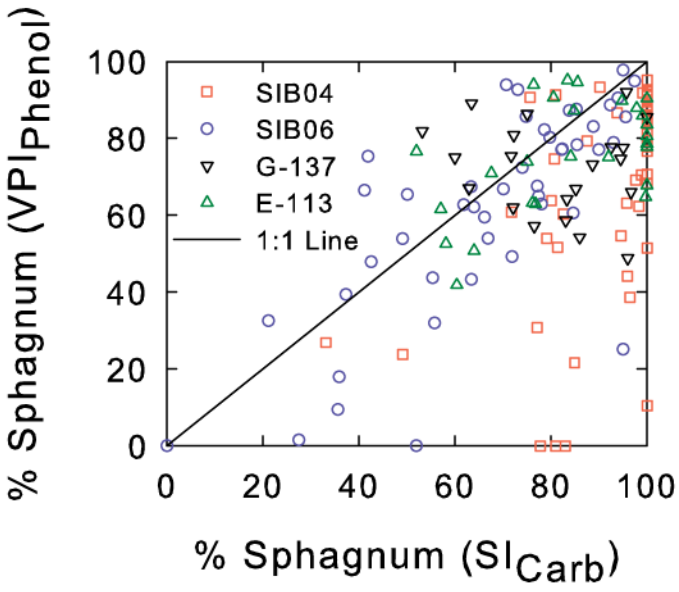

Figure 2.6 Correlation of carbohydrate- and lignin phenol-based estimates of peat vegetation. The solid line indicates a 1:1 relationship. Samples containing lichen remains (as indicated by LI_{Carb}) were excluded.

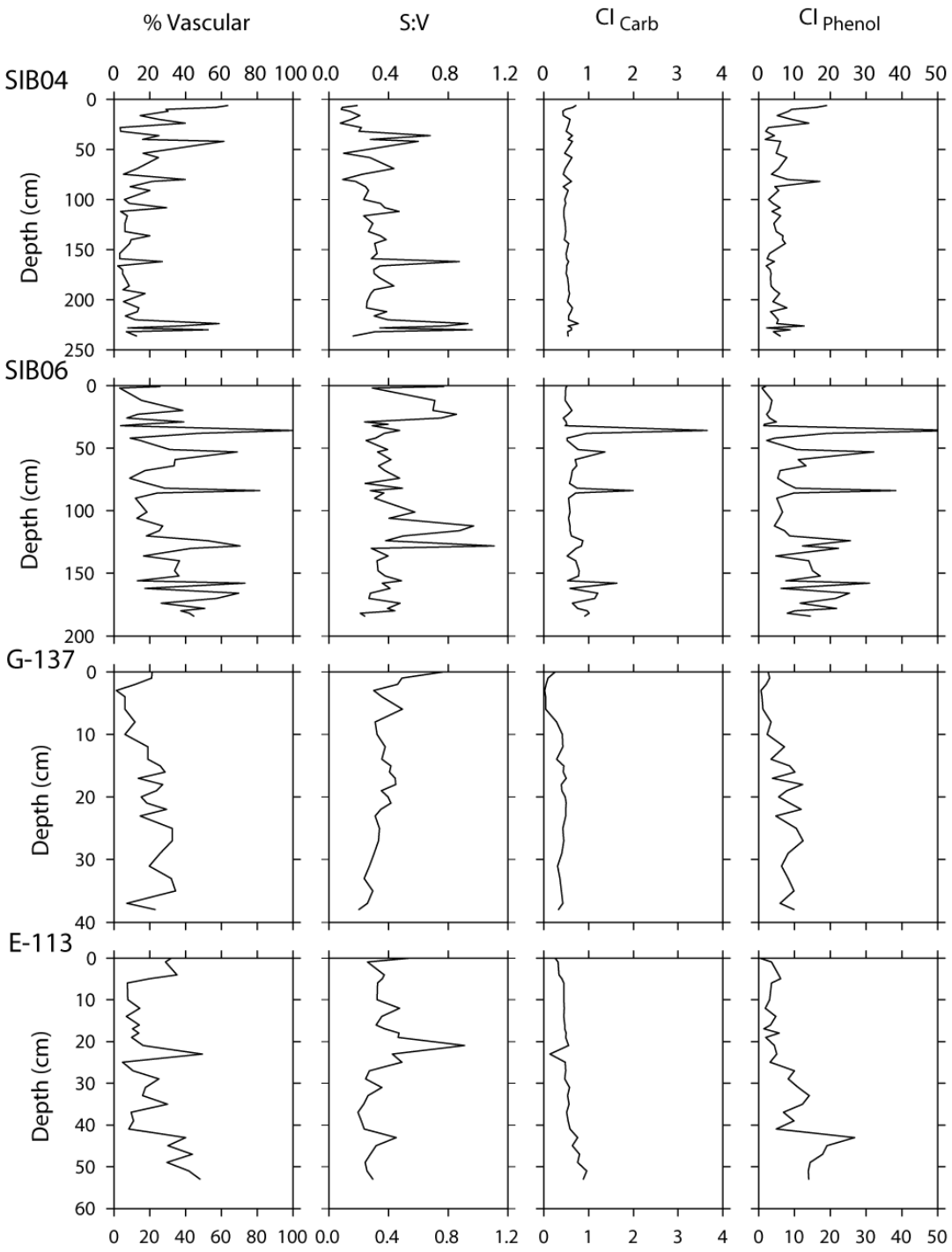

Figure 2.7 Qualitative vegetation indices in the four cores. See table 2 for index definitions. % Vascular was calculated as the average of the neutral sugar- and lignin phenol-based reconstructions.

CHAPTER 3

DOES OXYGEN EXPOSURE TIME CONTROL THE EXTENT OF ORGANIC MATTER DECOMPOSITION IN PEATLANDS?[3]

3.1. Introduction

Peatlands accumulate carbon (C) due to an imbalance between net primary production (NPP) and organic matter decomposition. NPP has exceeded decomposition in northern peatlands over most of the Holocene, resulting in the accumulation of approximately 550 Pg C [*Yu et al.,* 2010]. However, there is substantial concern that human activities will disrupt the current imbalance, transforming peatlands from a net C sink to a C source. Rising temperatures [*Lafleur et al.*, 2005; *Dorrepaal et al.*, 2009], changing precipitation patterns [*Ise et al.*, 2008; *Fenner and Freeman*, 2011], and increasing atmospheric nitrogen deposition [*Vitt et al.,* 2003; *Bragazza et al.*, 2012] to the boreal region will all affect both NPP and decomposition processes, and their net effect on peat C accumulation rates and C sequestration remain poorly understood.

Our ability to predict the response of peatland C accumulation to climate change rests on a mechanistic understanding of the factors that control NPP and decomposition. Experimental evidence shows that temperature, vegetation type, and availability of molecular oxygen can have a strong influence on rates of peat decomposition. Elevated

[3] Philben, M., K. Kaiser, and R. Benner (2014b), Does oxygen exposure time control the extent of organic matter decomposition in peatlands?, *Journal of Geophysical Research: Biogeosciences*.

temperatures stimulate microbial respiration, resulting in increased rates of organic matter decomposition [*Hobbie*, 1996; *Lafleur et al.*, 2005]. Vascular plant material decomposes at higher rates than *Sphagnum* mosses [*Hobbie*, 1996; *Moore et al.*, 2007], so a shift in the plant community composition could have a significant effect on peat decomposition. Aerobic decomposition of plant material in soils and sediments is typically an order of magnitude faster than anaerobic decomposition [*Benner et al.*, 1984]. It has been suggested that the residence time of peat in the acrotelm, the periodically oxic region between the peat surface and the lowest summer water table, is an important control on the extent of peat decomposition [*Belyea and Clymo*, 2001].

It is difficult to assess the importance of these effects on peat decomposition based on results of experimental manipulations. Temperature, vegetation, and water table are not fully independent of one another and tend to covary. For example, higher temperatures lead to increased evapotranspiration, which can lead to a lower water table. Drier conditions can promote vascular plant growth at the expense of *Sphagnum*, causing a change in the plant community. The depth of the water table is not only a function of climate, but is determined by the relative change in water storage and new peat formation [*Belyea*, 2009]. It is difficult for short-term experimental manipulations to capture the complex feedbacks among environmental variables. This limits the applicability of experimental results in predicting the long-term effects of environmental change on peat decomposition. It is also difficult to predict the relative importance of each of these factors in peatlands where all three are affecting the rate of peat decomposition.

The ratios of C:N and humification indices are commonly used to assess the extent of peat decomposition [*Aaby*, 1976; *Chambers et al.*, 1997; *Kuhry and Vitt*, 1996].

These approaches do not involve experimental manipulation of environmental conditions, but rather integrate natural variability of conditions both among cores and through time in individual cores. However, both C:N and humification indices are difficult to interpret and compare among sites. Use of the C:N ratio as a diagenetic index requires the assumption that plants have similar C:N ratios and that N is conserved while C is respired. The resulting enrichment of N relative to C can be used to estimate the extent of C loss [*Malmer and Holm*, 1984; *Kuhry and Vitt*, 1996]. However, this assumption is not necessarily met. *Sphagnum* mosses in ombrotrophic bogs receive most of their N from atmospheric deposition, and C:N ratios of *Sphagnum* litter are significantly correlated with the rate of N deposition [*Bragazza et al.*, 2006; *Gerdol et al.*, 2007; *Limpens et al.*, 2011]. Atmospheric deposition of reactive N has increased by an order of magnitude over the last century in many terrestrial environments due to anthropogenic N fixation [*Galloway et al.*, 2004]. Different levels of N deposition among sites and changing deposition with time can therefore affect peat C:N ratios independent of decomposition. In addition, denitrification rates can be significant in peatlands with greater N availability [*Francez et al.*, 2011], complicating the assumption of conservative N recycling. Similarly, humification indices are affected by the botanical composition of the peat [*Yeloff and Mauquoy*, 2006; *Hughes et al.*, 2012]. This limits their value in assessing controls on peat decomposition among sites with different plant communities.

Biochemical indices of the diagenetic state of organic matter can be useful for deciphering the controls on the extent of peat decomposition. Amino acids are common to all organisms and they typically comprise half or more of the total N in biomass, thereby providing insights about N recycling as well as the extent of decomposition

[*Tremblay and Benner*, 2006]. Hydroxyproline (Hyp) is an amino acid found in all plants, including mosses, but is not synthesized by microbes [*Kieliszewski and Lamport*, 1994]. Hyp is found in structural glycoproteins and is typically more resistant to microbial decomposition than bulk C. The yield of Hyp increased with increasing bulk C loss during a litter bag decomposition study of three vascular plant tissues, indicating Hyp is a useful diagenetic indicator (Chapter 1). Lignin is found only in vascular plants, and its CuO oxidation produces phenols that reflect the sources and extent of decomposition of vascular plant tissues [*Benner et al.*, 1991]. Ratios of vanillic acid to vanillin and syringic acid to syringaldehyde are low in fresh plant tissues but increase with microbial decomposition and are useful indicators of diagenetic alterations [*Hedges et al.*, 1988; *Opsahl and Benner*, 1995].

We analyzed samples from four cores collected along a latitudinal gradient in the West Siberian Lowland (WSL), which contains the world's largest peat-forming complex. Two cores were collected from the southern WSL, which has experienced relatively warm conditions and high rates of peat accumulation during the last 2000 years [*Smith et al.*, 2004; *Beilman et al.*, 2009]. Two cores were collected from the northern WSL, which has experienced lower temperatures, permafrost and much lower accumulation rates [*Kremenetski et al.*, 2003; *Beilman et al.*, 2009; *Smith et al.*, 2012]. Carbohydrate and lignin phenol compositions indicate that plant communities were variable in the southern cores, alternating between periods of *Sphagnum* and vascular plant dominance, while the northern cores were generally *Sphagnum*-dominated (Chapter 2). The latitudinal gradient presents a natural experiment for comparing the effects of the different hypothesized controls on peat decomposition. The southern cores experience

higher temperatures but are buried rapidly, shortening their exposure to oxygen and aerobic decomposition. The effect of vegetation on decomposition is assessed within each core, as layers dominated by vascular plants are hypothesized to be more decomposed than *Sphagnum*-dominated layers. Our objective is to test the relative importance of these factors in determining the extent of peat decomposition in these cores.

3.2. Materials and Methods

3.2.1. Study sites and sampling

Four peat cores were collected along a latitudinal gradient ranging from 56°N to 66°N in West Siberian Lowland, Russia [*Smith et al.*, 2004; *Beilman et al.*, 2009]. Cores were extracted with a 5-cm rotating sleeve side-cut Russian corer (non-permafrost sites) or a modified Cold Regions Research and Engineering Lab (CRREL) corer (permafrost sites). Cores were subsampled at 1 cm resolution and stored frozen in airtight plastic Whirl-pak sample bags until analysis. Two cores, SIB04 and SIB06, were collected from rapidly accumulating non-permafrost bogs in southern Siberia with depths of 400 and 395 cm, respectively. Core G-137 was collected from the discontinuous permafrost zone and had an active layer thickness of 50 cm and a total depth of 177 cm, whereas core E-113 was located in continuous permafrost and had an active layer thickness of 17 cm and a total depth of 327 cm [*Smith et al.*, 2012].

The four cores were radiocarbon dated to determine peat accumulation rates [*Beilman et al.* 2009]. The analyses herein focus on peat deposited in the last 2000 years. The apparent C accumulation rates at SIB04 and SIB06 over the last 2000 years (44 and 28 g C m^{-2} yr^{-1}, respectively) were significantly higher than the rates at G-137 and E-113 (10 and 15 g C m^{-2} yr^{-1}, respectively; Table 3.1). A vegetation reconstruction using the

lignin phenol and neutral sugar composition indicated all four cores were generally composed of *Sphagnum* remains but the southern cores indicated frequent shifts to vascular plant dominance on time scales <100 years (Chapter 2). Further details about the cores and their collection can be found in Sheng et al. [2004]; Smith et al. [2004, 2012]; and Beilman et al. [2009].

Samples of peat-forming vegetation and decomposers were also analyzed to identify their chemical signatures in the peat. While no vegetation was available from the coring sites, a variety of source materials were obtained from representative boreal ecosystems in North America. Bog vegetation from James Bay, QC, Canada was provided by Glen MacDonald and colleagues at UCLA. Keisuke Koba and Satoru Hobara provided tundra vegetation from Toolik Lake, AK, USA. Fungi and balsam fir needles and roots were collected from a boreal forest in Codroy Valley, NL, Canada by Sue Ziegler and Faye Murrin. Lyophilized bacteria cells were obtained from Sigma-Aldrich. The apical capitulum was removed from *Sphagnum* samples before analysis. Nitrogen is translocated from senescent stems to the actively growing capitula as they are buried [*Aldous*, 2002], so these capitula-free samples are more representative of *Sphagnum* litter on the peat surface.

3.2.2 Chemical Analyses

Frozen slices of peat (1 cm) were dried in a Savant SpeedVac vacuum centrifuge and ground in a Wiley mill to pass a 40-mesh screen. The C and N content of the peat was measured after combustion at 980 °C using a Costech ECS 4010 elemental analyzer. The mean % deviation for duplicate analyses was ±0.7% for C and ±3% for N.

Samples (10 mg) for total hydrolysable amino acid (THAA) analysis were added to glass ampules with 1 ml 6M HCl. The ampules were flame-sealed and heated to 110°C for 20 h. After hydrolysis, the ampules were opened and aliquots of the hydrolysates were dried under a stream of N_2. Samples were then dissolved in 200 µL deionized water and norvaline was added as an internal standard. Amino acids were recovered using solid phase extraction and derivatized with propyl chloroformate using the commercially available EZ:Faast kit for amino acid profiling (Phenomenex, USA). Derivatized samples were separated using gas chromatography (Phenomenex ZB-AAA column; 110-320°C at 30° min^{-1}) with flame ionization detection. The 16 quantified amino acids were: alanine (Ala), glycine (Gly), valine (Val), leucine (Leu), isoleucine (Ile), threonine (Thr), serine (Ser), proline (Pro), aspartic acid (Asp), hydroxyproline (Hyp), glutamic acid (Glu), phenylalanine (Phe), lysine (Lys), histidine (His), tyrosine (Tyr), and diaminopimelic acid (DAPA).

The amino acid yield was expressed as a percentage of C or N using the equation:

$$\text{THAA (\%C or N)} = \Sigma[\text{Yield}_{AA}/(\text{C or N})] \times [\text{Wt \% (C or N)}]_{AA} \quad (3.1)$$

for each of the 16 amino acids, where Yield_{AA}/C or N is the C- or N- normalized yield of the amino acid in mg AA (100 mg C or N)$^{-1}$ and $[\text{Wt \% (C or N)}]_{AA}$ is the weight % C or N in the amino acid. All amino acid data can be found in the supplementary information (Tables S1 and S2).

Lignin phenols were analyzed by gas chromatography/mass spectrometry (GC/MS) following CuO oxidation [*Kaiser and Benner*, 2012]. Dry peat samples (10-15 mg) were reacted with 330 mg CuO, 106 mg of $Fe(NH_4)_2(SO_4)_2 \cdot 6H2O$ and 2.5 mL of 2 mol L^{-1} NaOH in a Monel reaction vessel. Trans-cinnamic acid (CiAD) and ethyl-vanillin

(EVAL) were added as internal standards following oxidation. Samples were purified by solid phase extraction (SPE) using Oasis HLB cartridges and a vacuum manifold. After SPE, samples were dried under a stream of argon and redissolved in 200-400 μL of dry pyridine.

Gas chromatography was carried out using an Agilent 7890 system with an Agilent 5975C triple axis mass detector using electron impact ionization. Samples were derivatized with BSTFA/TMCS before analysis. Typically, 15 μL of sample was reacted with 15 μL of BSTFA/TMCS reagent at 75 °C for 15 min. The analytical precision of duplicate analysis was ±4 %. Mass spectrometer settings are described in detail by Kaiser and Benner [2012].

3.2.3 Statistical Analyses

All statistical analyses were performed using the open-source statistical package R (R Core team, 2013). A principle component analysis (PCA) was conducted to identify differences in amino acid composition among peat samples. The PCA compressed the mole percentages of 15 amino acids (all but DAPA) in each peat sample (n=150) into the two axes that explained the greatest amount of variance in the data set. The mole % of each amino acid in the peats was normalized by subtracting the mean value and dividing by the standard deviation of the mole % of the amino acid in the full data set.

3.3. Results

3.3.1. Composition of source materials

The *Sphagnum* mosses analyzed were very N-poor, with C:N ratios ranging from 91-170. Vascular plants had lower C:N than *Sphagnum* (32-61), but higher than fungi (11-21) or bacteria (3.7-4.7; Table 3.2). Amino acids accounted for a large fraction of the

N in all four types of organisms, ranging from 38% of the N in the stems of *Cortinarius armillatus* fungi to 71% in *Sphagnum magellanicum* (Table 3.2). *Sphagnum* had the highest average fraction of N as amino acids with 65%, while fungi had the lowest with 47%. The %C as amino acids was strongly correlated with the N:C ratio in the source materials analyzed (r^2=0.97), reflecting the relatively constant fraction of N as amino acids in all of the vegetation and microbes analyzed.

Hyp was found in all plants analyzed but not in bacteria or fungi (Table 3.2). The C-normalized Hyp yield was higher in vascular plants (10.4±2.7 s.d. nmol Hyp mg C^{-1}) than in *Sphagnum* (7.3±1.4 nmol Hyp mg C^{-1}). The highest Hyp yields (14.6 nmol mgC^{-1}) were found in *Abies balsamea* roots.

DAPA was found in four of the five bacteria analyzed but was not found in any other type of organism. The DAPA yield was 32 ±11 nmol mgC^{-1} in Gram negative bacteria (Table 2). The yield was higher in *Bacillus subtilis* (193 nmol mgC^{-1}), but DAPA was not found in *Micrococcus*, the other Gram positive bacterium analyzed. This is consistent with observations that the peptidoglycan layer is thicker in Gram positive than in Gram negative bacteria, but most Gram positive bacteria do not include DAPA in their peptidoglycan [*Schleifer and Kandler*, 1972].

3.3.2 Composition of peat cores

Patterns of C:N ratios varied significantly among the four cores. The average C:N ratio of the cores declined with increasing latitude, as SIB04 had the highest average C:N ratio (116) and E-113 had the lowest (56). The C:N ratios were generally high in SIB04 (100-150), but declined in the top 50 cm to a minimum of 45 (Fig. 3.1). The opposite trend was observed in SIB06, where C:N ratios were high near the surface (>275) but

declined to 60-120 below 50 cm depth. The samples at 26 and 29 cm depth had higher C:N ratios than any of the fresh vegetation analyzed. The G-137 core contained the narrowest range of C:N ratios; the ratio at the surface (69) increased rapidly to 109 at 2 cm and then generally declined with depth to a minimum of 53. The C:N ratio also generally declined with depth in core E-113, from a maximum of 113 at 17 cm to a minimum of 24 at the base of the core, the lowest ratio observed in the four cores (Fig. 3.1).

Amino acids accounted for a large fraction of the total N in all of the peats analyzed. This fraction was relatively constant in SIB04 and SIB06, generally ranging from 35-60% of the N with no apparent depth trend (Fig. 3.2). The two samples in SIB06 with C:N ratios >250 also had higher %N as THAA than the rest of the core. Amino acids constituted ~40% of the N at the surface in both northern cores, but this increased to >60% immediately below the surface layer. The THAA %N generally decreased with depth, reaching ~40% in the deepest samples analyzed in both cores. The THAA %N declined with depth in both northern cores, and the lower values in the northern cores were similar to typical values in the southern cores.

The PCA analysis identified two principle components (PC1 and PC2) that explained 25 and 19% of the variance of the amino acid composition, respectively. Among the individual amino acids, Hyp had the largest loading on PC1 (-0.45), indicating differences in mol % Hyp were the most significant drivers of variation in the peat AA composition (Fig. 3.3). Of the five AAs with loadings less than -0.2, four (Hyp, Lys, His, and Pro) are enriched in hydroxyproline-rich glycoproteins (HRGPs) relative to bulk plant N (Chapter 1). The five amino acids with significant negative loadings were all

polar amino acids, but Ser, Asp, and Thr are also polar amino acids and had positive loadings, indicating polarity did not control peat amino acid composition.

Hydroxyproline yields were significantly different between the northern and southern cores. Hyp yields were low throughout the SIB04 and SIB06 cores, falling within or slightly below the range of Hyp yields in *Sphagnum* and vascular plant source vegetation (6.1-14.6 nmol Hyp mg C^{-1}; Fig. 4). In contrast, Hyp yields in the northern cores were higher than those in source vegetation at most depths. The Hyp yield was within the range of vegetation yields in the top 12 cm of G-137 but increased below that depth to values higher than those measured in any plant tissue. The pattern in E-113 was similar, as the Hyp yield was relatively low near the surface but increased below 20 cm, reaching a maximum yield of 64 nmol Hyp mg C^{-1}, more than 4-fold higher than the most Hyp-rich source vegetation.

The acid/aldehyde (Ad/Al) ratios of lignin phenols, which indicate the extent of decomposition of vascular plant remains, followed the same general trends as the Hyp yields (Fig. 3.5). The Ad/Al ratio of vanillyl phenols was variable (0.1-0.7) near the peat surface in SIB04 and SIB06 cores, but was <0.5 below 50 cm in both cores (Fig. 3.5). In contrast, the Ad/Al ratios increased with depth to a maximal value of 0.9 at 37 cm in core G-137 and was >0.5 throughout core E-113. The Ad/Al ratios of vanillyl and syringyl phenols were strongly correlated (r^2=0.77, $p<0.0001$), and the ratio of syringyl phenols showed an even more pronounced difference between the northern and southern cores. The Ad/Al ratios were <0.4 throughout cores SIB04 and SIB06, but increased with depth in cores G-137 and E-113. The Ad/Al ratios of syringyl phenols reached maximal values of 0.6 in core G-137 and 0.8 in core E-113, the highest value in the four cores. The Ad/Al

ratios of the vanillyl and syringyl phenols were significantly correlated with the C-normalized Hyp yields (Fig. 3.6). The correlation was stronger between the Hyp yield and the Ad/Al ratios of syringyl phenols (r^2=0.664; p<0.001) than between Hyp and Ad/Al ratios of vanillyl phenols (r^2=0.485; p<0.001), but both relationships were statistically significant.

3.4. Discussion

3.4.1 Extent of peat decomposition

The C:N ratio of peat is often interpreted as an indicator of the extent of peat decomposition. This interpretation relies on the assumption that N is quantitatively recycled within the peatland, while C is lost as CO_2 during the remineralization of peat. The C:N ratio is therefore expected to decline with increasing C loss. This is supported by observations of low N concentrations in runoff from peatlands and low rates of gaseous N losses via denitrification [*Kuhry and Vitt*, 1996; *Malmer and Wallen*, 1993; 2004]. The C:N ratios are generally >100 below 50 cm in core SIB04 and <25 in the deepest layers of core E-113, with intermediate values in cores SIB06 and G-137. Based on C:N ratios, the extent of decomposition increases among the cores as follows: SIB04 < SIB06 = G-137 < E-113.

Several factors independent from microbial decomposition can affect the C:N ratios of peat, complicating its interpretation as a diagenetic indicator (see section 3.1). The cores analyzed in this study illustrate some these complications. Two samples in core SIB06 have C:N ratios >275, greater than those in fresh vegetation. This could indicate vertical transfer of N such as uptake by vascular plant roots, or preferential removal of N from the system via denitrification, runoff and volatilization. These processes challenge

the assumption of conservative N cycling in peatlands and complicate the interpretation of C:N ratios as diagenetic indices. Core SIB04 is unusual in that it has low C:N ratios near the surface and high ratios in the catotelm, the opposite of the trend in other peat profiles in which C:N ratios are highest at the surface and decline with depth in the acrotelm [*Kuhry and Vitt*, 1996; *Malmer and Wallen*, 2004]. Low C:N values near the surface of SIB04 coincide with a shift in the plant community from *Sphagnum* to vascular plant dominance (Chapter 2). This indicates vegetation change can have an effect on the peat C:N ratio as vascular plants are enriched in N compared to *Sphagnum* (Table 2.2). These effects illustrate the potential complications in interpreting C:N ratios as diagenetic indicators.

The %N as hydrolysable amino acids has also been used to estimate the extent of OM decomposition in other environments. In marine settings, it decreases along a continuum of increasing microbial alteration, from living phytoplankton, to sinking detritus, to sedimentary OM [*Cowie and Hedges*, 1992; 1994], and during microbial decomposition of DOM [*Amon et al.*, 2001]. A similar pattern appears to exist in mineral soils, as organic horizons typically have >70% N as amino acids [*Friedel and Scheller*, 2002; *Mikutta et al.*, 2010], and mineral horizons have <50% N as amino acids [*Christensen and Bechandersen*, 1989; *Friedel and Scheller*, 2002; *Schmidt et al.*, 2000; *Sowden et al.*, 1977]. This indicates amino acids are preferentially removed as plant litter is transformed into soil organic matter.

There does not appear to be selective removal of amino acids in the southern cores, which typically have 40-50 %N as amino acids throughout the cores. In the northern cores, the fraction of N as amino acids decreases from >70% near the surface to

about 40% at depth. This trend in the northern cores could be indicative of selective removal of amino acids with increasing decomposition, but this is complicated by the observation that the lowest %N as amino acids in the northern cores is within the range of typical values in the southern cores. This is likely due to the fact that the dominant sources of amino acids in the peats, plants and microbes, exhibit a broad range of values (36-71%) for the %N as amino acids. Yields of the bacterial biomarker DAPA typically vary between 50-150 nmol mg N^{-1}, a range similar to the yields in bacteria. This confirms that microbes and their remains constitute a significant portion of the peat N. However, microbes appear to use salvage pathways and resynthesize amino acids to conserve N, so the %N as amino acids remains relatively constant in peats during microbial decomposition.

The composition of amino acids also provides clues about the cycling of peat N. The PCA indicates the abundances of Hyp and other amino acids enriched in Hyp-rich glycoproteins (HRGPs) tended to covary, suggesting the selective preservation of HRGP molecules. Assuming each Hyp residue is associated with an intact HRGP molecule, the contribution of plant-derived HRGPs to peat amino acids (AA) can be calculated using the equation:

$$\%\,\mathrm{AA\,as\,HRGP} = 100 \times \frac{1}{\mathrm{THAA/C}} \times \sum\left(\mathrm{Hyp/C} \times \frac{\mathrm{Mol\%AA}_{HRGP}}{\mathrm{Mol\%Hyp}_{HRGP}} \right) \tag{3.2}$$

where THAA/C and Hyp/C are the yields of amino acids and Hyp in nmol mg C^{-1}, $\mathrm{Mol\%AA_{HRGP}}$ is the mol% of each individual amino acid in a typical HRGP, and $\mathrm{Mol\%Hyp_{HRGP}}$ is the mean mol% Hyp of a typical HRGP (Chapter 1). This calculation indicates HRGPs can account for 1% to 20% of the total amino acids in the peat cores.

Selective preservation of HRGPs appears to be an important driver of the peat amino acid composition.

Carbon-normalized Hyp yields are also useful proxies for C loss from plant tissues (Chapter 1). Evidence of the selective preservation of Hyp and HRGPs in the northern cores indicates these peats are extensively decomposed. Furthermore, the extent of diagenetic alteration of peat in the northern cores is greater than that in the southern cores, as indicated by the higher Hyp yields in the northern cores. A conservative estimate of C loss from the peat can be calculated using a starting Hyp yield of 9.3 nmol mgC^{-1} (the average yield measured in fresh vegetation) and assuming that Hyp is conserved according to the equation:

$$\%\text{C loss} = 100 - 100 \times \frac{\text{Hyp}_{Vegetation}}{\text{Hyp}_{Peat}} \tag{3.3}$$

where %C loss is the percentage of the original C that has been removed and $Hyp_{Vegetation}$ and Hyp_{Peat} are the C-normalized Hyp yields of fresh vegetation and the peat. This calculation indicates that C loss was >70% in G-137 (approximately 30 nmol Hyp mgC^{-1}) and >85% in E-113 (up to 64 nmol Hyp mgC^{-1}). These are conservative estimates of C loss because Hyp is lost during the decomposition of plant detritus (Chapter 1).

Acid/aldehyde (Ad/Al) ratios of lignin phenols support the conclusion that the northern cores are more extensively decomposed than the southern cores. Lignin phenols are specific to vascular plants [*Hedges and Mann*, 1979] and Ad/Al ratios increase with microbial decomposition of vascular plant material [*Hedges et al.*, 1988; *Opsahl and Benner*, 1995]. Lignin phenol Ad/Al ratios increase with depth in mineral soil profiles, reflecting increasing microbial decomposition of lignin [*Feng and Simpson*, 2007]. Increasing Ad/Al ratios of vanillyl and syringyl phenols with depth in the northern cores

indicate the extent of vascular plant decomposition increases with depth, but this evidence is lacking in the southern cores.

The lignin phenol Ad/Al ratios indicate the extent of vascular plant decomposition, whereas Hyp yields are indicative of C losses from all sources of vegetation in peatlands, including *Sphagnum*. The strong correlation between Ad/Al ratios of vanillyl and syringyl phenols indicates gymnosperm and angiosperm remains have experienced a similar extent of decomposition. In addition, the correlation between lignin phenol Ad/Al ratios and Hyp yields indicates the extent of decomposition of vascular plant tissue is generally representative of the extent of decomposition of bulk peat carbon. It appears the extent of decomposition of all plant types is controlled by similar environmental factors over timescales of centuries to millennia.

Hyp yields and lignin phenol Ad/Al ratios do not necessarily indicate that the southern cores are not significantly decomposed, only that they are less decomposed than the northern cores. The Ad/Al ratios of vanillyl phenols are consistently elevated above values in plants in the southern cores. Hyp is a minor component of fresh plant tissue and is concentrated with the loss of associated OM. The yields of recalcitrant biochemicals such as Hyp increase exponentially with decomposition, which is not apparent until an advanced stage of decomposition [*Hedges and Prahl,* 1993; Chapter 1].

Hyp yields, lignin phenol Ad/Al ratios, and C:N ratios all indicate cores SIB04 and E-113 are the least- and most-extensively decomposed, respectively. However, C:N ratios indicate SIB06 and G-137 have a similar extent of decomposition while Hyp and lignin phenol Ad/Al ratios indicate G-137 is more decomposed. The disparity is likely due to factors other than decomposition that can affect the C:N ratio, as discussed above. This

demonstrates the value of using multiple independent indicators to reveal differences in extent of decomposition.

3.4.2 Controls on the extent of peat decomposition

The integrative nature of the biochemical degradation indices used herein enables the testing of competing hypotheses regarding the key factors governing the extent of peat decomposition. Experimental evidence suggests that temperature, vegetation type, and oxygen availability can all have a significant influence on rates of peat decomposition. We evaluate the importance of each below in light of our findings that the northern cores were more extensively decomposed than the southern cores.

Temperature is hypothesized to be a major control on peat decomposition due to stimulation of microbial activity [*Lafleur et al.*, 2005; *Dorrepaal et al.*, 2009]. This is supported by laboratory and field experiments that show increased mass loss of peat and respiration at elevated temperatures [*Clymo*, 1965; *Updegraff et al.*, 2001; *Lafleur et al.*, 2005]. However, this study shows that temperature is not the dominant variable in determining the extent of peat decomposition. The mean annual air temperature at the southern sites is 4-7°C warmer than those at the northern sites, yet the northern cores were more extensively decomposed than the southern cores despite being of similar age. This is the opposite pattern from that expected if temperature was the dominant control on the extent of peat decomposition.

Changes in the composition of the plant community can also affect decomposition of the peats. *Sphagnum* is consistently more resistant to decomposition than vascular plants when incubated under equivalent conditions [*Hobbie*, 1996; *Scheffer et al.*, 2001; *Moore et al.*, 2007], suggesting that vascular plant-dominated peat should be more

extensively decomposed than *Sphagnum*-dominated peat. This does not appear to be the case in the peat cores analyzed here. Vegetation in cores SIB04 and SIB06 was generally *Sphagnum*-dominated, but periodic shifts to vascular plant dominance were evident (Chapter 2). Vascular plants accounted for over half of the peat C during these periods, but the Hyp yields and lignin phenol Ad/Al ratios indicated they were not more decomposed than *Sphagnum*-dominated peat layers. *Sphagnum* remains generally accounted for >50% of the C in the northern cores, yet they were more extensively decomposed than any vascular plant-dominated layers in the southern cores. This indicates that despite differences between the rates of decomposition of mosses and vascular plant litter, vegetation composition is not the primary control on the extent of decomposition of these peats.

We developed the oxygen exposure time hypothesis as a third explanation for the observed trends in peat decomposition. The free energy yield of organic matter oxidation is greatest when oxygen is used as the terminal electron acceptor. Other oxidized ions that can be used as terminal electron acceptors (e.g. NO^{3-}, Fe^{3+}, SO_4^{2-}) have limited availability in peatlands, so the thermodynamic favorability of C remineralization declines rapidly below the water table [*Shotyk,* 1988]. Consequently, the rate of peat decomposition is an order of magnitude higher under aerobic conditions [*Belyea*, 1996; *Clymo*, 1965]. Lowering of the water table and expansion of the acrotelm consistently results in higher rates of C loss, at least in the short term [*Laiho*, 2006]. Therefore, some models recognize acrotelm residence time as an important control on peat accumulation [*Clymo*, 1984; *Belyea and Clymo*, 2001; *Belyea and Malmer*, 2004].

Many factors that influence decomposition vary between the acrotelm and catotelm. Peat bulk density increases and hydrological conductivity decreases in the catotelm. Lack of water transport can result in the accumulation of CO_2 and CH_4 in catotelm porewaters, further reducing the energy yield of C remineralization [*Beer and Blodau*, 2007; *Beer et al.*, 2008]. Higher water and solute mobility in the acrotelm could also enhance microbial nutrient availability in the acrotelm. In addition, oscillating redox conditions like those found in the acrotelm can result in more rapid decomposition than aerobic conditions alone [*Aller*, 1994; *Hulthe et al*., 1998]. These factors contribute to the observed differences in C remineralization rates between the acrotelm and catotelm, but the large difference in energy yield between aerobic C oxidation and methanogenesis is likely the primary driver.

We therefore propose oxygen exposure time as the primary control of organic matter decomposition in peatlands. This concept is similar to acrotelm residence time, but has a direct mechanistic link to decomposition. In addition, oxygen availability is not restricted to the acrotelm because vascular plants transport oxygen to their roots, which can extend into the catotelm [*Anderson and Beckett*, 1987]. Oxygen exposure time therefore avoids the inflexibility of the acrotelm/catotelm model, which indicates a discrete boundary (the drought water table level) separates zones of fast and slow decomposition [*Morris et al*., 2011]. Oxygen exposure time is also proposed to control the extent of decomposition of marine sedimentary organic matter [*Hartnett et al.*, 1998; *Hedges et al*., 1999]. Oxygen exposure time could have a greater influence on decomposition in peatlands than in marine sediments due to the more limited availability of alternative terminal electron acceptors in peats.

Oxygen exposure time is primarily controlled by the depth of the water table and rate of peat accumulation. More rapid accumulation results in faster burial beneath the water table, where oxygen availability is lower. Oxygen exposure time is likely higher in vascular plant-dominated peats due to oxygen transport in roots below the water table. Peats with lower accumulation rates and lower water tables are expected to be more extensively decomposed due to longer oxygen exposure times (Fig. 3.7).

The observed differences in decomposition between the northern and southern cores support the oxygen exposure time hypothesis. The vertical growth rate is several times higher in the southern cores, so peat is more rapidly buried and entrained into the catotelm at these sites. In addition, the northern cores are affected by permafrost [*Smith et al.*, 2012], which causes cryogenic heaving and uplift of the soil relative to the water table [*Robinson and Moore,* 2000]. This further increases oxygen exposure time by causing a deeper water table than in the non-permafrost southern cores. Accordingly, the water content of northern cores is lower than in the southern cores [*Smith et al.*, 2012]. The northern cores had higher hydroxyproline yields and lignin phenol acid:aldehyde ratios than the southern cores, indicating more extensive decomposition and supporting the oxygen exposure time hypothesis. Oxygen exposure time was therefore a better predictor of the extent of decomposition than temperature or plant composition, which have received considerable attention in assessing the future of carbon storage in peatlands.

Oxygen exposure time is changing as a function of plant growth and hydrology, which will influence future trends in peat C loss or accumulation. Warmer temperatures will likely lead to higher plant production. Other things being equal, this will reduce

oxygen exposure time by accelerating burial below the water table, and will ultimately increase peatland C sequestration. However, if peat accumulation outpaces water storage, the water table will decline, promoting decomposition. Changes in water storage will likely vary regionally due to changing patterns of precipitation and evaporation. This interaction between plant growth and hydrology will ultimately determine the future of peatland C storage and its feedback on climate change.

Table 3.1 Locations, mean annual air temperatures, and accumulation rates of the four peat cores.

Core	Latitude	Longitude	Mean annual air temperature (°C)[a]	Vertical growth rate (mm yr^{-1})[b]	C-accumulation rate (gC m^{-2} yr^{-1})[b,c]	N-accumulation rate (gN m^{-2} yr^{-1})[b]
SIB4	56°48'14"N	78°44'13"E	-1.8	1.36	44	0.41
SIB6	58°26'09"N	83°26'03"E	-1.1	0.92	28	0.31
G137	63°45'01"N	75°45'58"E	-5.3	0.15	10	0.13
E113	66°26'59"N	79°19'24"E	-8.0	0.28	15	0.37

[a]Average 1930-2000; Matsuura and Willmott, data set, 2004; available at http://climate.geog.udel.edu/~climate/html_pages/archive.html
[b]Since 2000 years bp
[c]Beilman et al., 2009

Table 3.2 C:N ratio and amino acid and biomarker yields in peat-forming vegetation, bacteria, and fungi.

Sample	n	C:N (molar)	THAA %C	THAA %N	Hyp (nmol/mgC)	DAPA (nmol/mgC)
Mosses[a]						
Sphagnum fuscum	6	110	2.5	69	8.8	nd
Spagnum magellanicum	4	170	1.8	71	7.2	nd
Sphagnum angustifolium	2	79	2.8	54	6.1	nd
Vascular Plants						
Carex leaves	1	61	3.5	50	7.8	nd
Eriophorum leaves	1	32	7.7	57	10.1	nd
Ledum leaves	1	50	5.3	61	11.3	nd
Abies balsamea needle litter	3	55	5.2	66	8.3	nd
Abies balsamea roots	3	48	3.4	40	14.6	nd
Bacteria						
Gram negative						
Pseudomonus fluorescens	1	4.1	48	47	nd	39
Azobacter vinelandii	1	3.8	64	58	nd	19
Aerobacter sp.	1	3.7	56	49	nd	37
Gram positive						
Bacillus subtilis	1	4.5	57	61	nd	193
Micrococcus sp.	1	4.7	57	67	nd	nd
Fungi						
Cortinarius armillatus stems	1	21	7.3	36	nd	nd
Cortinarius armillatus caps	1	14	19	63	nd	nd
Albatrellus ovinus (whole)	1	21	8.8	43	nd	nd
Clitocybe sp. (whole)	1	12	17	48	nd	nd
Russula paludosa stem	1	24	9.5	53	nd	nd
Russula paludosa cap	1	11	14.0	38	nd	nd

[a]Fields samples with capitula removed

nd, not detected

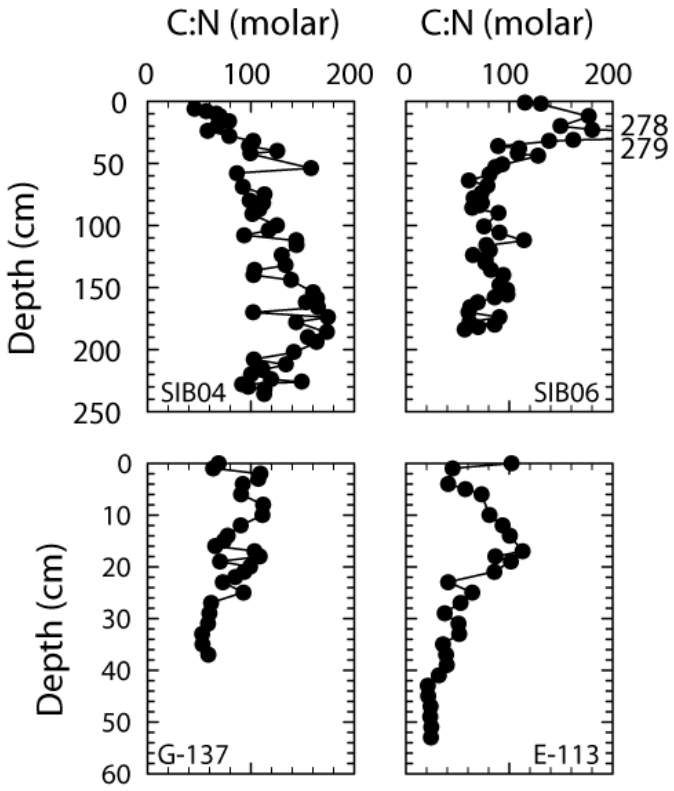

Figure 3.1 Peat C:N ratios in the four cores.

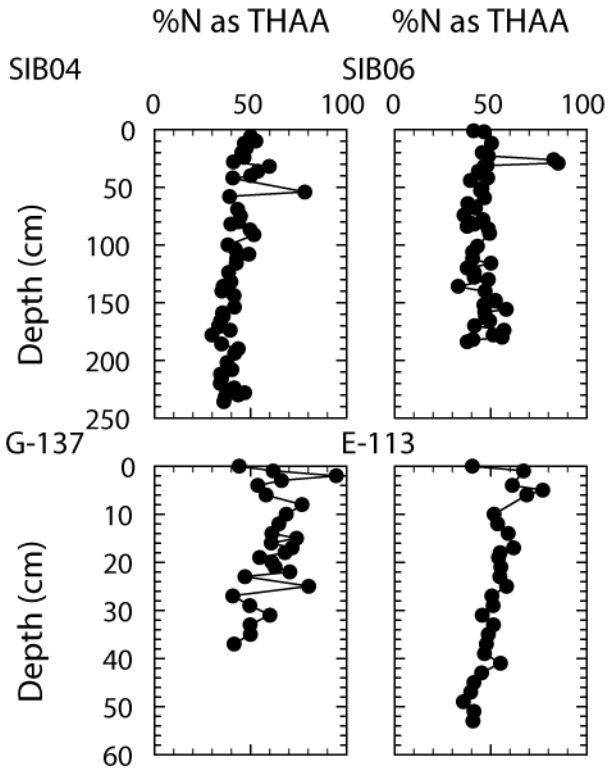

Figure 3.2 Percentage of total peat N accounted for by total hydrolysable amino acids in the four cores.

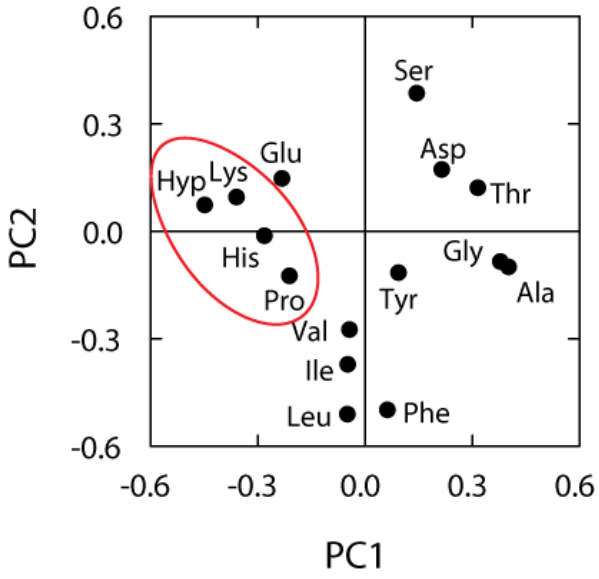

Figure 3.3 Loadings of amino acids on PC1 and PC2. Circled amino acids are enriched in hydroxyproline-rich glycoproteins (HRGPs) compared to bulk amino acids (Chapter 1).

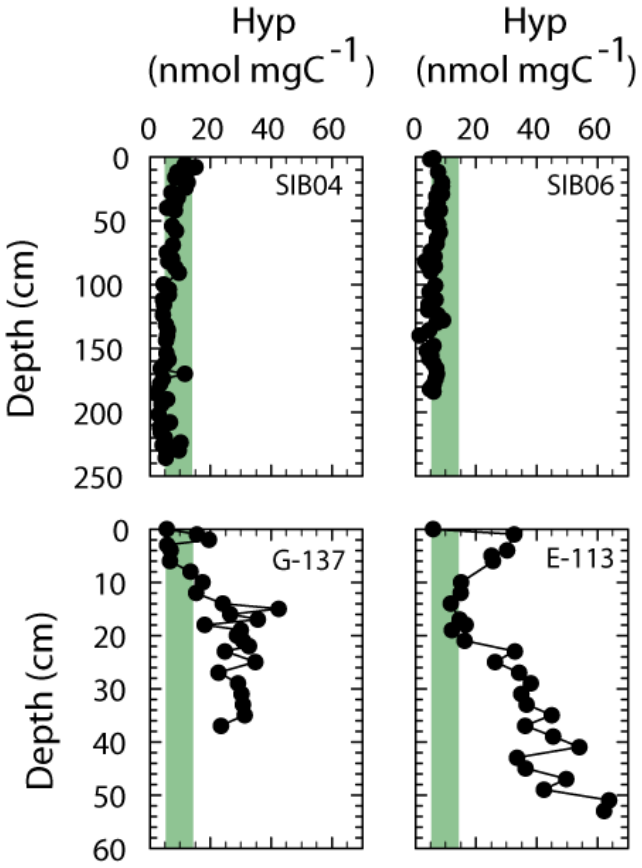

Figure 3.4 Hydroxyproline (Hyp) yields in the four cores. The shaded area represents the range of Hyp yields in fresh vegetation (6.1–14.6 nmol mg C^{-1}).

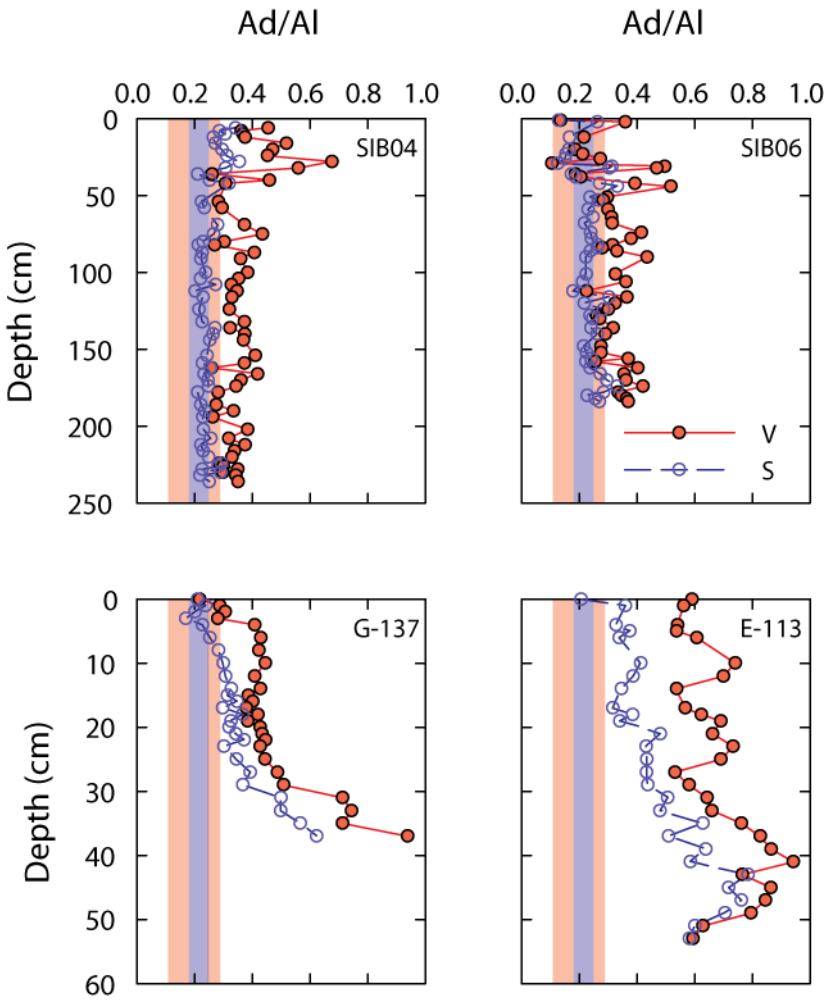

Figure 3.5 Profile of acid/aldehyde ratios of vanillyl (V) phenols (solid red symbols) and syringyl (S) phenols (open blue symbols) in the four cores. The red and blue shaded areas represent the range of Ad/Al ratios of vanillyl and syringyl phenols, respectively, in fresh vegetation (average ± 1 standard deviation).

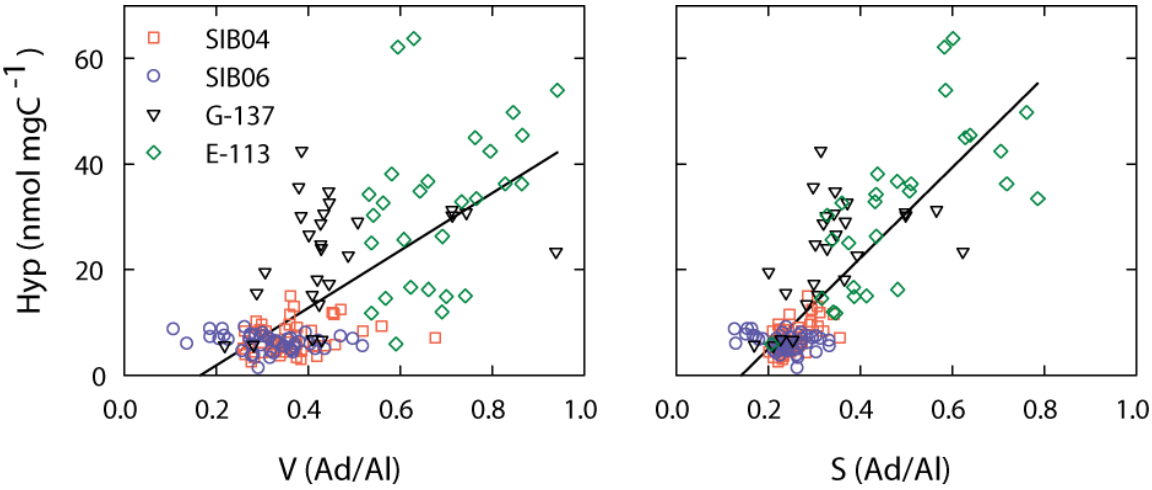

Figure 3.6 Correlation between C-normalized hydroxyproline yields and acid/aldehyde ratios of (a) vanillyl phenols and (b) syringyl phenols.

CHAPTER 4

TEMPERATURE AND OXYGEN CONTROLS ON DECOMPOSITION IN A JAMES BAY PEATLAND[4]

4.1. Introduction

Boreal peatlands are important sinks for atmospheric carbon dioxide and currently contain ~550 Pg C due to an imbalance between net primary production and organic matter decomposition [*Yu et al.*, 2010]. Organic matter storage in peatlands is several times higher than in other ecosystems despite lower rates of primary production, indicating net accumulation is primarily due to limited decomposition [*Schlesinger and Bernhardt*, 2013; *Thormann et al.*, 1999]. Decomposition is likely incomplete due to a variety of factors including low temperatures [*Lafleur et al.*, 2005], restricted oxygen exposure [Chapter 3; *Belyea and Clymo*, 2001], and the poor litter quality of *Sphagnum*, the dominant moss in many peatland plant communities [*Hobbie*, 1996; *Moore et al.*, 2007]. However, the relative importance of these factors remains poorly understood. The lack of a mechanistic understanding of peat decomposition reduces our ability to predict the responses of peatland carbon reservoirs to future changes in temperature, growing season, and precipitation.

The duration of peat exposure to oxygen (oxygen exposure time) has been proposed as an important control on the extent of peat decomposition (Chapter 3).

[4] Philben, M., Holmquist, J., MacDonald, G., Duan, D., Kaiser, K., and Benner, R. (submitted), Temperature and oxygen controls on decomposition in a James Bay peatland, *Global Biogeochemical Cycles*.

Decomposition is rapid in the oxic surface layer and peat decomposition models indicate litter loses 80-90% of its initial mass before burial beneath the water table [*Clymo*, 1992]. Oxygen is rapidly depleted below the water table by heterotrophic respiration. The remineralization of organic carbon to carbon dioxide is much less thermodynamically favorable in the absence of oxygen, and decomposition is slower under anaerobic conditions by an order of magnitude or more [*Belyea*, 1996; *Benner et al.*, 1984; *Clymo*, 1965]. Oxygen exposure time is mainly a function of water table depth and peat accumulation rate, as drier conditions and lower accumulation rates result in slower burial beneath the oxic layer.

A recent study comparing the extent of peat decomposition along a latitudinal transect in the West Siberian Lowland (WSL), Russia found that differences in oxygen exposure time were more important in determining the extent of decomposition than temperature or vegetation change (Chapter 3). Peat cores collected from the northern WSL were formed under cooler conditions, with mean annual temperatures as much as 7°C lower than in the south. In contrast, oxygen exposure time was longer in the north, as peat was buried beneath the water table less rapidly. The northern cores were more extensively decomposed, indicating oxygen exposure time was more important than temperature in determining the extent of decomposition.

However, the variability of environmental conditions between the northern and southern WSL cores was likely greater than those driven by climatic change. Accumulation rates were as much as five-fold higher in the south, presumably resulting in similar differences in oxygen exposure time. Climate-driven changes in the water table depth will likely be significant but less dramatic. The temperature difference of 7°C

between the sites is similar to the upper extreme of the 3-7°C estimate for warming in the subarctic region by 2100 [*IPCC*, 2013]. It is possible that temperature is more important to peat decomposition over naturally occurring ranges of environmental conditions.

The goal of this study is to test the oxygen exposure time hypothesis by examining temporal variability in the extent of peat decomposition in a core from James Bay, Canada. The core represents over 7000 years of peat accumulation [*Holmquist et al.*, 2014], providing an opportunity to evaluate peatland responses to natural climate change. . Elevated summer insolation associated with the Holocene Thermal Maximum (HTM) increased temperatures across the western Arctic by an average of 1-2 above the 20th century average between about 10000 and 5000 yr B.P [*Kaufman et al*., 2004]. 120 of 140 sites analyzed showed qualitative evidence of increased temperature during this period, although the few records collected from the vicinity of James Bay Lowlands have been equivocal [*Bunbury et al*., 2012; *O'Reilly et al*., 2014]. In addition, the Medieval Climate Anomaly produced a temperature anomaly of about 2°C across northern Canada between 1000 and 700 yr B.P., including the James Bay Lowland [*Viau and Gajewski*, 2009; *Bunbury et al*., 2012]. The ~2°C temperature anomalies experienced during both of these events is analogous to the projected warming over the next 20 years [*IPCC*, 2013]. This enables the estimation of the temperature sensitivity of peat decomposition in a natural system without experimental manipulation.

The historical variability of oxygen exposure time can be estimated using the testate amoebae record. Each species of amoebae inhabits a characteristic range of moisture conditions [*Charman and Warner*, 1992]. The testate amoebae community can therefore yield a reconstruction of the water table level at the site during peat formation

[*Booth*, 2002; *Woodland et al.*, 1998]. Calibration with modern analogues has resulted in a quantitative transfer function specific to eastern North America and a better understanding of the uncertainty associated with this approach [*Booth*, 2008]. Oxygen is rapidly depleted below the water table, making the water table reconstruction a useful proxy for past changes in oxygen exposure time.

We used the biochemical composition of peat as an integrative indicator of its extent of decomposition. The major classes of biological macromolecules are degraded at varying rates, and their carbon-normalized yields can reveal the extent of organic matter decomposition. Hydrolysable neutral sugars are initially abundant in plant litter, primarily in cellulose and hemicellulose, but are among its most labile components and are removed rapidly [*Opsahl and Benner*, 1999]. Hydrolysable amino acids, in contrast, are enriched in microbes compared to plant litter, and their yields generally increase with decomposition [*Hobara et al.*, 2014; *Tremblay and Benner*, 2006]. Hydroxyproline, an amino acid found in all plants but not in microbes, is generally less reactive than bulk plant carbon and its yield tends to increase with decomposition (Chapter 1). The ratio of the acid and aldehyde monomers of vanillyl and syringyl phenols is also low in plant material but increases with decomposition [*Hedges et al.*, 1988; *Opsahl and Benner*, 1995]. While these indicators are often effective over various stages of decomposition, using multiple independent diagenetic indicators can increase confidence and improve understanding of the mechanics of individual indicators. We hypothesize that these indicators will show more extensive decomposition in the sections of the core with longer oxygen exposure time.

4.2. Materials and methods

4.2.1 Study site and collection

This study uses a peat core selected from a network of eight cores collected in 2008 along a latitudinal transect in the Ontario James Bay Lowland, Canada [*Holmquist and MacDonald*, 2014; *Holmquist et al.*, 2014]. The JBL7 core (54°23'43"N, 89°31'20"W) was collected from an ombrotrophic, permafrost-free *Sphagnum* bog using a Russian auger. The core was covered in plastic wrap and aluminum foil and frozen upon return to the laboratory. Subsamples (1 cm) were collected using a bandsaw [*Holmquist et al.*, 2014]. An age-depth model for the core was constructed using ^{14}C dating and the Bayesian "Bacon" model [*Blaauw and Christen*, 2011]. JBL7 had a basal age of 7731 cal yr B.P. and had an apparent long-term carbon accumulation rate of 16.7 g C m^{-2} yr^{-1} [*Holmquist et al.*, 2014]. Subsamples were dried in a Savant Speedvac vacuum centrifuge and ground in a Wiley mill for chemical analysis.

Samples of surface vegetation were collected from James Bay and were supplemented by samples from Toolik Lake, Alaska, and Codroy Valley, NL, Canada. These samples were analyzed to identify the chemical signatures of fresh plant inputs to the peat. Their chemical compositions are reported elsewhere (Chapters 2 and 3) and summarized herein (Table 4.1).

4.2.2 Chemical analyses

Carbon and nitrogen content were determined using a Costech ECS 4010 elemental analyzer after combustion at 980°C. The mean % deviation was ±0.7% for carbon and ±3% for nitrogen. Hydrolysable neutral sugars were analyzed according to Skoog and Benner [1997] with some modifications. Samples (~5 mg dry weight) were

placed in 2 mL glass ampules and immersed in 12 mol L^{-1} sulfuric acid for two hours at room temperature. Ampules were then flame-sealed after the addition of 1.8 mL deionized water and immersed in a water bath at 100°C for 3 hours. The hydrolysis was terminated in an ice bath. Ampules were cracked open and deoxyribose was added as an internal standard. About 400 μL of hydrolysate were neutralized with 2 mL self-absorbed ion retardation resin (Biorad AG11 A8) [*Kaiser and Benner*, 2000]. The sample was then deionized using a mixture of cation and anion exchange resins (Biorad AG50 and AG2).

Neutral sugars were separated isocratically using 25 mmol L^{-1} NaOH on a PA1 column in a Dionex 500 system with a pulsed amperiometric detector. Detector settings were based on Skoog and Benner [1997]. The seven neutral sugars measured were fucose, rhamnose, arabinose, galactose, glucose, mannose, and xylose. The analytical precision of duplicate analyses performed on different days was ±2% for glucose and ±4% for other sugars.

Samples for hydrolysable amino acid analysis were added to glass ampules with 1 mL of 6 mol L^{-1} hydrochloric acid. The ampules were flame sealed and heated to 110°C for 20 hours. The ampules were opened after hydrolysis and aliquots were dried under a stream of N_2 gas. Samples were redissolved in deionized water and norvaline was added as an internal standard.

Amino acids were purified by solid phase extraction and derivatized with propyl chloroformate using the commercially available EZ:Faast kit for amino acid profiling (Phenomenex, USA). Derivatized samples were separated and quantified using gas chromatography (Phenomenex ZB-AAA column; 110–320°C at 30° min^{-1}) with flame ionization detection. The 16 quantified amino acids were alanine, glycine, valine, leucine,

isoleucine, threonine, serine, proline, aspartic acid, hydroxyproline, glutamic acid, phenylalanine, lysine, histidine, tyrosine, and diaminopimelic acid.

Lignin phenols were analyzed by gas chromatography/mass spectrometry following CuO oxidation [*Kaiser and Benner*, 2012]. Samples (8-10 mg) were mixed with 330 mg CuO, 106 mg of $Fe(NH_4)_2(SO_4)_2 \cdot 6H_2O$, and 2.5mL of 2 mol L^{-1} NaOH in Monel reaction vessels. Vessels were kept in argon-filled containers to exclude molecular oxygen. A mixture of transcinnamic acid and ethyl-vanillin was added as internal standards after oxidation. Samples were purified by solid-phase extraction using Oasis HLB cartridges and were dried under a stream of argon. Samples were then redissolved in 200 µL dry pyridine and stored frozen until analysis.

Phenols were quantified using an Agilent 7890 gas chromatography system with an Agilent 5975C triple axis mass detector with electron impact ionization. Samples were derivatized with BSTFA/TMCS reagent at 75°C for 15 minutes prior to analysis. Mass spectrometer settings are described in detail by Kaiser and Benner [2012]. Analyzed phenols included p-hydroxy (P) phenols (p-hydroxybenzaldehyde, p-hydroxyacetophenone, and p-hydroxybenzoic acid), vanillyl (V) phenols (vanillin, acetovanillone, and vanillic acid), syringyl (S) phenols (syringaldehyde, acetosyringone, and syringic acid), cinnamyl (C) phenols (coumaric acid and ferulic acid), and 3,5-dihydroxy-benzoic acid. The analytical precision of duplicate analysis was ±4%.

4.2.3 Vegetation reconstruction

The plant community at JBL7 was reconstructed using the carbohydrate composition and the lignin phenol yield of the peat. The carbohydrate approach exploited

differences in carbohydrate composition between vascular plants and *Sphagnum* to calculate a carbohydrate *Sphagnum* index using the molar ratio of sugars:

$$\text{Carbohydrate } Sphagnum \text{ index} = \frac{\text{Rhamnose}}{\text{Mannose+Xylose}} \quad (4.1)$$

This index was converted to a quantitative estimate of the *Sphagnum* contribution to total peat carbon using the equation:

$$f\text{Sphagnum} = 2.6998(SI_{Carb})^3 - 4.5889(SI_{Carb})^2 + 4.3775(SI_{Carb}) - 0.2161 \quad (4.2)$$

where SI_{Carb} is the carbohydrate *Sphagnum* index and *f*Sphagnum is the fractional contribution of *Sphagnum* to the peat carbon (Chapter 2). The vascular plant contribution was calculated by difference.

Lignin phenols were used as an independent estimate of the paleovegetation according to the equation:

$$f\text{Vascular} = \frac{VPI_{Phenol}}{220} \quad (4.3)$$

where *f*Vascular is the fraction of carbon from vascular plants, VPI_{Phenol} is the phenol vascular plant index (nmol V+S phenols mg C^{-1}) and 220 is the average VPI_{Phenol} in fresh vascular plants (Chapter 2). The *Sphagnum* contribution was calculated by difference.

4.2.4 Water table reconstruction

The water table was reconstructed by testate amoebae analysis using a method modified from Charman [2001] and Booth [2008]. Peat samples were boiled gently and spiked with a known number of exotic *Lycopodium* spores to aid quantification. Testate amoebae were separated from the peat by filtering through a 250 um filter and reverse-filtering through a 7 um filter. Samples were centrifuged and mixed with Saffron dye and glycerol as a preservative. Tests were counted under a compound microscope with 400x magnification and identified according to Charman [2000] as modified by Booth [2008]. At least 150 tests were counted for samples with >6000 tests cm^{-3} and 50 tests were counted for other samples [*Payne and Mitchell*, 2009]. Water table depth was calculated, omitting the problematic taxa *Difflugia pristis* type, and using weighted-average transfer function developed from 776 North American surface samples [*Booth*, 2008; *Markel et al*. 2010]. Stratigraphic plots, additional methodological data, and a list of taxa recorded are available in Holmquist [2013].

4.3. Results

4.3.1. Chemical composition of peat-forming vegetation

Approximately 40% of the total carbon in fresh vegetation was characterized as hydrolysable neutral sugars, amino acids, and lignin phenols (±2% for *Sphagnum* and ±11% for vascular plants). Vascular plants had slightly higher carbon (C) content (45.9±4.8 standard deviation wt. %C) and substantially higher nitrogen (N) content (1.15±0.35 wt. %N) than *Sphagnum* mosses (40.5±1.4 and 0.43±0.15 wt. %, respectively; Table 4.1). *Sphagnum* therefore had a much higher C:N ratio than vascular plants (119±43 vs. 50±13). The N content of all vegetation was strongly correlated with the

amino acid yield (r^2=0.99), so the percentage of C as amino acids in vascular plants (5.43±1.7 %C as amino acids) was also approximately double that of *Sphagnum* (2.37±0.51 %C as amino acids). Hydroxyproline yields were slightly higher on average in vascular plants than in *Sphagnum* (9.4±1.6 vs. 7.3±1.4 nmol Hyp mg C^{-1}). Neutral sugar yields were similar in both plant types, but were more variable in vascular plants (31.2±9.4 %C as neutral sugars) than in *Sphagnum* (35.6±2.1 %C as neutral sugars).

4.3.2 Environmental history of JBL7

The paleovegetation reconstruction based on lignin phenols consistently indicated a greater contribution of vascular plant material than the reconstruction based on carbohydrates. The carbohydrate method indicated a larger vascular plant contribution in only five of the 70 peat samples analyzed. Although the two methods indicated differing magnitudes of vegetation change, they showed consistent patterns. From the surface to 150 cm depth, both methods indicated the plant community was >50% *Sphagnum*, except at 31 cm and 84-86 cm depths, where the phenol method indicated greater vascular plant inputs (Fig. 4.1). Both methods indicated a sustained shift to vascular plant dominance between 150 and 250 cm depth, where the phenol method indicated 16 of the 21 samples were >50% vascular plant C. The carbohydrate method indicated a smaller vascular plant contribution in this zone but a distinct transition was still apparent, as 15 of the 21 samples had >20% vascular plant C, compared to a baseline of about 0-10% above 150 cm. This period of vascular plant dominance lasted approximately 2140 years (4730-2590 cal. yr. B.P.) according to the calibrated radiocarbon age model [*Holmquist et al.*, 2014]. The plant community was more variable below 250 cm and appeared to be mostly *Sphagnum* except for vascular plant invasions at 259, 303, 315, and 327 cm.

The testate amoebae-derived water table record indicated conditions were relatively wet (water table close to the peat surface) above 150 cm depth (Fig. 4.2), although a trend toward drier conditions over the last two centuries was also visible. The water table was generally lower below 150 cm, indicating drier conditions during peat formation, including the driest conditions in the core at 172 cm depth (36±8 cm water table depth). The average water table depth below 150 cm was 17 cm, compared to 13 cm above 150 cm. Like the vegetation record, the water table reconstruction indicated rapid change near 150 cm depth. However, the generally drier conditions persisted to the base of the core, unlike the vascular plant vegetation which was mostly confined to the 150-250 cm interval.

4.3.3. Chemical composition of JBL7 peat

The C content of the peat varied between 39 and 51 wt. % C through most of the core. The deepest samples had lower C content (as little as 32%), likely due to dilution by the underlying mineral soil during the initial establishment of the peatland on the mineral surface. The N content was much more variable than the C content, with a nearly seven-fold difference between the highest and lowest N concentrations (2.0 and 0.3 wt. % N, respectively; Fig. 4.3). The N content was highest in the vascular plant-dominated zone between 150 and 250 cm depth. Samples at 183 and 215-227 cm were particularly enriched in N (>1.5 Wt. %N). N content decreased beneath this zone and was <1.1 between 250 cm and the bottom of the core. The C:N ratio primarily reflected changes in N because the C content was relatively constant. The C:N ratio was highest in the upper 50 cm (>90) and generally declined with depth. The lowest values were found between 150-250 cm, with C:N ratios as low as 28 (Fig. 4.3).

The analyzed biochemicals accounted for 29±6% of the peat C in the core. The percentage of C accounted for by neutral sugars (%C as NS) was highest in the upper 50 cm, where the yield in the peat was within the range of yields found in fresh plant material (Fig. 4.4). The sugar yield declined with depth but was lowest in the zone 150-250 cm (16±4 %C as NS). The yield was higher below 250 cm (22±3 %C as NS), but was still lower than in fresh plant material.

Differences in botanical composition could influence the sugar yield independent of decomposition because vascular plants had a lower average and wider range of neutral sugar yields (Table 4.1). An "expected" range of neutral sugar yields was calculated for each sample based on its reconstructed plant composition to correct for variable neutral sugar yields in vegetation. The expected sugar yield was calculated using the formula:

$$\text{Expected yield} = \left(\frac{\%\text{Vascular}}{100}\right)(\%\text{C as NS})_{\text{Vascular}} + \left(\frac{\%\textit{Sphagnum}}{100}\right)(\%\text{C as NS})_{\textit{Sphagnum}} \quad (4.4)$$

where "%Vascular" and %*Sphagnum*" are the vascular plant and *Sphagnum* contents, respectively, based on an average of the carbohydrate and phenol reconstructions. $(\%\text{C as NS})_{\textit{Sphagnum}}$ and $(\%\text{C as NS})_{\text{Vascular}}$ refer to the neutral sugar yields of fresh *Sphagnum* and vascular plant tissues, respectively. A range of expected yields was generated by performing the calculation with the highest and lowest sugar yield found in each plant type.

The "Sugar degradation index" was calculated as the ratio of the expected sugar yield to the observed yield. The index was calculated using the minimum and maximum expected yields to generate a range of depletion factors for each sample, and the average

of these two values was reported. The sugar degradation index was <1.2 in the upper 50 cm of the core, indicating the peat had similar neutral sugar yields compared to fresh vegetation (Fig. 4.4). The index was highest between 150-250 cm (on average 2.2±0.5), reaching a maximum value of 3.1 at 183 cm, the sample which also had the lowest C:N ratio. The index was lower below 250 cm (<2.0) but remained above 1. The sugar degradation index was strongly correlated with the N:C ratio ($n=70$; $r^2=0.71$, $p<0.001$; Fig.4.5), as samples between 150 and 250 cm generally had higher N:C ratios and degradation indices than samples above or below.

The amino acid yield (%C as amino acids) followed a trend similar to the N content and the sugar degradation index (Fig. 4.6). The yield was lowest near the surface (1.9-2.3 in the upper 50 cm) and was highest between 150 and 250 cm (3.8±1.0 %C as amino acids). Like the other indicators, the amino acid yield was highest at 183 and 219 cm, with values of 5.4 and 5.8 %C as amino acids, respectively. However, the amino acid yield was also relatively high at 64 cm (5.2 % C as amino acids) unlike the N content or the sugar degradation index. Overall, the amino acid yield was strongly correlated with the total nitrogen content ($n=70$; $r^2=0.82$; $p<0.001$; Fig. 7). The slope of the best-fit line (0.34) indicated that on average, amino acids accounted for 34% of the total nitrogen and the strong correlation indicates this ratio was relatively constant throughout the core.

Yields of hydroxyproline (Hyp) generally followed the patterns of the other indicators, with some differences. Yields in the upper 50 cm were low and within the range of fresh vegetation, while yields were highest between 150 and 250 cm (Fig. 4.7). The highest yield in the core was 49 nmol Hyp mg C^{-1}, more than double the highest yield found in fresh plant material. However, the pattern of peaks in the Hyp yield was

somewhat different than peaks in the other indicators. The local maximum at 183 cm co-occurred with maxima in the sugar degradation index and nitrogen content, but the peak in Hyp yield at 155 cm was not reflected in the other indicators. The peak at 64 cm was also found in the N content but not the sugar degradation index. In addition, Hyp yields below 250 cm were generally in the same range as fresh plant material and similar to peat near the surface, while the N content and sugar degradation index were elevated compared to the surface.

The C:N ratio, sugar degradation index, and hydroxyproline yield indicated the extent of bulk peat decomposition, whereas acid:aldehyde (Ad/Al) ratios of lignin phenols were used to assess the degree of oxidation of vascular plant detritus. The Ad/Al ratios of both vanillyl and syringyl phenols were low (<0.4) throughout the core. The ratio of vanillyl phenols did not match the pattern of the other degradation indices. The ratio was higher and more variable near the surface, with the highest ratio found at 38 cm, but the total yield of vanillyl phenols was low in this interval due to the *Sphagnum*-dominated plant community, so the ratio was likely sensitive to minor variations in plant composition. Unlike the other indicators, the Ad/Al ratio of vanillyl phenols was not elevated between 150 and 250 cm. The Ad/Al ratio of syringyl phenols was more similar to the patterns of other indices. The syringyl phenol Ad/Al ratio was elevated in the 150-250 cm zone and was higher than values above or below, with the exception of a single sample at 31 cm.

4.4. Discussion

4.4.1. Environmental history and oxygen exposure time

The lignin phenol method for paleovegetation reconstruction consistently indicated a greater contribution of vascular plants to the peat than the carbohydrate method. The differences were relatively minor near the peat surface but were greatest in the highly decomposed interval between 150 and 250 cm, where the phenol method often indicated 100% of the C was from vascular plants compared to <50% using the carbohydrate method. The lignin phenol method overestimated the vascular plant abundance in this interval, as both *Sphagnum* and vascular plant macrofossils were present [*Holmquist and MacDonald*, 2014]. This supports the assessment in Chapter 2 that the lignin phenol method likely overestimates the vascular plant contribution in extensively decomposed peats because lignin is more resistant to biodegradation than bulk plant C, especially under anaerobic conditions [*Benner et al.*, 1984]. The carbohydrate method, in contrast, likely overestimates the *Sphagnum* contribution due to relatively higher microbial production of rhamnose compared to other sugars and differences in reactivity between *Sphagnum* and vascular plant-derived sugars (Chapter 2). However, it is also possible that differences between the methods are due to biases in the vegetation indices given the variability of lignin phenol yields among vascular plants and the relatively small sample set.

The position of the water table is a key factor in determining the duration of peat exposure to molecular oxygen, i.e. oxygen exposure time, because the oxygen concentration in air is much greater than in water. The average water table level was lower in the bottom portion of the core (>150 cm) than in the upper portion, so oxygen

exposure time was correspondingly longer. Based on the water table reconstruction and the Bacon age-depth model, peat in the 150-250 cm interval was buried below the water table after 320 years on average, compared to 230 years for peat above 150 cm. Although peat around 200 cm depth formed under relatively wet conditions, the very dry interval at 172 cm would have re-exposed this peat to oxic conditions. In addition, the abundant vascular plant input between 150-250 cm represents an environment that is likely to have increased oxygen exposure time in this interval. Wetland plant roots release oxygen into the otherwise anoxic rhizosphere [*Armstrong and Beckett*, 1987]. The magnitude of rhizosphere oxidation in peatlands varies by species but is sufficient to have a substantial impact on methane oxidation rates [*Fritz et al.*, 2011; *Watson et al.*, 1997]. The vascular plant-dominated interval from 150-250 cm likely had a higher oxygen exposure time than the deeper (>250 cm) depth interval due to oxygen release by vascular plant roots.

The water table was also relatively low in the upper 50 cm of the core. The most recently deposited peat formed with a water table depth of 28±8 cm, comparable to or drier than most of the samples below 150 cm. However, oxygen exposure time was likely lower for recent peat due to higher accumulation rates. The most recent radiocarbon date, at 51 cm depth, had a best-fit age of 225 cal. yr B.P., resulting in an average accumulation rate of 2.3 mm/yr for the upper 50 cm. This indicates peat in the upper 50 cm was buried below the water table in about 50 years on average, compared to 320 years in the 150-250 cm interval. The higher accumulation rate near the surface means oxygen exposure time was likely low during this interval despite relatively dry conditions. Therefore, the interval between 150 and 250 cm likely experienced the longest oxygen exposure time in the core.

4.4.2. Peat decomposition

Several independent indicators showed the peat between 150 and 250 cm experienced the highest degree of decomposition. The C:N ratio, which was lowest in the 150-250 cm interval, is often used as a diagenetic indicator in peats based on the assumption of conservative N recycling. While organic C is respired to CO_2 during decomposition, N is retained by microbes and mostly remains within the system [*Kuhry and Vitt*, 1996; *Malmer and Holm*, 1984; *Malmer and Wallen*, 2004]. Although the C:N ratio can be influenced by changes in atmospheric N deposition and vegetation change [*Bragazza et al.*, 2006; *Gerdol et al.*, 2007], it is strongly correlated with independent indicators of decomposition, including the syringyl phenol acid:aldehyde ratios and hydroxyproline yields used in this study [Chapter 3; *Zaccone et al.*, 2008].

Hydrolysable amino acids provide a molecular perspective of the C:N ratio, as they accounted for ~ 46% of total nitrogen in the peat. The amino acid yield was strongly correlated with the N:C ratio, showing that this fraction was relatively constant throughout the core. Even in the extensively decomposed 150-250 cm interval, which had a nitrogen content up to four times higher than the rest of the core, the fraction of nitrogen as amino acids varied between 32-51%, similar to peat in surrounding layers. Amino acids are preferentially removed during decomposition of marine organic matter [*Amon et al.*, 2001; *Cowie and Hedges*, 1992; 1994] and during the formation of soil organic matter [*Friedel and Scheller*, 2002; *Schmidt et al.*, 2000], resulting in a decline in %N as amino acids, but this is not observed in peatlands (this study; Chapter 3). This supports the hypothesis that nitrogen is conservatively recycled in peatlands [*Malmer and Holm*, 1984], as substantial losses would likely result in the preferential removal of

amino acids and a lower % nitrogen as amino acids in highly decomposed peats. Instead, it appears that microbes continuously regenerate amino acids, maintaining them as a relatively constant fraction of total nitrogen.

Hydrolysable neutral sugars are the most abundant class of biochemicals in peat-forming plants, accounting for up to 41% of the peat C (Table 4.1). Hydrolysable neutral sugars are removed more rapidly than bulk C in decaying plant detritus, so lower sugar yields are indicative of more extensive decomposition [*Opsahl and Benner*, 1999]. This can be complicated by vegetation change, but even accounting for the difference in neutral sugar yields between *Sphagnum* and vascular plants by using the sugar degradation index, the 150-250 cm interval was more decomposed than the surrounding peat. The strong correlation between the sugar degradation index and the N:C ratio increases confidence in its use as a diagenetic indicator.

A number of other diagenetic indicators have been proposed based on the composition of neutral sugars, such as the mole % of glucose [*Hedges et al.*, 1994; *Opsahl and Benner*, 1999] or the ratio of plant-derived sugars (arabinose and xylose) to microbial-derived sugars (rhamnose, fucose, galactose, and mannose) [*Glaser et al.*, 2000; *Guggenberger et al.*, 1994]. The mole % glucose profile is consistent with the other indicators of decomposition, as it is generally high (55-70%) in the peat but is considerably lower (<45%) at 183, 219-227, and 243 cm, zones of extensive decomposition according to the other indicators. Unlike the other indicators, however, only peat from these five depths was significantly different from the rest of the core and the mole % glucose was not typically lower in the 150-250 cm interval. Compositional indices related to plant vs. microbial-derived sugars did not correlate with the sugar yield

or other indicators of decomposition used in this study. This is likely due to the substantial differences in sugar composition between vascular plants and *Sphagnum*. *Sphagnum* is relatively rich in rhamnose and fucose, whereas vascular plants are enriched in arabinose and xylose [*Comont et al.*, 2006; *Jia et al.*, 2008]. Vegetation change can therefore cause dramatic changes in the mole % of these sugars. This makes the neutral sugar composition very useful for vegetation reconstruction, but complicates its utility in assessing decomposition in peatlands.

Hydroxyproline (Hyp) is of similar or greater resistance to decomposition than bulk plant C and its yield commonly increases with decomposition even though it is not synthesized by bacteria or fungi (Chapter 1). Yields above the range found in vascular plants can therefore be interpreted as another independent indicator of extensive decomposition. Hydroxyproline yields, like the C:N ratio and the sugar degradation index, indicate the most highly degraded peats between 150 and 250 cm and in particular samples at 183 and 219 cm. The yields found in these samples (up to 49 nmol Hyp mg C^{-1}) are similar to those found in highly decomposed peat in West Siberian Lowland, Russia (Chapter 3).

In contrast to the other indicators, the acid:aldehyde (Ad/Al) ratios of lignin phenols do not clearly indicate extensive decomposition in the 150-250 cm zone. The Ad/Al ratio of syringyl phenols was elevated in this interval, but there was no apparent change in the Ad/Al ratio of the vanillyl phenols compared to the baseline of surrounding peat. In addition, both Ad/Al ratios were relatively low (<0.4 for V phenols, <0.3 for S phenols) compared with those (0.6-1.5) in highly decomposed peat (Chapter 3; [*Williams*

and Yavitt, 2003]), and mineral soils (>1.5; [*Feng and Simpson*, 2007; *Otto and Simpson*, 2006]).

The apparent disagreement between the Ad/Al ratios and the other independent indicators of decomposition (C:N ratios, amino acid yields, Hyp yields, and sugar degradation indices) is not unexpected because these indicators have widely varying sensitivities and are therefore useful over different time scales. Decomposition models indicate peat entering the catotelm has lost approximately 80-90% of its initial mass [*Clymo*, 1992], so the ideal diagenetic indicator would be most sensitive over this range. In a four-year decomposition study of three types of vascular plant litter, the neutral sugar yield was most sensitive in the early and middle stages of decomposition and declined 30-80% after 80% mass loss [*Opsahl and Benner*, 1999]. Hydroxyproline yields doubled after 80% mass loss and increased another 40% between 80 and 90% mass loss (Chapter 1). Lignin phenol Ad/Al ratios, in contrast, increased little up to 90% mass loss but increased exponentially with subsequent mass loss [*Opsahl and Benner*, 1995]. This suggests sugar and hydroxyproline yields are more sensitive to differences in decomposition between peat samples, while substantial changes to the Ad/Al ratios only occur with more extensive decomposition. Differences in sensitivity among the various indicators emphasize the utility of using multiple indicators in interpreting the extent of decomposition.

4.4.3. Controls on decomposition

The pattern of decomposition in the JBL7 core, with extensively decomposed peat between 150 and 250 cm and less decomposed peat above and below, provides a unique opportunity to examine the controls on peat decomposition. First, it illustrates that the

extent of decomposition is not always correlated with peat age. The vegetation succession at JBL7 differs from most peat sequences in that it shows a transition from *Sphagnum*-dominated after initiation, to vascular plant dominated, and then a shift back to *Sphagnum* dominance. This pattern is consistent with the plant macrofossil record of the core [*Holmquist and MacDonald*, 2014]. Most peatlands begin as minerotrophic fens inhabited mainly by sedges and become increasingly ombrotrophic, allowing *Sphagnum* to outcompete vascular plants [*van Breemen*, 1995]. The unusual pattern in the present core provides an opportunity to evaluate the effects of vegetation and associated environmental conditions on decomposition. In a common peat profile with a *Sphagnum* layer underlain by a vascular plant-dominated interval, both the age of the peat and the contribution of vascular plants increase with depth, making it difficult to separate the effects of peat age and litter quality on decomposition.

The JBL7 core contains a layer of mostly vascular plant remains in the middle of the core, avoiding the covariance of age and vegetation type found in most peat profiles. Peat near the base of the core was thousands of years older than peat between 150 and 250 cm, yet the latter was more extensively decomposed according to several independent indicators. This demonstrates that differences in litter quality and environmental conditions in the acrotelm can be more significant for the extent of peat decomposition than lengthy exposure to decomposition under anaerobic conditions in the catotelm. This is remarkable because peat typically spends only tens or hundreds of years in the acrotelm compared to thousands of years in the catotelm, but it is consistent with theoretical modeling of peat decomposition [*Frolking et al.*, 2001].

The results also indicate temperature was not the primary driver of decomposition in this core. The Holocene Thermal Maximum (HTM) lasted from approximately 7000-4000 years B.P. at sites near James Bay, with temperatures up to 1-2°C warmer than present [*Kaufman et al.*, 2004]. This event approximately corresponds to the interval between 241-326 cm according to the "Bacon" age-depth model [*Holmquist et al.*, 2014], so the bottom ~55 cm of the core likely formed under warmer conditions than the rest of the core. However, the extent of decomposition in this layer was similar to the 100-150 cm interval, where the plant community was also *Sphagnum*-dominated, and lower than in the 150-250 cm interval.

Samples at 86 and 88 cm were formed during the Medieval Climate Anomaly (1000-700 yr B.P.), with temperature about 2°C above the 20th century average [*Viau and Gajewski*, 2009; *Bunbury et al*., 2012]. Like those formed during the Holocene Thermal Maximum, there is no evidence that the warmer temperatures enhanced decomposition, as the sugar degradation index, amino acid yield, and hydroxyproline yield remained low during this interval. The sample at 84 cm had an elevated sugar degradation index, but was formed after the Medieval Climate Anomaly according the "Bacon" model (688 yr B.P.). The extent of peat decomposition was low during both the Holocene Thermal Maximum and the Medieval Climate Anomaly despite higher temperatures, indicating temperature is not the primary control of decomposition. The low apparent temperature sensitivity of decomposition is consistent with results from the West Siberian Lowland (WSL), where cores from the northern WSL were more decomposed than those from the southern WSL despite experiencing mean annual temperatures as much as 7°C cooler than those in the south (Chapter 3).

The zone of elevated decomposition in the JBL7 core coincided with a sustained transition to vascular plant vegetation and the interval with the longest oxygen exposure time. Both factors provide a plausible mechanism explaining elevated decomposition in this zone, as vascular plant detritus decays faster than *Sphagnum* when decomposed under aerobic conditions [*Moore et al.*, 2007]. It is difficult to separate the effects of the two factors, as they co-occur in the highly decomposed interval, but details of the vegetation record and pattern of decomposition provide some insight. The deepest three samples in the 150-250 cm interval (235, 239, and 247 cm) were mostly *Sphagnum*, but still appeared to be highly decomposed. The elevated decomposition in these samples cannot be explained by differences in litter quality between *Sphagnum* and vascular plants, as these samples contained mainly *Sphagnum* remains. Instead, it is likely that the subsequent transition to vascular plant dominance increased oxygen penetration into these layers due to their root systems and the elevated decomposition is due to greater oxygen exposure time.

There were two additional shifts to vascular plant dominance at 259 and 303-307 cm. Unlike the sustained vegetation shift in the 150-250 cm interval of extensive decomposition, these appeared to be transient (100-200 yr) vascular plant invasions and it appears they did not experience extensive decomposition. This is consistent with the findings of Chapter 3, in which no connection between vegetation type and extent of decomposition was observed in cores from the West Siberian Lowland. Together, these suggest differences in litter quality between vascular plants and *Sphagnum* are not sufficient to drive major differences in extent of decomposition. In contrast, a brief shift to drier conditions at 296 cm did appear to affect decomposition, as the sample directly

below (299 cm) exhibited a local maximum in the amino acid yield, hydroxyproline yield, and the sugar degradation index. This demonstrates changes in oxygen exposure time can have a direct effect on the extent of decomposition.

Decomposition was substantially greater from 150-250 cm even though vegetation type alone does not appear to have an effect on decomposition. Oxygen exposure time appears to be more important, but the water table was relatively low from 150 cm to the bottom of the core. This apparent contradiction is best explained by synergistic effects of vascular plant vegetation and oxygen exposure time. Vascular plants directly increase oxygen exposure time through the release of oxygen from roots, and by influencing the relative decomposition rates of *Sphagnum* and vascular plant litter. The decomposition of vascular plant litter can be several times faster than that of *Sphagnum* under aerobic conditions, but this difference is not apparent under anaerobic conditions. Decomposition rates of *Carex, Typha,* and *Chamaedaphne* all decreased substantially when incubated at 60 cm depth compared to at the surface [*Moore et al.*, 2007]. The effect of anoxia on *Sphagnum* decay is muted and its rate of anaerobic decay is similar to that of vascular plants [*Johnson and Damman,* 1991]. This is likely due to the absence of lignin in mosses [*Verhoeven and Liefveld*, 1997; *Wilson et al.*, 1989]. Lignin decomposition is much slower in the absence of oxygen and other macromolecules are physically shielded from enzymes within the lignocellulosic matrix [*Benner et al*., 1984].

Our finding that peat decomposition is primarily controlled by oxygen exposure time rather than temperature has important implications for future changes in peatland C balance. It suggests warmer temperatures in the arctic will have little direct impact on

peatland decomposition. In contrast, *Sphagnum* net primary production is strongly correlated with photosynthetically available radiation integrated over the growing season (PAR0), which is increasing due to climate change [*Loisel et al.*, 2012]. This is consistent with observations that net C accumulation over the last 2000 years is correlated with mean annual temperature in the West Siberian Lowland [*Beilman et al.*, 2009] and in the James Bay Lowland [*Holmquist et al.*, 2014]. In addition, global peat C accumulation rates declined during the transition from the Medieval Climate Anomaly to the Little Ice Age, likely due to decreasing temperature [*Charman et al.*, 2013]. This indicates net primary production is more sensitive to temperature than decomposition and suggests net C accumulation in peatlands could increase with future warming in the arctic and subarctic.

Table 4.1 Elemental and biochemical composition of peat-forming vegetation.

Sample	n	Wt. %N[a]	Wt. %C[a]	C:N[b] (molar)	Hyp[b] (nmol/mgC)	THAA[b] (%C)	THNS[a] (%C)
Sphagnum							
Sphagnum fuscum	2	0.42	39.6	109.2	8.8	2.5	33.8
Sphagnum magellanicum	2	0.29	42.1	170.0	7.2	1.8	37.9
Sphagnum angustifolium	2	0.59	39.8	78.9	6.1	2.8	35.3
Vascular Plants							
Carex leaves	2	0.76	39.6	61.0	7.8	3.5	40.5
Eriophorum leaves	2	1.62	44.8	32.0	10.1	7.7	38.1
Ledum leaves	3	1.16	49.0	50.0	11.3	5.3	23.9
Abies balsamea needle litter	3	1.07	50.1	55.0	8.3	5.2	22.4

[a]From Chapter 2

[b]From Chapter 3

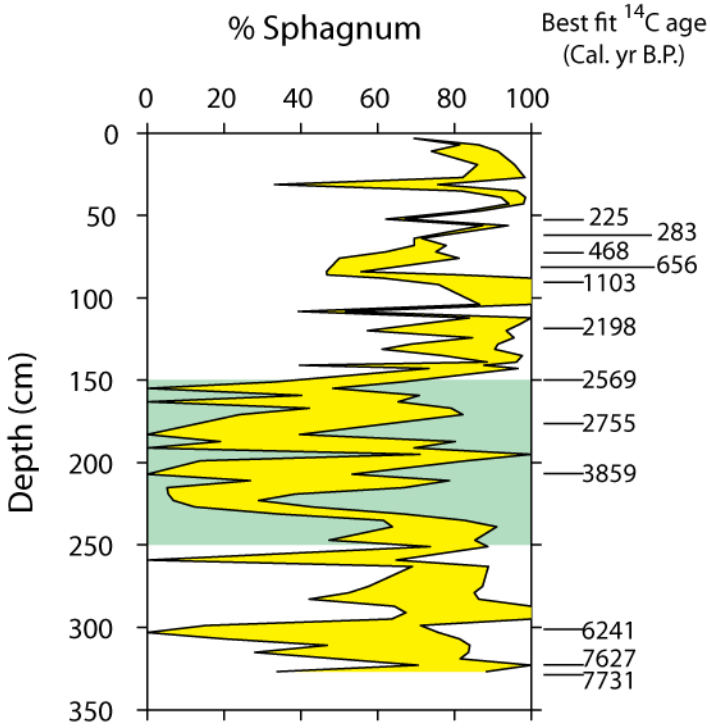

Figure 4.1 Vegetation reconstruction using the lignin phenol and carbohydrate methods. The yellow fill shows the range of values obtained using the two methods. Best fit radiocarbon ages are from Holmquist et al. [2014]. The green bar highlights the interval from 150-250 cm with vascular plant vegetation and higher oxygen exposure time.

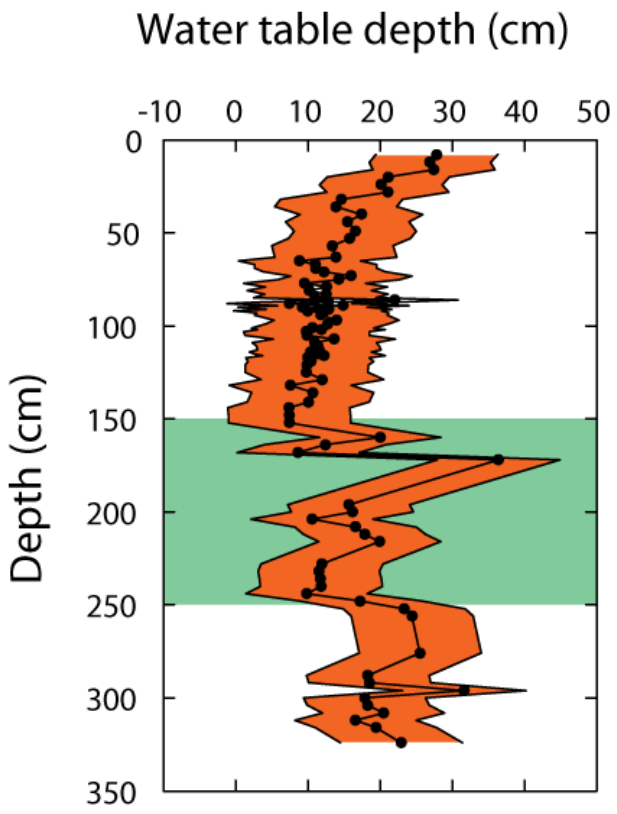

Figure 4.2 Water table reconstruction based on the testate amoebae analysis. The line represents the mean estimate of water table depth while the shaded area shows the maximum and minimum estimates. The green bar highlights the interval from 150-250 cm with vascular plant vegetation and higher oxygen exposure time.

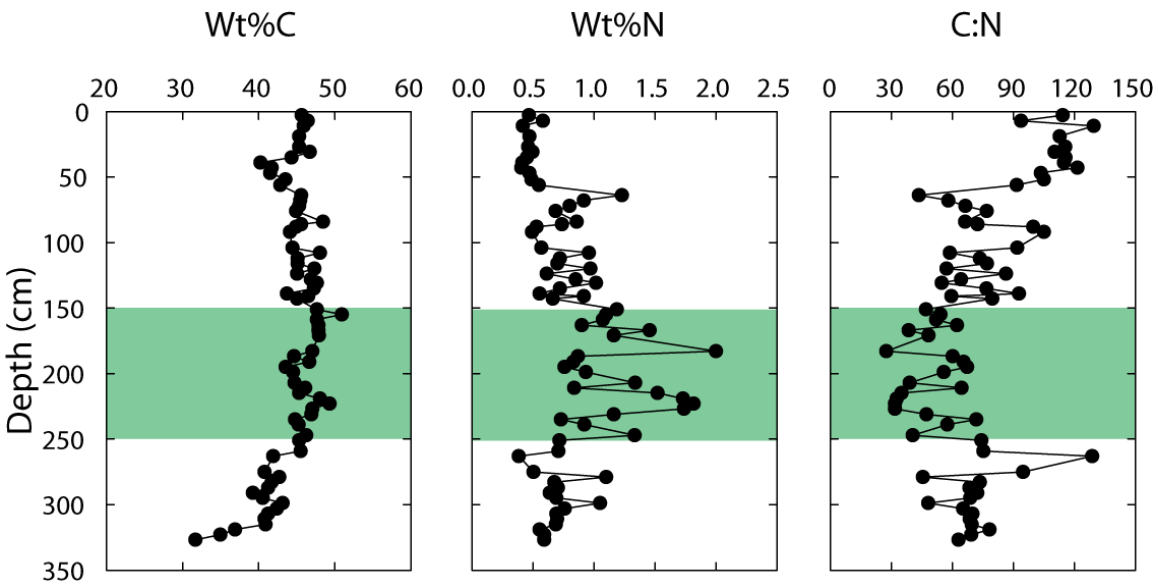

Figure 4.3 Elemental composition and C:N ratio of the peat. The green bar highlights the interval from 150-250 cm with vascular plant vegetation and higher oxygen exposure time.

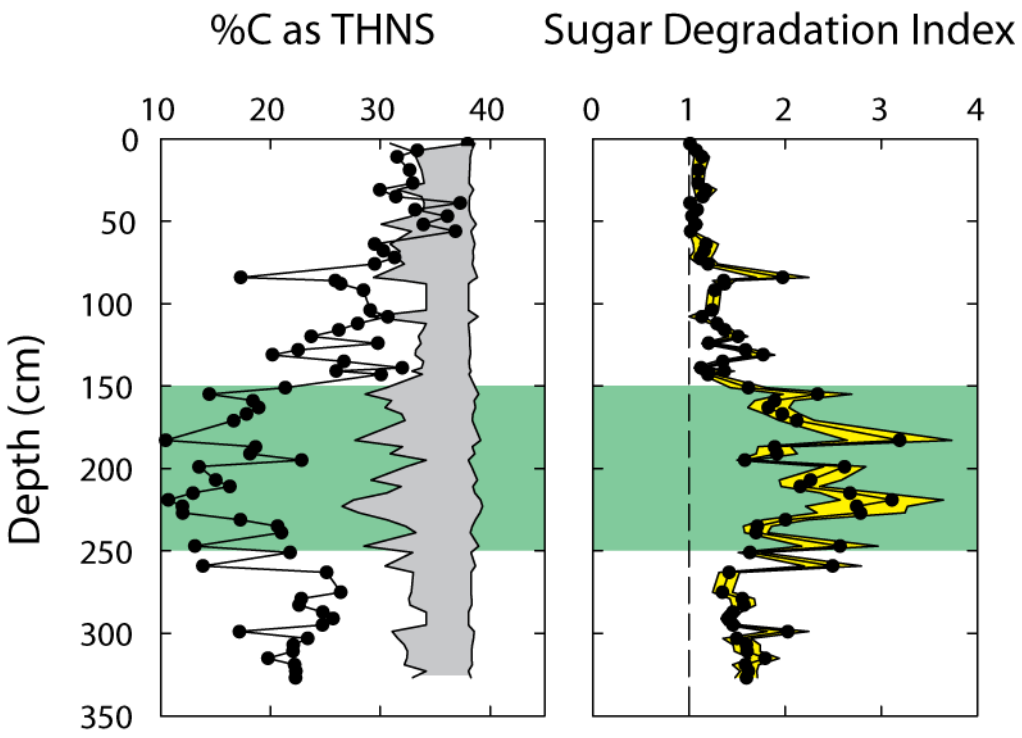

Figure 4.4 Profile of the percentage carbon as neutral sugars and the sugar degradation index in the core. The gray shaded area on the left indicates the "expected" sugar yield based on the vegetation reconstruction and neutral sugar yields in fresh vegetation. The sugar degradation index is the ratio of the "expected" sugar yield to the observed yield. The green bar highlights the interval from 150-250 cm with vascular plant vegetation and higher oxygen exposure time.

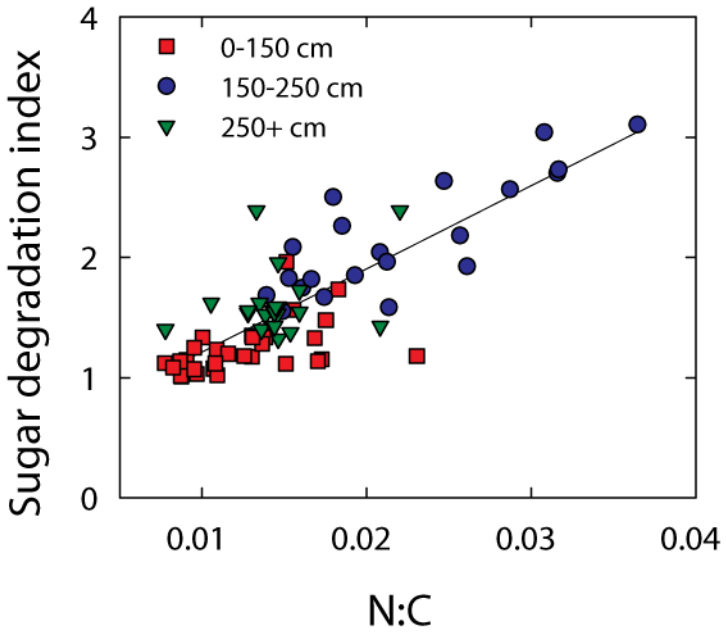

Figure 4.5 Correlation between the sugar degradation index and the N:C ratio.

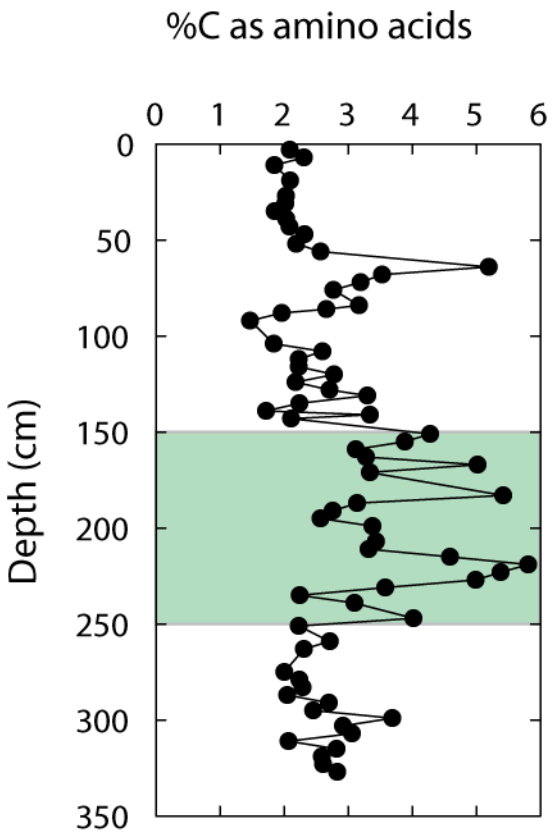

Figure 4.6 Percentage of carbon as total hydrolysable amino acids with depth in the core. The green bar highlights the interval from 150-250 cm with vascular plant vegetation and higher oxygen exposure time.

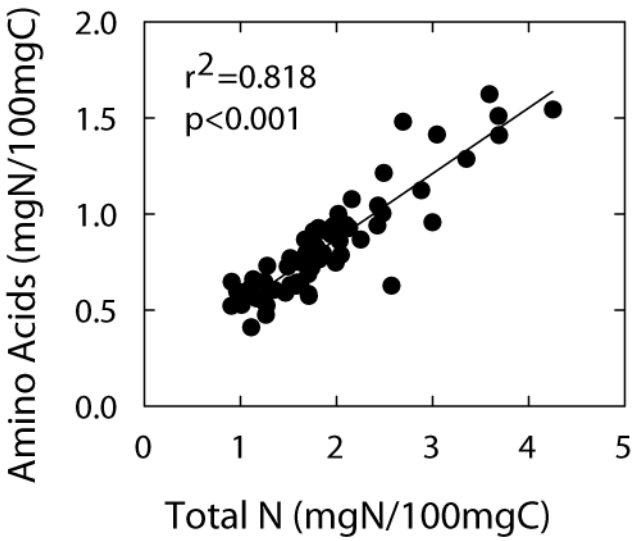

Figure 4.7 Correlation between total hydrolysable amino acids and nitrogen in the peat core, with both variables normalized to 100 mg C.

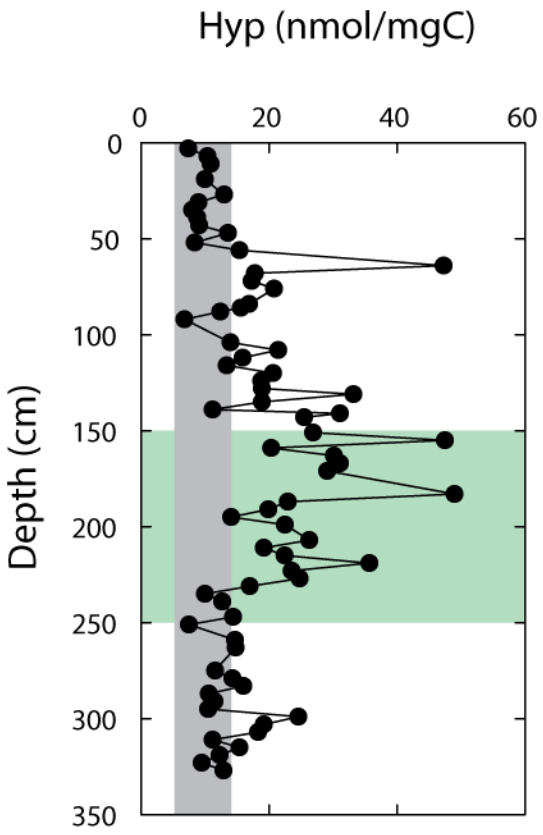

Figure 4.8 Profile of carbon-normalized hydroxyproline (Hyp) yields with depth in the core. The gray bar indicates the range of Hyp yields in fresh plant material (Table 4.1) and the green bar indicates the interval from 150-250 cm with vascular plant vegetation and higher oxygen exposure time.

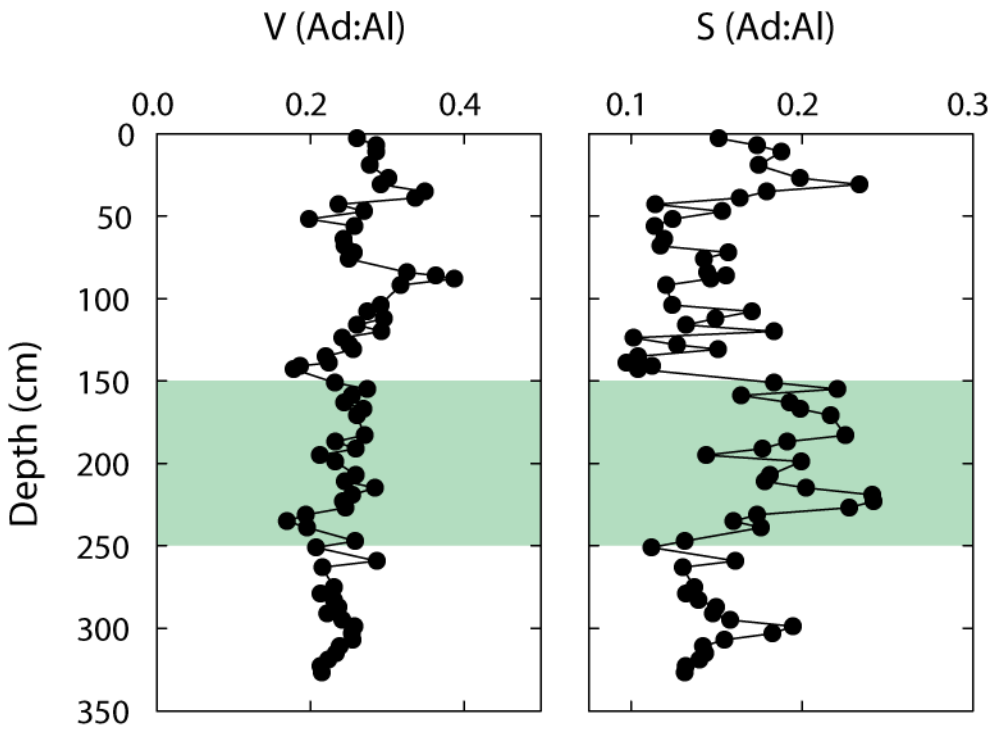

Figure 4.9 Profile of acid:aldehyde (Ad:Al) ratios of vanillyl (left) and syringyl (right) phenols in the core. The green bar highlights the interval from 150-250 cm with vascular plant vegetation and higher oxygen exposure time.

REFERENCES

Aaby, B. (1976), Cyclic climatic variations in climate over past 5,500 yr reflected in raised bogs, *Nature*, *263*(5575), 281-284.

Aaby, B., and H. Tauber (1975), Rates of peat formation in relation to degree of humification and local environment, as shown by studies of a raised bog in Deninark, *Boreas*, *4*(1), 1-17.

Adams, E., 1978. Invertebrate collagens. *Science* 202, 591-598.

Aerts, R., 1996. Nutrient resorption from senescing leaves of perennials: Are there general patterns? *Journal of Ecology* 84, 597-608.

Aldous, A. R. (2002), Nitrogen translocation in Sphagnum mosses: effects of atmospheric nitrogen deposition, *New Phytol.*, *156*(2), 241-253.

Amelung, W., 2001. Methods using amino sugars as markers for microbial residues in soil. In: Lal, R., Kimble, J., Follett, R., Stewart, B. (Eds.), Assessment Methods for Soil Carbon Pools. Lewis Publishers, Boca Raton, FL, pp. 233-270.

Amelung, W., 2003. Nitrogen biomarkers and their fate in soil. *Journal of Plant Nutrition and Soil Science* 166, 677-686.

Amon, R. M. W., H. P. Fitznar, and R. Benner (2001), Linkages among the bioreactivity, chemical composition, and diagenetic state of marine dissolved organic matter, *Limnol. Oceanogr.*, *46*(2), 287-297.

Armstrong, W., and P. Beckett (1987), Internal aeration and development of stela anoxia in submerged roots, *New Phytol.*, *105*(2), 221-245.

Baas, M., R. Pancost, B. van Geel, and J. S. S. Damste (2000), A comparative study of lipids in Sphagnum species, *Org. Geochem.*, *31*(6), 535-541, doi:10.1016/s0146-6380(00)00037-1.

Ballance, S., K. Y. Borsheim, K. Inngjerdingen, B. S. Paulsen, and B. E. Christensen (2007), A re-examination and partial characterisation of polysaccharides released by mild acid hydrolysis from the chlorite-treated leaves of Sphagnum papillosum, *Carbohydr. Polym.*, *67*(1), 104-115, doi:10.1016/j.carbpol.2006.04.020.

Barber, K. E., F. Chambers, D. Maddy, R. Stoneman, and J. Brew (1994), A sensitive high-resolution record of late Holocene climatic change from a raised bog in northern England, *The Holocene*, *4*(2), 198-205

Barber, K., L. Dumayne-Peaty, P. Hughes, D. Mauquoy, and R. Scaife (1998), Replicability and variability of the recent macrofossil and proxy-climate record from raised bogs: field stratigraphy and macrofossil data from Bolton Fell Moss and Walton Moss, Cumbria, England, *J. Quat. Sci.*, *13*(6), 515-528.

Barber, K. E., D. Maddy, N. Rose, A. C. Stevenson, R. Stoneman, and R. Thompson (2000), Replicated proxy-climate signals over the last 2000 yr from two distant UK peat bogs: new evidence for regional palaeoclimate teleconnections, *Quat. Sci. Rev.*, *19*(6), 481-487, doi:10.1016/s0277-3791(99)00102-x.

Beer, J., and C. Blodau (2007), Transport and thermodynamics constrain belowground carbon turnover in a northern peatland, *Geochim. Cosmochim. Acta*, *71*(12), 2989-3002, doi: 10.1016/j.gca.2007.03.010

Beilman, D. W. (2006), Carbon Accumulation and Development of Peatlands over the Holocene, West Siberia, Russia, Ph.D thesis, University of California, Los Angeles, California, USA.

Beilman, D. W., G. M. MacDonald, L. C. Smith, and P. J. Reimer (2009), Carbon accumulation in peatlands of West Siberia over the last 2000 years, *Global biogeochemical cycles*, *23*, doi:10.1029/2007GB003112.

Belyea, L. R. (1996), Separating the effects of litter quality and microenvironment on decomposition rates in a patterned peatland, *Oikos*, 529-539.

Belyea, L. R. (2009), Nonlinear Dynamics of Peatlands and Potential Feedbacks on the Climate System, in *Carbon Cycling in Northern Peatlands*, edited by A. J. Baird, L. R. Belyea, X. Comas, A. S. Reeve and L. D. Slater, American Geophysical Union, Washington, D.C.

Belyea, L. R., and R. Clymo (2001), Feedback control of the rate of peat formation, *Proc. R. Soc. London, Ser. B*, *268*(1473), 1315-1321.

Belyea, L. R. and Malmer, N. (2004), Carbon sequestration in peatland: patterns and mechanisms of response to climate change. *Global Change Biol*., 10, 1043–1052. doi: 10.1111/j.1529-8817.2003.00783.x

Benner, R., Hodson, R.E., 1985. Microbial degradation of the leachable and lignocellulosic components of leaves and wood from *Rhizophora mangle* in a tropical mangrove swamp. *Marine Ecology-Progress Series* 23, 221-230.

Benner, R., Maccubbin, A.E., Hodson, R.E., 1984. Anaerobic biodegradation of the lignin and polysaccharide components of lignocellulose and synthetic lignin by sediment microflora. *Applied and Environmental Microbiology* 47, 998-1004.

Benner, R., M. L. Fogel, E. K. Sprague, and R. E. Hodson (1987), Depletion of C-13 in lignin and its implications for stable carbon isotope studies, *Nature*, *329*(6141), 708-710.

Benner, R., M. L. Fogel, and E. K. Sprague (1991), Diagenesis of belowground biomass of Spartina alterniflora in salt marsh sediments, *Limnol. Oceanogr.*, *36*(7), 1358-1374.

Blaauw, M., and J. A. Christen (2011), Flexible paleoclimate age-depth models using an autoregressive gamma process(3), 457-474 doi: 10.1214/ba/1339616472.

Booth, R. K. (2002), Testate amoebae as paleoindicators of surface-moisture changes on Michigan peatlands: modern ecology and hydrological calibration, *Journal of Paleolimnology, 28*(3), 329-348.

Booth, R. K. (2008), Testate amoebae as proxies for mean annual water-table depth in Sphagnum-dominated peatlands of North America, *J. Quat. Sci., 23*(1), 43-57.

Borch, N.H., Kirchman, D.L., 1999. Protection of protein from bacterial degradation by submicron particles. *Aquatic Microbial Ecology* 16, 265-272.

Bourdon, S., F. Laggoun-Defarge, J. R. Disnar, O. Maman, B. Guillet, S. Derenne, and C. Largeau (2000), Organic matter sources and early diagenetic degradation in a tropical peaty marsh (Tritrivakely, Madagascar). Implications for environmental reconstruction during the Sub-Atlantic, *Org. Geochem., 31*(5), 421-438, doi:10.1016/s0146-6380(00)00010-3.

Brady, J.D., Sadler, I.H., Fry, S.C., 1996. Di-isodityrosine, a novel tetrameric derivative of tyrosine in plant cell wall proteins: A new potential cross-link. *Biochemical Journal* 315, 323-327.

Bragazza, L., A. Buttler, A. Siegenthaler, and E. A. D. Mitchell (2009), Plant Litter Decomposition and Nutrient Release in Peatlands, in *Carbon Cycling in Northern Peatlands*, edited by A. J. Baird, L. R. Belyea, X. Comas, A. S. Reeve and L. D. Slater, American Geophysical Union, Washington, D.C.

Bragazza, L., A. Buttler, J. Habermacher, L. Brancaleoni, R. Gerdol, H. Fritze, P. Hanajik, R. Laiho, and D. Johnson (2012), High nitrogen deposition alters the decomposition of bog plant litter and reduces carbon accumulation, *Global Change Biol., 18*(3), 1163-1172, doi: 10.1111/j.1365-2486.2011.02585.x

Bragazza, L., C. Freeman, T. Jones, H. Rydin, J. Limpens, N. Fenner, T. Ellis, R. Gerdol, M. Hajek, T. Hajek, P. Lacumin, L. Kutnar, T. Tahvanainen, and H. Toberman (2006), Atmospheric nitrogen deposition promotes carbon loss from peat bogs, *Proc. Natl. Acad. Sci. U. S. A., 103*(51), 19386-19389 doi: 10.1073/pnas.0606629104.

Briffa, K. R. (2000), Annual climate variability in the Holocene: interpreting the message of ancient trees, *Quat. Sci. Rev., 19*(1-5), 87-105, doi:10.1016/s0277-3791(99)00056-6.

Brownleader, M.D., Dey, P.M., 1993. Purification of extensin from cell walls of tomato (hybrid of *Lycopersicon esculentum* and *Lycopersicon peruvianum*) cells in supension culture. *Planta* 191, 457-469.

Bunbury, J., S. A. Finkelstein, and J. Bollmann (2012), Holocene hydro-climatic change and effects on carbon accumulation inferred from a peat bog in the Attawapiskat River watershed, Hudson Bay Lowlands, Canada, *Quat. Res., 78*(2), 275-284.

Buranov, A. U., and G. Mazza (2008), Lignin in straw of herbaceous crops, *Ind. Crop. Prod.*, *28*(3), 237-259, doi:10.1016/j.indcrop.2008.03.008

Carpita, N. C. (1996), Structure and biogenesis of the cell walls of grasses, *Annual Review of Plant Physiology and Plant Molecular Biology*, *47*, 445-476.

Cassab, G.I., 1998. Plant cell wall proteins. *Annual Review of Plant Physiology and Plant Molecular Biology* 49, 281-309.

Cassab, G.I., Nietosotelo, J., Cooper, J.B., Vanholst, G.J., Varner, J.E., 1985. A developmentally regulated hydroxyproline-rich glycoprotein from the cell walls of soybean seed coats. *Plant Physiology* 77, 532-535.

Cegelski, L., O'Connor, R.D., Stueber, D., Singh, M., Poliks, B., Schaefer, J., 2010. Plant Cell-Wall Cross-Links by REDOR NMR Spectroscopy. *Journal of the American Chemical Society* 132, 16052-16057.

Celerin, M., Ray, J.M., Schisler, N.J., Day, A.W., StetlerStevenson, W.G., Laudenbach, D.E., 1996. Fungal fimbriae are composed of collagen. *Embo Journal* 15, 4445-4453.

Chambers, F., K. Barber, D. Maddy, and J. Brew (1997), A 5500-year proxy-climate and vegetation record from blanket mire at Talla Moss, Borders, Scotland, *Holocene*, *7*(4), 391-399.

Charman, D. (2001), Biostratigraphic and palaeoenvironmental applications of testate amoebae, *Quat. Sci. Rev.*, *20*(16), 1753-1764.

Charman, D. J., A. Blundell, R. C. Chiverrell, D. Hendon, and P. G. Langdon (2006), Compilation of non-annually resolved Holocene proxy climate records: stacked Holocene peatland palaeo-water table reconstructions from northern Britain, *Quat. Sci. Rev.*, *25*(3-4), 336-350, doi:10.1016/j.quascirev.2005.05.005.

Charman, D., and B. Warner (1992), Relationship between testate amoebae (Protozoa: Rhizopoda) and microenvironmental parameters on a forested peatland in northeastern Ontario, *Canadian Journal of Zoology*, *70*(12), 2474-2482.

Christensen, B. T., and S. Bechandersen (1989), Influence of straw disposal on distribution of amino acids in soil particle size-fractions, *Soil Biol.Biochem.*, *21*(1), 35-40.

Clymo, R. (1965), Experiments on breakdown of Sphagnum in two bogs, *J. Ecol.*, 747-758.

Clymo, R. (1984), The limits to peat bog growth, *Philos. Trans. R. Soc., B.*, *303*(1117), 605-654.

Comont, L., F. Laggoun-Defarge, and J. R. Disnar (2006), Evolution of organic matter indicators in response to major environmental changes: The case of a formerly cut-over peat bog (Le Russey, Jura Mountains, France), *Org. Geochem.*, *37*(12), 1736-1751, doi:10.1016/j.orggeochem.2006.08.005

Cooper, J.B., Varner, J.E., 1984. Cross-linking of soluble extensin in isolated cell walls. *Plant Physiology* 76, 414-417.

Cowie, G. L., and J. I. Hedges (1992), Sources and reactivities of amino acids in a coastal marine environment, *Limnol. Oceanogr.*, *37*(4), 703-724.

Cowie, G. L., and J. I. Hedges (1994), Biochemical indicators of diagenetic alteration in natural organic matter mixtures, *Nature*, *369*(6478), 304-307.

Crook, E.M., Johnston, I.R., 1962. The qualitative analysis of cell walls of selected species of fungi. *Biochemical Journal* 83, 325-331.

Datta, K., Schmidt, A., Marcus, A., 1989. Characterization of 2 soybean repetitive proline-rich proteins and a cognate cDNA from germinated axes. *Plant Cell* 1, 945-952.

Delarue, F., F. Laggoun-Defarge, J. R. Disnar, N. Lottier, and S. Gogo (2011), Organic matter sources and decay assessment in a Sphagnum-dominated peatland (Le Forbonnet, Jura Mountains, France): impact of moisture conditions, *Biogeochemistry*, *106*(1), 39-52, doi:10.1007/s10533-010-9410-0.

Deniro, M.J., 1985. Postmortem preservation and alteration of *in vivo* bone-collagen isotope ratios in relation to paleodietary reconstruction. *Nature* 317, 806-809.

Derrien, D., C. Marol, and J. Balesdent (2007), Microbial biosyntheses of individual neutral sugars among sets of substrates and soils, *Geoderma*, *139*(1-2), 190-198, doi:10.1016/j.geoderma.2007.01.017.

Dey, P.M., Brownleader, M.D., Pantelides, A.T., Trevan, M., Smith, J.J., Saddler, G., 1997. Extensin from suspension-cultured potato cells: A hydroxyproline-rich glycoprotein, devoid of agglutinin activity. *Planta* 202, 179-187.

Dixon, R.K., Brown, S., Houghton, R.A., Solomon, A.M., Trexler, M.C., Wisniewski, J., 1994. Carbon pools and flux of global forest ecosystems. *Science* 263, 185-190.

Dorrepaal, E., S. Toet, R. S. P. van Logtestijn, E. Swart, M. J. van de Weg, T. V. Callaghan, and R. Aerts (2009), Carbon respiration from subsurface peat accelerated by climate warming in the subarctic, *Nature*, *460*(7255), 616-620, doi: 10.1038/nature08216.

Epstein, L., Lamport, D.T.A., 1984. An intramolecular linkage involving isodityrosine in extensin. *Phytochemistry* 23, 1241-1246.

Esquerre-Tugaye, M.T., Lamport, D.T.A., 1979. Cell surfaces in plant-microorganism interactions 1. Structural investigation of cell wall hydroxyproline-rich glycoproteins which accumulate in fungus-infected plants. *Plant Physiology* 64, 314-319.

Everdeen, D.S., Kiefer, S., Willard, J.J., Muldoon, E.P., Dey, P.M., Li, X.B., Lamport, D.T.A., 1988. Enzymic cross-linkage of monomeric extensin precursors *in vitro*. *Plant Physiology* 87, 616-621.

Feng, X., and M. J. Simpson (2007), The distribution and degradation of biomarkers in Alberta grassland soil profiles, *Org. Geochem.*, *38*(9), 1558-1570, doi: 10.1016/j.orggeochem.2007.05.001.

Fenner, N., and C. Freeman (2011), Drought-induced carbon loss in peatlands, *Nat. Geosci.*, *4*(12), 895-900, doi: 10.1038/ngeo1323.

Francez, A.-J., G. Pinay, N. Josselin, and B. L. Williams (2011), Denitrification triggered by nitrogen addition in Sphagnum magellanicum peat, *Biogeochemistry*, *106*(3), 435-441, doi: 10.1007/s10533-010-9523-5.

Friedel, J. K., and E. Scheller (2002), Composition of hydrolysable amino acids in soil organic matter and soil microbial biomass, *Soil Biol. Biochem.*, *34*(3), 315-325.

Fritz, C., V. A. Pancotto, J. Elzenga, E. J. Visser, A. P. Grootjans, A. Pol, R. Iturraspe, J. G. Roelofs, and A. J. Smolders (2011), Zero methane emission bogs: extreme rhizosphere oxygenation by cushion plants in Patagonia, *New Phytol.*, *190*(2), 398-408.

Frolking, S., N. T. Roulet, T. R. Moore, P. J. Richard, M. Lavoie, and S. D. Muller (2001), Modeling northern peatland decomposition and peat accumulation, *Ecosystems*, *4*(5), 479-498.

Frolking, S., N. Roulet, E. Tuittila, J. Bubier, A. Quillet, J. Talbot, and P. Richard (2010), A new model of Holocene peatland net primary production, decomposition, water balance, and peat accumulation, *Earth System Dynamics*, *1*, 1-21, doi:10.5194/esd-1-1-2010.

Fry, S.C., 1982. Isodityrosine, a new cross-linking amino acid from plant cell-wall gycoprotein. *Biochemical Journal* 204, 449-455.

Galloway, J. N., F. J. Dentener, D. G. Capone, E. W. Boyer, R. W. Howarth, S. P. Seitzinger, G. P. Asner, C. C. Cleveland, P. A. Green, E. A. Holland, D. M. Karl, A. F. Michaels, J. H. Porter, A. R. Townsend, and C. J. Vorosmarty (2004), Nitrogen cycles: past, present, and future, *Biogeochemistry*, *70*(2), 153-226 doi: 10.1007/s10533-004-0370-0.

Gerdol, R., A. Petraglia, L. Bragazza, P. Iacumin, and L. Brancaleoni (2007), Nitrogen deposition interacts with climate in affecting production and decomposition rates in Sphagnum mosses, *Global Change Biol.*, *13*(8), 1810-1821 doi: 10.1111/j.1365-2486.2007.01380.x..

Glaser, B., M.-B. Turrion, D. Solomon, A. Ni, and W. Zech (2000), Soil organic matter quantity and quality in mountain soils of the Alay Range, Kyrgyzia, affected by land use change, *Biology and Fertility of Soils*, *31*(5), 407-413.

Goni, M. A., K. C. Ruttenberg, and T. I. Eglinton (1998), A reassessment of the sources and importance of land-derived organic matter in surface sediments from the Gulf of Mexico, *Geochimica Et Cosmochimica Acta*, *62*(18), 3055-3075, doi:10.1016/s0016-7037(98)00217-8.

Gorham, E. (1991), Northern peatlands: role in the carbon cycle and probable responses to climatic warming, *Ecological Applications*, *1*(2), 182-195, doi:10.2307/1941811.

Gotelli, I.B., Cleland, R., 1968. Differences in occurrence and distributions of hydroxyproline-proteins among algae. *American Journal of Botany* 55, 907-914.

Guggenberger, G., B. T. Christensen, and W. Zech (1994), Land-use effects on the composition of organic matter in particle-size separates of soil: I. Lignin and carbohydrate signature, *European Journal of Soil Science*, *45*(4), 449-458.

Guggenberger, G., Frey, S.D., Six, J., Paustian, K., Elliott, E.T., 1999. Bacterial and fungal cell-wall residues in conventional and no-tillage agroecosystems. *Soil Science Society of America Journal* 63, 1188-1198.

Guiot, J., C. Corona, and Escarsel (2010), Growing Season Temperatures in Europe and Climate Forcings Over the Past 1400 Years, *PLoS One*, *5*(3), doi:10.1371/journal.pone.0009972.

Hagerman, A.E., Butler, L.G., 1981. The specificity of proanthocyanidin-protein interactions. *Journal of Biological Chemistry* 256, 4494-4497.

Hagerman, A.E., Rice, M.E., Ritchard, N.T., 1998. Mechanisms of protein precipitation for two tannins, pentagalloyl glucose and epicatechin(16) (4 -> 8) catechin (procyanidin). *Journal of Agricultural and Food Chemistry* 46, 2590-2595.

Hajek, T., S. Ballance, J. Limpens, M. Zijlstra, and J. T. A. Verhoeven (2011), Cell-wall polysaccharides play an important role in decay resistance of Sphagnum and actively depressed decomposition in vitro, *Biogeochemistry*, *103*(1-3), 45-57, doi:10.1007/s10533-010-9444-3.

Hartnett, H. E., R. G. Keil, J. I. Hedges, and A. H. Devol (1998), Influence of oxygen exposure time on organic carbon preservation in continental margin sediments, *Nature*, *391*(6667), 572-574 doi: 10.1038/35351.

Hedges, J. I., and D. C. Mann (1979), Lignin geochemistry of marine sediments from the southern Washington coast, *Geochimica Et Cosmochimica Acta*, *43*(11), 1809-1818, doi:10.1016/0016-7037(79)90029-2.

Hedges, J. I., R. A. Blanchette, K. Weliky, and A. H. Devol (1988), Effects of fungal degradation on the CuO oxidation products of lignin: a controlled laboratory study, *Geochimica Et Cosmochimica Acta*, *52*(11), 2717-2726.

Hedges, J. I., G. L. Cowie, J. E. Richey, P. D. Quay, R. Benner, M. Strom, and B. R. Forsberg (1994), Origins and processing of organic matter in the Amazon River as indicatated by carbohydrates and amino acids, *Limnology and Oceanography*, *39*(4), 743-761.

Hedges, J. I., F. S. Hu, A. H. Devol, H. E. Hartnett, E. Tsamakis, and R. G. Keil (1999), Sedimentary organic matter preservation: A test for selective degradation under oxic conditions, *Am. J. Sci.*, *299*(7-9), 529-555.

Hedges, J. I., and R. G. Keil (1995), Sedimentary organic matter preservation: an assessment and speculative synthesis, *Mar. Chem.*, *49*(2), 81-115.

Hedges, J. I., and F. G. Prahl (1993), Early Diagenesis: Consequences for Applications of Molecular Biomarkers, in Organic Geochemistry, edited by M. H. Engel and S. A. Macko, Plenum Press, New York.

Held, M.A., Tan, L., Kamyab, A., Hare, M., Shpak, E., Kieliszewski, M.J., 2004. Di-isodityrosine is the intermolecular cross-link of isodityrosine-rich extensin analogs cross-linked in vitro. *Journal of Biological Chemistry* 279, 55474-55482.

Hernes, P.J., Hedges, J.I., 2004. Tannin signatures of barks, needles, leaves, cones, and wood at the molecular level. *Geochimica et Cosmochimica Acta* 68, 1293-1307.

Hobara, S., T. Osono, D. Hirose, K. Noro, M. Hirota, and R. Benner (2014), The roles of microorganisms in litter decomposition and soil formation, *Biogeochemistry*, *118*(1-3), 471-486.

Hobbie, S. E. (1996), Temperature and plant species control over litter decomposition in Alaskan tundra, *Ecol. Monogr.*, *66*(4), 503-522.

Holmquist, J. R. (2013), Holocene Peatland Carbon Accumulation, Ecology, and Hydrology in the Canadian James Bay Lowlands, PhD Dissertation, Univ. of California, Los Angeles, Los Angeles, California, USA.

Holmquist, J. R., and G. M. MacDonald (2014), Peatland succession and long-term apparent carbon accumulation in central and northern Ontario, Canada, *The Holocene*, 0959683614538074.

Holmquist, J. R., G. M. MacDonald, and A. Gallego-Sala (2014), Peatland initiation, carbon accumulation, and 2 ka depth in the James Bay Lowland and adjacent regions, *Arctic, Antarctic, and Alpine Research*, *46*(1), 19-39.

Hood, E.E., Qing, X.S., Varner, J.E., 1988. A developmentally regulated hydroxyproline-rich glycoprotein in maize pericarp cell walls. *Plant Physiology* 87, 138-142.

Howard, P.J.A., Howard, D.M., 1993. Ammonification of complexes prepared from gelatin and aqueous extracts of leaves and freshly-fallen litter of trees on different soil types. *Soil Biology & Biochemistry* 25, 1249-1256.

Hughes, P. D. M., A. Blundell, D. Charman, S. Bartlett, J. Daniell, A. Wojatschke, and F. Chambers (2006), An 8500cal. year multi-proxy climate record from a bog in eastern Newfoundland: contributions of meltwater discharge and solar forcing, *Quat. Sci. Rev.*, *25*(11), 1208-1227 doi: 10.1016/j.quascirev.2005.11.001.

Hughes, P. D. M., G. Mallon, H. J. Essex, M. J. Amesbury, D. J. Charman, A. Blundell, F. M. Chambers, T. J. Daley, and D. Mauquoy (2012), The use of k-values to examine plant 'species signals' in a peat humification record from Newfoundland, *Quat. Inter.*, *268*, 156-165 doi: 10.1016/j.quaint.2011.11.023.

Ise, T., A. L. Dunn, S. C. Wofsy, and P. R. Moorcroft (2008), High sensitivity of peat decomposition to climate change through water-table feedback, *Nat. Geosci.*, *1*(11), 763-766 doi: 10.1038/ngeo331.

Jaatinen, K., R. Laiho, A. Vuorenmaa, U. del Castillo, K. Minkkinen, T. Pennanen, T. Penttila, and H. Fritze (2008), Responses of aerobic microbial communities and soil respiration to water-level drawdown in a northern boreal fen, *Environmental Microbiology*, *10*(2), 339-353 doi: 10.1111/j.1462-2920.2007.01455.x.

Jia, G. D., J. A. J. Dungait, E. M. Bingham, M. Valiranta, A. Korhola, and R. P. Evershed (2008), Neutral monosaccharides as biomarker proxies for bog-forming plants for application to palaeovegetation reconstruction in ombrotrophic peat deposits, *Org. Geochem.*, *39*(12), 1790-1799, doi:10.1016/j.orggeochem.2008.07.002.

Johnson, L. C., and A. W. Damman (1991), Species-controlled Sphagnum decay on a south Swedish raised bog, *Oikos*, 234-242.

Kaiser, K., Benner, R., 2000. Determination of amino sugars in environmental samples with high salt content by high performance anion exchange chromatography and pulsed amperometric detection. *Analytical Chemistry* 72, 2566-2572.

Kaiser, K., Benner, R., 2008. Major bacterial contribution to the ocean reservoir of detrital organic carbon and nitrogen. *Limnology and Oceanography* 53, 99-112.

Kaiser, K., Benner, R., 2009. Biochemical composition and size distribution of organic matter at the Pacific and Atlantic time-series stations. *Marine Chemistry* 113, 63-77.

Kaiser, K., and R. Benner (2012), Characterization of lignin by gas chromatography and mass spectrometry using a simplified CuO oxidation method, *Analytical Chemistry*, *84*(1), 459-464, doi:10.1021/ac202004r.

Kaiser, K., and G. Guggenberger (2000), The role of DOM sorption to mineral surfaces in the preservation of organic matter in soils, *Org. Geochem.*, *31*(7), 711-725.

Kalbitz, K., S. Solinger, J.-H. Park, B. Michalzik, and E. Matzner (2000), Controls on the dynamics of dissolved organic matter in soils: a review, *Soil science*, *165*(4), 277-304.

Katz, E., Kamal, F., Mason, K., 1979. Biosynthesis of *trans*-4-hydroxy-L-proline by *Streptomyces griseoviridus*. *Journal of Biological Chemistry* 254, 6684-6690.

Kaufman, D., T. Ager, N. Anderson, P. Anderson, J. Andrews, P. Bartlein, L. Brubaker, L. Coats, L. C. Cwynar, and M. Duvall (2004), Holocene thermal maximum in the western Arctic (0–180 W), *Quat. Sci. Rev.*, *23*(5), 529-560.

Keil, R.G., Kirchman, D.L., 1993. Dissolved combined amino acids: chemical form and utilization by marine bacteria. *Limnology and Oceanography* 38, 1256-1270.

Keil, R. G., D. B. Montluçon, F. G. Prahl, and J. I. Hedges (1994), Sorptive preservation of labile organic matter in marine sediments.

Kieliszewski, M., Dezacks, R., Leykam, J.F., Lamport, D.T.A., 1992a. A repetitive proline-rich protein from the gymnosperm Douglas Fir is a hydroxyproline-rich glycoprotein. *Plant Physiology* 98, 919-926.

Kieliszewski, M.J., Kamyab, A., Leykam, J.F., Lamport, D.T.A., 1992b. A histidine-rich extensin from *Zea mays* is an arabinogalactan protein. *Plant Physiology* 99, 538-547.

Kieliszewski, M., Lamport, D.T.A., 1987. Purification and partial characterization of a hydroxyproline-rich glycoprotein in a gramineous monocot, *Zea mays*. *Plant Physiology* 85, 823-827.

Kieliszewski, M.J., Lamport, D.T.A., 1994. Extensin: repetitive motifs, functional sites, posttranslational codes, and phylogeny. *Plant Journal* 5, 157-172.

Kieliszewski, M.J., Leykam, J.F., Lamport, D.T.A., 1990. Structure of the threonine-rich extensin from *Zea mays*. *Plant Physiology* 92, 316-326.

Kindler, R., Miltner, A., Richnow, H.-H., Kaestner, M., 2006. Fate of gram-negative bacterial biomass in soil - mineralization and contribution to SOM. *Soil Biology & Biochemistry* 38, 2860-2870.

Knicker, H., Hatcher, P.G., 1997. Survival of protein in an organic-rich sediment: Possible protection by encapsulation in organic matter. *Naturwissenschaften* 84, 231-234.

Kremenetski, K. V., A. A. Velichko, O. K. Borisova, G. M. MacDonald, L. C. Smith, K. E. Frey, and L. A. Orlova (2003), Peatlands of the Western Siberian lowlands: current knowledge on zonation, carbon content and Late Quaternary history, *Quat. Sci. Rev.*, *22*(5-7), 703-723, doi:10.1016/s0277-3791(02)00196-8.

Kuhry, P. (1994), The role of fire in the development of *Sphagnum*-dominated peatlands in western boreal Canada, *J. Ecol.*, *82*(4), 899-910, doi:10.2307/2261453.

Kuhry, P., B. J. Nicholson, L. D. Gignac, D. H. Vitt, and S. E. Bayley (1993), Development of *Sphagnum*-dominated peatlands in boreal continental Canada, *Can. J. Bot.-Rev. Can. Bot.*, *71*(1), 10-22.

Kuhry, P., and D. H. Vitt (1996), Fossil carbon/nitrogen ratios as a measure of peat decomposition, *Ecology*, *77*(1), 271-275.

Lafleur, P. M., T. R. Moore, N. T. Roulet, and S. Frolking (2005), Ecosystem respiration in a cool temperate bog depends on peat temperature but not water table, *Ecosystems*, *8*(6), 619-629 doi: 10.1007/s10021-003-0131-2.

Laiho, R. (2006), Decomposition in peatlands: reconciling seemingly contrasting results on the impacts of lowered water levels, *Soil Biol. Biochem.*, *38*(8), 2011-2024 doi: 10.1016/j.soilbio.2006.02.017.

Lamport, D.T.A., Miller, D.H., 1971. Hydroxyproline arabinosides in the plant kingdom. *Plant Physiology* 48, 454-456.

Larson, J., 1980. The Boreal Ecosystem. Academic Press, New York.

Leach, J.E., Cantrell, M.A., Sequeira, L., 1982. Hydroxyproline-rich bacterial agglutinin from potato: extraction, purification, and characterization. *Plant Physiology* 70, 1353-1358.

Li, X.B., Kieliszewski, M., Lamport, D.T.A., 1990. A chenopod extensin lacks repetitive tetrahydroxyproline blocks. *Plant Physiology* 92, 327-333.

Limpens, J., G. Granath, U. Gunnarsson, R. Aerts, S. Bayley, L. Bragazza, J. Bubier, A. Buttler, L. J. L. van den Berg, A. J. Francez, R. Gerdol, P. Grosvernier, M. Heijmans, M. R. Hoosbeek, S. Hotes, M. Ilomets, I. Leith, E. A. D. Mitchell, T. Moore, M. B. Nilsson, J. F. Nordbakken, L. Rochefort, H. Rydin, L. J. Sheppard, M. Thormann, M. M. Wiedermann, B. L. Williams, and B. Xu (2011), Climatic modifiers of the response to nitrogen deposition in peat-forming Sphagnum mosses: a meta-analysis, *New Phytol.*, *191*(2), 496-507 doi: 10.1111/j.1469-8137.2011.03680.x.

Loisel, J., and M. Garneau (2010), Late Holocene paleoecohydrology and carbon accumulation estimates from two boreal peat bogs in eastern Canada: Potential and limits of multi-proxy archives, *Paleogeogr. Paleoclimatol. Paleoecol.*, *291*(3-4), 493-533, doi:10.1016/j.palaeo.2010.03.020.

Lomstein, B.A., Niggemann, J., Jorgensen, B.B., Langerhuus, A.T., 2009. Accumulation of prokaryotic remains during organic matter diagenesis in surface sediments off Peru. *Limnology and Oceanography* 54, 1139-1151.

Mack, M.C., Treseder, K.K., Manies, K.L., Harden, J.W., Schuur, E.A.G., Vogel, J.G., Randerson, J.T., Chapin, F.S., III, 2008. Recovery of aboveground plant biomass and productivity after fire in mesic and dry black spruce forests of interior alaska. *Ecosystems* 11, 209-225.

Malmer, N., and E. Holm (1984), Variation in the C/N-quotient of peat in relation to decomposition rate and age determination with 210 Pb, *Oikos*, 171-182.

Malmer, N., and B. Wallen (1993), Accumulation and release of organic matter in ombrotrophic bog hummocks: processes and regional variation, *Ecography*, *16*(3), 193-211.

Malmer, N., and B. Wallen (2004), Input rates, decay losses and accumulation rates of carbon in bogs during the last millennium: internal processes and environmental changes, *Holocene*, *14*(1), 111-117 doi: 10.1191/0959683604h1693rp.

Mambelli, S., Bird, J.A., Gleixner, G., Dawson, T.E., Torn, M.S., 2011. Relative contribution of foliar and fine root pine litter to the molecular composition of soil organic matter after in situ degradation. *Organic Geochemistry* 42, 1099-1108.

Mann, M. E., R. S. Bradley, and M. K. Hughes (1998), Global-scale temperature patterns and climate forcing over the past six centuries, *Nature*, *392*(6678), 779-787, doi:10.1038/33859.

Mann, M. E., Z. H. Zhang, S. Rutherford, R. S. Bradley, M. K. Hughes, D. Shindell, C. Ammann, G. Faluvegi, and F. B. Ni (2009), Global Signatures and Dynamical Origins of the Little Ice Age and Medieval Climate Anomaly, *Science, 326*(5957), 1256-1260, doi:10.1126/science.1177303.

Mannino, A., Harvey, H.R., 2000. Biochemical composition of particles and dissolved organic matter along an estuarine gradient: Sources and implications for DOM reactivity. *Limnology and Oceanography* 45, 775-788.

Markel, E. R., R. K. Booth, and Y. Qin (2010), Testate amoebae and $\delta^{13}C$ of *Sphagnum* as surface-moisture proxies in Alaskan peatlands, *The Holocene*.

Mauquoy, D., T. Engelkes, M. Groot, F. Markesteijn, M. Oudejans, J. Van Der Plicht, and B. Van Geel (2002), High-resolution records of late-Holocene climate change and carbon accumulation in two north-west European ombrotrophic peat bogs, *Paleogeogr. Paleoclimatol. Paleoecol.*, *186*(3), 275-310.

Mauquoy, D., B. van Geel, M. Blaauw, and J. van der Plicht (2002), Evidence from northwest European bogs shows 'Little Ice Age' climatic changes driven by variations in solar activity, *Holocene*, *12*(1), 1-6, doi:10.1191/0959683602hl514rr.

McClymont, E. L., E. M. Bingham, C. J. Nott, F. M. Chambers, R. D. Pancost, and R. P. Evershed (2011), Pyrolysis GC-MS as a rapid screening tool for determination of peat-forming plant composition in cores from ombrotrophic peat, *Org. Geochem*., 42(11), 1420-1435 doi: 10.1016/j.orggeochem.2011.07.004.

Melillo, J., Naiman, R., Aber, J., Linkins, A., 1984. Factors controlling mass loss and nitrogen dynamics of plant litter decaying in northern streams. *Bulletin of Marine Science* 35, 341-356.

Mikutta, R., K. Kaiser, N. Doerr, A. Vollmer, O. A. Chadwick, J. Chorover, M. G. Kramer, and G. Guggenberger (2010), Mineralogical impact on organic nitrogen across a long-term soil chronosequence (0.3-4100 kyr), *Geochim. Cosmochim. Acta*, *74*(7), 2142-2164 doi: 10.1016/j.gca.2010.01.006.

Miltner, A., Kindler, R., Knicker, H., Richnow, H.H., Kastner, M., 2009. Fate of microbial biomass-derived amino acids in soil and their contribution to soil organic matter. *Organic Geochemistry* 40, 978-985.

Mole, S., 1993. The systematic distribution of tannins in the leaves of angiosperms: a tool for ecological studies. *Biochemical Systematics and Ecology* 21, 833-846.

Moore, E.K., Nunn, B.L., Goodlett, D.R., Harvey, H.R., 2012. Identifying and tracking proteins through the marine water column: Insights into the inputs and preservation mechanisms of protein in sediments. *Geochimica et Cosmochimica Acta* 83, 324-359.

Moore, T. R., J. L. Bubier, and L. Bledzki (2007), Litter decomposition in temperate peatland ecosystems: The effect of substrate and site, *Ecosystems*, *10*(6), 949-963, doi:10.1007/s10021-007-9064-5.

Nagata, T., Fukuda, R., Koike, I., Kogure, K., Kirchman, D.L., 1998. Degradation by bacteria of membrane and soluble protein in seawater. *Aquatic Microbial Ecology* 14, 29-37.

Nguyen, R.T., Harvey, H.R., 2003. Preservation via macromolecular associations during *Botryococcus braunii* decay: proteins in the Pula Kerogen. *Organic Geochemistry* 34, 1391-1403.

Nichols, J. E., and Y. S. Huang (2007), C-23-C-31 n-alkan-2-ones are biornarkers for the genus Sphagnum in freshwater peatlands, *Org. Geochem.*, *38*(11), 1972-1976, doi:10.1016/j.orggeochem.2007.07.002.

Nichols, J. E., R. K. Booth, S. T. Jackson, E. G. Pendall, and Y. S. Huang (2006), Paleohydrologic reconstruction based on n-alkane distributions in ombrotrophic peat, *Org. Geochem.*, *37*(11), 1505-1513, doi:10.1016/j.orggeochem.2006.06.020.

Nunez, A., Fishman, M.L., Fortis, L.L., Cooke, P.H., Hotchkiss, A.T., Jr., 2009. Identification of extensin protein associated with sugar beet pectin. *Journal of Agricultural and Food Chemistry* 57, 10951-10958.

Opsahl, S., Benner, R., 1995. Early diagenesis of vascular plant tissues: Lignin and cutin decomposition and biogeochemical implications. *Geochimica et Cosmochimica Acta* 59, 4889-4904.

Opsahl, S., Benner, R., 1999. Characterization of carbohydrates during early diagenesis of five vascular plant tissues. *Organic Geochemistry* 30, 83-94.

O'Reilly, B. C., S. A. Finkelstein, and J. Bunbury (2014), Pollen-Derived Paleovegetation Reconstruction and Long-Term Carbon Accumulation at a Fen Site in the Attawapiskat River Watershed, Hudson Bay Lowlands, Canada, *Arctic, Antarctic, and Alpine Research*, *46*(1), 6-18.

Osborn, T. J., and K. R. Briffa (2006), The spatial extent of 20th-century warmth in the context of the past 1200 years, *Science*, *311*(5762), 841-844, doi:10.1126/science.1120514.

Otto, A., and M. J. Simpson (2006), Evaluation of CuO oxidation parameters for determining the source and stage of lignin degradation in soil, *Biogeochemistry*, *80*(2), 121-142.

PAGES 2k Consortium (2013), Continental-scale temperature variability during the past two millennia, *Nature Geoscience*, *6*(5), 339-346, doi:10.1038/ngeo1797.

Pancost, R. D., M. Baas, B. van Geel, and J. S. S. Damste (2002), Biomarkers as proxies for plant inputs to peats: an example from a sub-boreal ombrotrophic bog, *Org. Geochem.*, *33*(7), 675-690, doi:10.1016/s0146-6380(02)00048-7.

Pancost, R. D., M. Baas, B. van Geel, and J. S. S. Damste (2003), Response of an ombrotrophic bog to a regional climate event revealed by macrofossil, molecular and carbon isotopic data, *Holocene*, *13*(6), 921-932, doi:10.1191/0959683603hl674rp.

Parton, W., Silver, W.L., Burke, I.C., Grassens, L., Harmon, M.E., Currie, W.S., King, J.Y., Adair, E.C., Brandt, L.A., Hart, S.C., Fasth, B., 2007. Global-scale similarities in nitrogen release patterns during long-term decomposition. *Science* 315, 361-364.

Payne, R. J., and E. A. Mitchell (2009), How many is enough? Determining optimal count totals for ecological and palaeoecological studies of testate amoebae, *Journal of Paleolimnology*, *42*(4), 483-495.

Peteet, D., A. Andreev, W. Bardeen, and F. Mistretta (1998), Long-term Arctic peatland dynamics, vegetation and climate history of the Pur-Taz region, Western Siberia, *Boreas*, *27*(2), 115-126.

Pitkanen, A., J. Turunen, T. Tahvanainen, and K. Tolonen (2002), Holocene vegetation history from the Salym-Yugan Mire Area, West Siberia, *Holocene*, *12*(3), 353-362, doi:10.1191/0959683602hl533rp.

Popper, Z.A., 2008. Evolution and diversity of green plant cell walls. *Current Opinion in Plant Biology* 11, 286-292.

Prahl, F. G., J. R. Ertel, M. A. Goni, M. A. Sparrow, and B. Eversmeyer (1994), Terrestrial organic carbon contributions to sediments on the Washington margin, *Geochimica Et Cosmochimica Acta*, *58*(14), 3035-3048, doi:10.1016/0016-7037(94)90177-5.

Qi, X.Y., Behrens, B.X., West, P.R., Mort, A.J., 1995. Solubilization and partial characterization of extensin fragments from cell walls of cotton suspension cultures: evidence for a covalent cross-link between extensin and pectin. *Plant Physiology* 108, 1691-1701.

Rasmussen, M., Jacobsson, M., Bjorck, L., 2003. Genome-based identification and analysis of collagen-related structural motifs in bacterial and viral proteins. *Journal of Biological Chemistry* 278, 32313-32316.

Rasmussen, S., C. Wolff, and H. Rudolph (1995), Compartmentalization of phenolic constituents in *Sphagnum*, *Phytochemistry*, *38*(1), 35-39, doi:10.1016/0031-9422(94)00650-i.

Robinson, D., 2001. delta N-15 as an integrator of the nitrogen cycle. *Trends in Ecology & Evolution* 16, 153-162.

Robinson, S., and T. Moore (2000), The influence of permafrost and fire upon carbon accumulation in high boreal peatlands, Northwest Territories, Canada, *Arct. Antarct. Alp. Res.*, 155-166.

Ronkainen, T., E. L. McClymont, M. Valiranta, and E. S. Tuittila (2013), The n-alkane and sterol composition of living fen plants as a potential tool for palaeoecological studies, *Org. Geochem.*, *59*, 1-9 doi: 10.1016/j.orggeochem.2013.03.005.

Sannel, A. B. K., and P. Kuhry (2008), Long-term stability of permafrost in subarctic peat plateaus, west-central Canada, *Holocene, 18*(4), 589-601, doi:10.1177/0959683608089658.

Sarkanen, K. V., and C. H. Ludwig (1971), *Lignins: occurence, formation, structure, and reactions*, 916 pp., Wiley-Interscience, N.Y.

Sarkar, P., Bosneaga, E., Auer, M., 2009. Plant cell walls throughout evolution: towards a molecular understanding of their design principles. *Journal of Experimental Botany* 60, 3615-3635.

Scheffer, R. A., R. S. P. van Logtestijn, and J. T. A. Verhoeven (2001), Decomposition of Carex and Sphagnum litter in two mesotrophic fens differing in dominant plant species, *Oikos, 92*(1), 44-54.

Schleifer, K., and O. Kandler (1972), Peptidoglycan types of bacterial cell walls and their taxonomic implications, *Bacteriological Reviews, 36*(4), 407-477.

Schlesinger, W. H., and E. S. Bernhardt (2013), *Biogeochemistry: an analysis of global change*, Academic press.

Schmidt, M. W. I., H. Knicker, and I. Kögel-Knabner (2000), Organic matter accumulating in Aeh and Bh horizons of a Podzol— chemical characterization in primary organo-mineral associations, *Org. Geochem., 31*(7–8), 727-734.

Schnabelrauch, L.S., Kieliszewski, M., Upham, B.L., Alizedeh, H., Lamport, D.T.A., 1996. Isolation of pl 4.6 extensin peroxidase from tomato cell suspension cultures and identification of Val-Tyr-Lys as putative intermolecular cross-link site. *Plant Journal* 9, 477-489.

Sheng, Y. W., L. C. Smith, G. M. MacDonald, K. V. Kremenetski, K. E. Frey, A. A. Velichko, M. Lee, D. W. Beilman, and P. Dubinin (2004), A high-resolution GIS-based inventory of the west Siberian peat carbon pool, *Global biogeochem. cycles*, 18(3) doi: 10.1029/2003gb002190.

Shotyk, W. (1988), Review of the inorganic geochemistry of peats and peatland waters, *Earth-Sci. Rev., 25*(2), 95-176.

Shibasaki, T., Mori, H., Chiba, S., Ozaki, A., 1999. Microbial proline 4-hydroxylase screening and feme cloning. *Applied and Environmental Microbiology* 65, 4028-4031.

Sillasoo, U., M. Valiranta, and E. S. Tuittila (2011), Fire history and vegetation recovery in two raised bogs at the Baltic Sea, *J. Veg. Sci., 22*(6), 1084-1093, doi:10.1111/j.1654-1103.2011.01307.x.

Simpson, A.J., Simpson, M.J., Smith, E., Kelleher, B.P., 2007. Microbially derived inputs to soil organic matter: Are current estimates too low? *Environmental Science & Technology* 41, 8070-8076.

Skoog, A., and R. Benner (1997), Aldoses in various size fractions of marine organic matter: Implications for carbon cycling, *Limnology and Oceanography*, *42*(8), 1803-1813.

Smith, J.J., Muldoon, E.P., Lamport, D.T.A., 1984. Isolation of extensin precursors by direct elution of intact tomato cell suspension cultures. *Phytochemistry* 23, 1233-1239.

Smith, J.J., Muldoon, E.P., Willard, J.J., Lamport, D.T.A., 1986. Tomato extensin precursors P1 and P2 are highly periodic structures. *Phytochemistry* 25, 1021-1030.

Smith, L. C., G. MacDonald, A. Velichko, D. Beilman, O. Borisova, K. Frey, K. Kremenetski, and Y. Sheng (2004), Siberian peatlands a net carbon sink and global methane source since the early Holocene, *Science*, *303*(5656), 353-356.

Smith, L. C., D. W. Beilman, K. V. Kremenetski, Y. W. Sheng, G. M. MacDonald, R. B. Lammers, A. I. Shiklomanov, and E. D. Lapshina (2012), Influence of permafrost on water storage in West Siberian peatlands revealed from a new database of soil properties, *Permafrost and Periglacial Processes*, *23*(1), 69-79, doi:10.1002/ppp.735.

Sowden, F. J., Y. Chen, and M. Schnitzer (1977), Nitrogen distribution in soils formed under widely differing climatic conditions, *Geochim. Cosmochim. Acta*, *41*(10), 1524-1526.

Stafstrom, J.P., Staehelin, L.A., 1986a. Cross-linking patterns in salt-extractable extensin from carrot cell walls. *Plant Physiology* 81, 234-241.

Stafstrom, J.P., Staehelin, L.A., 1986b. The role of carbohydrate in maintaining extensin in an extended conformation. *Plant Physiology* 81, 242-246.

Stocker, T. F., D. Qin, G.-K. Plattner, M. Tignor, S. K. Allen, J. Boschung, A. Nauels, Y. Xia, V. Bex, and P. M. Midgley (2013), Climate change 2013: The physical science basis, *Intergovernmental Panel on Climate Change, Working Group I Contribution to the IPCC Fifth Assessment Report (AR5)(Cambridge Univ Press, New York)*.

Stout, S.A., Boon, J.J., Spackman, W., 1988. Molecular aspects of the peatification and early coalification of angiosperm and gymnosperm woods. *Geochimica et Cosmochimica Acta* 52, 405-414.

Strobel, G.A., Miller, R.V., Martinez-Miller, C., Condron, M.M., Teplow, D.B., Hess, W.M., 1999. Cryptocandin, a potent antimycotic from the endophytic fungus Cryptosporiopsis cf. quercina. *Microbiology-UK* 145, 1919-1926.

Stuart, D.A., Varner, J.E., 1980. Purification and characterization of a salt-extractable hydroxyproline-rich glycoprotein from aerated carrot disks. *Plant Physiology* 66, 787-792.

Swindles, G. T., G. Plunkett, and H. M. Roe (2007), A delayed climatic response to solar forcing at 2800 cal. BP: multiproxy evidence from three Irish peatlands, *Holocene*, *17*(2), 177-182, doi:10.1177/0959683607075830.

Swindles, G. T., R. T. Patterson, H. M. Roe, and J. M. Galloway (2012), Evaluating periodicities in peat-based climate proxy records, *Quat. Sci. Rev.*, *41*, 94-103, doi:10.1016/j.quascirev.2012.03.003.

Szpak, P., 2011. Fish bone chemistry and ultrastructure: implications for taphonomy and stable isotope analysis. *Journal of Archaeological Science* 38, 3358-3372.

Tareq, S. M., N. Tanaka, and K. Ohta (2004), Biomarker signature in tropical wetland: lignin phenol vegetation index (LPVI) and its implications for reconstructing the paleoenvironment, *Sci. Total Environ.*, *324*(1-3), 91-103, doi:10.1016/j.scitotenv.2003.10.020.

Thormann, M., A. Szumigalski, and S. Bayley (1999), Aboveground peat and carbon accumulation potentials along a bog-fen-marsh wetland gradient in southern boreal Alberta, Canada, *Wetlands*, *19*(2), 305-317 doi: 10.1007/bf03161761.

Tremblay, L., Benner, R., 2006. Microbial contributions to N-immobilization and organic matter preservation in decaying plant detritus. *Geochimica et Cosmochimica Acta* 70, 133-146.

Turunen, J., T. Tahvanainen, K. Tolonen, and A. Pitkanen (2001), Carbon accumulation in West Siberian mires, Russia, *Global biogeochemical cycles*, *15*(2), 285-296, doi:10.1029/2000gb001312

Updegraff, K., S. D. Bridgham, J. Pastor, P. Weishampel, and C. Harth (2001), Response of CO2 and CH4 emissions from peatlands to warming and water table manipulation, *Ecol. Appl.*, *11*(2), 311-326.

Valiranta, M., A. Korhola, H. Seppa, E. S. Tuittila, K. Sarmaja-Korjonen, J. Laine, and J. Alm (2007), High-resolution reconstruction of wetness dynamics in a southern boreal raised bog, Finland, during the late Holocene: a quantitative approach, *Holocene*, *17*(8), 1093-1107, doi:10.1177/0959683607082550.

van Breemen, N. (1995), How Sphagnum bogs down other plants, *Trends in Ecology & Evolution*, *10*(7), 270-275.

Vanholst, G.J., Varner, J.E., 1984. Reinforced polyproline II conformation in a hydroxyproline-rich cell wall glycoprotein from carrot root. *Plant Physiology* 74, 247-251.

Verhoeven, J., and W. Liefveld (1997), The ecological significance of organochemical compounds in Sphagnum, *Acta Botanica Neerlandica*, *46*(2), 117-130.

Vitt, D. H., K. Wieder, L. A. Halsey, and M. Turetsky (2003), Response of Sphagnum fuscum to nitrogen deposition: a case study of ombrogenous peatlands in Alberta, Canada, *Bryologist*, *106*(2), 235-245 doi: 10.1639/0007-2745(2003)106[0235:ROSFTN]2.0.CO;2.

Watson, A., K. D. Stephen, D. B. Nedwell, and J. R. Arah (1997), Oxidation of methane in peat: Kinetics of CH_4 and O_2 removal and the role of plant roots, *Soil Biology and Biochemistry*, *29*(8), 1257-1267.

White, D.S., Howes, B.L., 1994. Nitrogen incorporation into decomposing litter of Spartina alterniflora. *Limnology and Oceanography*, 133-140.

Williams, C. J., and J. B. Yavitt (2003), Botanical composition of peat and degree of peat decomposition in three temperate peatlands, *Ecoscience*, *10*(1), 85-95.

Williams, C. J., J. B. Yavitt, R. K. Wieder, and N. L. Cleavitt (1998), Cupric oxide oxidation products of northern peat and peat-forming plants, *Can. J. Bot.-Rev. Can. Bot.*, *76*(1), 51-62.

Wilson, L.G., Fry, J.C., 1986. Extensin - a major cell wall glycoprotein. *Plant Cell and Environment* 9, 239-260.

Wilson, M. A., J. Sawyer, P. G. Hatcher, and H. E. Lerch (1989), 1,3,5-Hydroxybenezene structures in mosses, *Phytochemistry*, *28*(5), 1395-1400, doi:10.1016/s0031-9422(00)97754-9.

Woodland, W. A., D. J. Charman, and P. C. Sims (1998), Quantitative estimates of water tables and soil moisture in Holocene peatlands from testate amoebae, *The Holocene*, *8*(3), 261-273.

Yamada, N., Tanoue, E., 2003. Detection and partial characterization of dissolved glycoproteins in oceanic waters. *Limnology and Oceanography* 48, 1037-104.

Yeloff, D., and D. Mauquoy (2006), The influence of vegetation composition on peat humification: implications for palaeoclimatic studies, *Boreas*, *35*(4), 662-673 doi: 10.1080/03009480600690860.

Yu, Z. C., J. Loisel, D. P. Brosseau, D. W. Beilman, and S. J. Hunt (2010), Global peatland dynamics since the Last Glacial Maximum, *Geophys. Res. Lett.*, *37* doi: 10.1029/2010gl043584.

Zaccone, C., D. Said-Pullicino, G. Gigliotti, and T. Miano (2008), Diagenetic trends in the phenolic constituents of *Sphagnum*-dominated peat and its corresponding humic acid fraction, *Org. Geochem.*, *39*(7), 830-838.

Zhou, W. J., S. C. Xie, P. A. Meyers, and Y. H. Zheng (2005), Reconstruction of late glacial and Holocene climate evolution in southern China from geolipids and pollen in the Dingnan peat sequence, *Org. Geochem.*, *36*(9), 1272-1284, doi: 10.1016/j.orggeochem.2005.04.005.

Zhou, W. J., Y. H. Zheng, P. A. Meyers, A. J. T. Jull, and S. C. Xie (2010), Postglacial climate-change record in biomarker lipid compositions of the Hani peat sequence, Northeastern China, *Earth Planet. Sci. Lett.*, *294*(1-2), 37-46, doi:10.1016/j.epsl.2010.02.035.

Zoltai, S. C. (1993), Cyclic development of permafrost in the peatlands of northwestern Alberta, Canada, *Arct. Alp. Res.*, *25*(3), 240-246, doi:10.2307/1551820.

APPENDIX A – SUPPLEMENTARY FIGURES

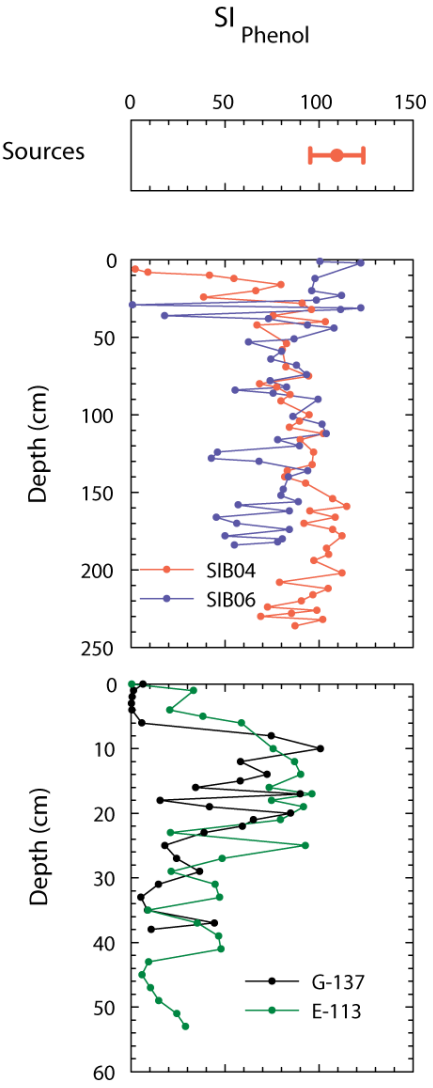

Figure A.1 Profile of PON yield (SI_{Phenol}) in the 4 peat cores. The average and standard deviation of SIPhenol in Sphagnum is shown at the top of the profile

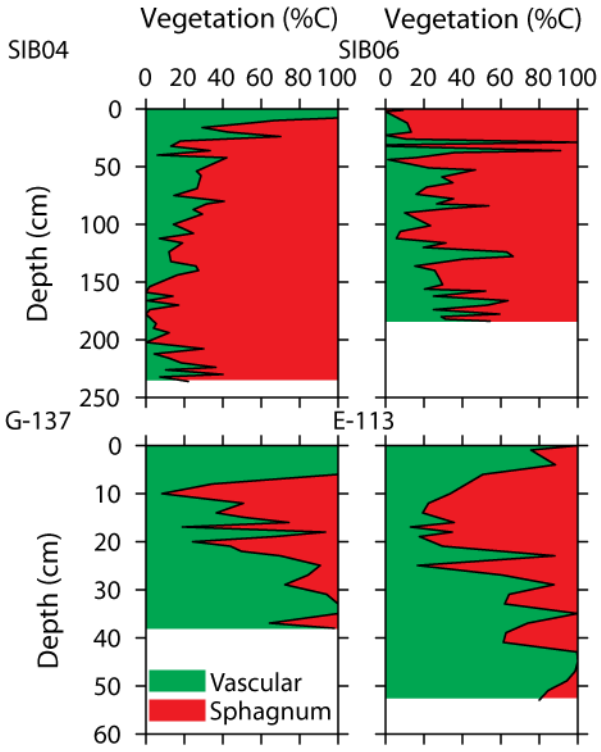

Figure A.2 Vegetation reconstruction using SI_{Phenol} in the four peat cores. SI_{Phenol} was used to calculate the *Sphagnum* input and % vascular plant was calculated by subtraction.

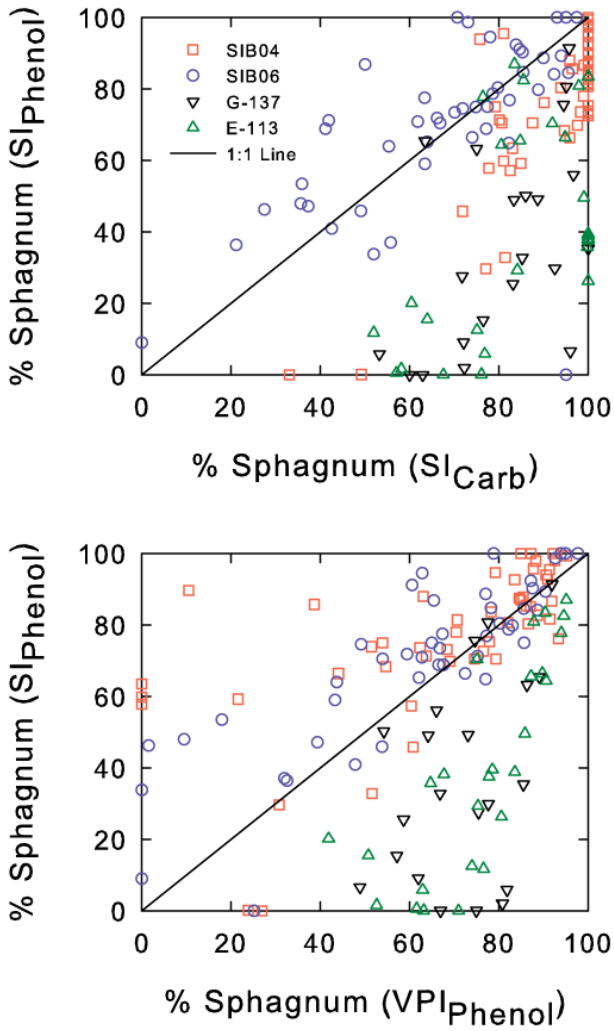

Figure A.3 Correlation of PON-based vegetation reconstruction with neutral sugar- (a) and lignin phenol-based reconstructions (b). The solid line indicates a 1:1 relationship. Samples containing lichen remains (as indicated by LI_{Carb}) were excluded.

APPENDIX B – PERMISSION TO REPRINT

ELSEVIER LICENSE
TERMS AND CONDITIONS

Sep 18, 2014

This is a License Agreement between Michael Philben ("You") and Elsevier ("Elsevier") provided by Copyright Clearance Center ("CCC"). The license consists of your order details, the terms and conditions provided by Elsevier, and the payment terms and conditions.

All payments must be made in full to CCC. For payment instructions, please see information listed at the bottom of this form.

Supplier	Elsevier Limited The Boulevard,Langford Lane Kidlington,Oxford,OX5 1GB,UK
Registered Company Number	1982084
Customer name	Michael Philben
Customer address	Department of Biological Sciences COLUMBIA, SC 29208
License number	3471950288461
License date	Sep 18, 2014
Licensed content publisher	Elsevier
Licensed content publication	Organic Geochemistry
Licensed content title	Reactivity of hydroxyproline-rich glycoproteins and their potential as biochemical tracers of plant-derived nitrogen
Licensed content author	Michael Philben,Ronald Benner
Licensed content date	April 2013
Licensed content volume number	57
Licensed content issue number	n/a
Number of pages	12
Start Page	11

End Page	22
Type of Use	reuse in a thesis/dissertation
Portion	full article
Format	both print and electronic
Are you the author of this Elsevier article?	Yes
Will you be translating?	No
Title of your thesis/dissertation	Climatic Controls on Organic Matter Decomposition in Boreal Peatlands
Expected completion date	Dec 2014
Estimated size (number of pages)	150
Elsevier VAT number	GB 494 6272 12
Permissions price	0.00 USD
VAT/Local Sales Tax	0.00 USD / 0.00 GBP
Total	0.00 USD
Terms and Conditions	

INTRODUCTION

1. The publisher for this copyrighted material is Elsevier. By clicking "accept" in connection with completing this licensing transaction, you agree that the following terms and conditions apply to this transaction (along with the Billing and Payment terms and conditions established by Copyright Clearance Center, Inc. ("CCC"), at the time that you opened your Rightslink account and that are available at any time at http://myaccount.copyright.com).

GENERAL TERMS

2. Elsevier hereby grants you permission to reproduce the aforementioned material subject to the terms and conditions indicated.

3. Acknowledgement: If any part of the material to be used (for example, figures) has appeared in our publication with credit or acknowledgement to another source, permission must also be sought from that source. If such permission is not obtained then that material may not be included in your publication/copies. Suitable acknowledgement to the source must be made, either as a footnote or in a reference list at the end of your publication, as follows:

"Reprinted from Publication title, Vol /edition number, Author(s), Title of article / title of chapter, Pages No., Copyright (Year), with permission from Elsevier [OR APPLICABLE SOCIETY COPYRIGHT OWNER]." Also Lancet special credit - "Reprinted from The Lancet, Vol. number, Author(s), Title of article, Pages No., Copyright (Year), with permission from Elsevier."

4. Reproduction of this material is confined to the purpose and/or media for which permission is hereby given.

5. Altering/Modifying Material: Not Permitted. However figures and illustrations may be altered/adapted minimally to serve your work. Any other abbreviations, additions, deletions and/or any other alterations shall be made only with prior written authorization of Elsevier Ltd. (Please contact Elsevier at permissions@elsevier.com)

6. If the permission fee for the requested use of our material is waived in this instance, please be advised that your future requests for Elsevier materials may attract a fee.

7. Reservation of Rights: Publisher reserves all rights not specifically granted in the combination of (i) the license details provided by you and accepted in the course of this licensing transaction, (ii) these terms and conditions and (iii) CCC's Billing and Payment terms and conditions.

8. License Contingent Upon Payment: While you may exercise the rights licensed immediately upon issuance of the license at the end of the licensing process for the transaction, provided that you have disclosed complete and accurate details of your proposed use, no license is finally effective unless and until full payment is received from you (either by publisher or by CCC) as provided in CCC's Billing and Payment terms and conditions. If full payment is not received on a timely basis, then any license preliminarily granted shall be deemed automatically revoked and shall be void as if never granted. Further, in the event that you breach any of these terms and conditions or any of CCC's Billing and Payment terms and conditions, the license is automatically revoked and shall be void as if never granted. Use of materials as described in a revoked license, as well as any use of the materials beyond the scope of an unrevoked license, may constitute copyright infringement and publisher reserves the right to take any and all action to protect its copyright in the materials.

9. Warranties: Publisher makes no representations or warranties with respect to the licensed material.

10. Indemnity: You hereby indemnify and agree to hold harmless publisher and CCC, and their respective officers, directors, employees and agents, from and against any and all claims arising out of your use of the licensed material other than as specifically authorized pursuant to this license.

11. No Transfer of License: This license is personal to you and may not be sublicensed, assigned, or transferred by you to any other person without publisher's written permission.

12. No Amendment Except in Writing: This license may not be amended except in a writing signed by both parties (or, in the case of publisher, by CCC on publisher's behalf).

13. Objection to Contrary Terms: Publisher hereby objects to any terms contained in any purchase order, acknowledgment, check endorsement or other writing prepared by you,

which terms are inconsistent with these terms and conditions or CCC's Billing and Payment terms and conditions. These terms and conditions, together with CCC's Billing and Payment terms and conditions (which are incorporated herein), comprise the entire agreement between you and publisher (and CCC) concerning this licensing transaction. In the event of any conflict between your obligations established by these terms and conditions and those established by CCC's Billing and Payment terms and conditions, these terms and conditions shall control.

14. Revocation: Elsevier or Copyright Clearance Center may deny the permissions described in this License at their sole discretion, for any reason or no reason, with a full refund payable to you. Notice of such denial will be made using the contact information provided by you. Failure to receive such notice will not alter or invalidate the denial. In no event will Elsevier or Copyright Clearance Center be responsible or liable for any costs, expenses or damage incurred by you as a result of a denial of your permission request, other than a refund of the amount(s) paid by you to Elsevier and/or Copyright Clearance Center for denied permissions.

LIMITED LICENSE

The following terms and conditions apply only to specific license types:

15. **Translation**: This permission is granted for non-exclusive world **English** rights only unless your license was granted for translation rights. If you licensed translation rights you may only translate this content into the languages you requested. A professional translator must perform all translations and reproduce the content word for word preserving the integrity of the article. If this license is to re-use 1 or 2 figures then permission is granted for non-exclusive world rights in all languages.

16. **Posting licensed content on any Website**: The following terms and conditions apply as follows: Licensing material from an Elsevier journal: All content posted to the web site must maintain the copyright information line on the bottom of each image; A hyper-text must be included to the Homepage of the journal from which you are licensing athttp://www.sciencedirect.com/science/journal/xxxxx or the Elsevier homepage for books athttp://www.elsevier.com; Central Storage: This license does not include permission for a scanned version of the material to be stored in a central repository such as that provided by Heron/XanEdu.

Licensing material from an Elsevier book: A hyper-text link must be included to the Elsevier homepage at http://www.elsevier.com . All content posted to the web site must maintain the copyright information line on the bottom of each image.

Posting licensed content on Electronic reserve: In addition to the above the following clauses are applicable: The web site must be password-protected and made available only to bona fide students registered on a relevant course. This permission is granted for 1 year

only. You may obtain a new license for future website posting.

For journal authors: the following clauses are applicable in addition to the above: Permission granted is limited to the author accepted manuscript version* of your paper.

***Accepted Author Manuscript (AAM) Definition:** An accepted author manuscript (AAM) is the author's version of the manuscript of an article that has been accepted for publication and which may include any author-incorporated changes suggested through the processes of submission processing, peer review, and editor-author communications. AAMs do not include other publisher value-added contributions such as copy-editing, formatting, technical enhancements and (if relevant) pagination.

You are not allowed to download and post the published journal article (whether PDF or HTML, proof or final version), nor may you scan the printed edition to create an electronic version. A hyper-text must be included to the Homepage of the journal from which you are licensing at http://www.sciencedirect.com/science/journal/xxxxx. As part of our normal production process, you will receive an e-mail notice when your article appears on Elsevier's online service ScienceDirect (www.sciencedirect.com). That e-mail will include the article's Digital Object Identifier (DOI). This number provides the electronic link to the published article and should be included in the posting of your personal version. We ask that you wait until you receive this e-mail and have the DOI to do any posting.

Posting to a repository: Authors may post their AAM immediately to their employer's institutional repository for internal use only and may make their manuscript publically available after the journal-specific embargo period has ended.

Please also refer to Elsevier's Article Posting Policy for further information.

18. **For book authors** the following clauses are applicable in addition to the above: Authors are permitted to place a brief summary of their work online only.. You are not allowed to download and post the published electronic version of your chapter, nor may you scan the printed edition to create an electronic version. **Posting to a repository:** Authors are permitted to post a summary of their chapter only in their institution's repository.

20. **Thesis/Dissertation**: If your license is for use in a thesis/dissertation your thesis may be submitted to your institution in either print or electronic form. Should your thesis be published commercially, please reapply for permission. These requirements include permission for the Library and Archives of Canada to supply single copies, on demand, of the complete thesis and include permission for UMI to supply single copies, on demand, of the complete thesis. Should your thesis be published commercially, please reapply for permission.

Elsevier Open Access Terms and Conditions

Elsevier publishes Open Access articles in both its Open Access journals and via its Open Access articles option in subscription journals.

Authors publishing in an Open Access journal or who choose to make their article Open Access in an Elsevier subscription journal select one of the following Creative Commons user licenses, which define how a reader may reuse their work: Creative Commons Attribution License (CC BY), Creative Commons Attribution – Non Commercial - ShareAlike (CC BY NC SA) and Creative Commons Attribution – Non Commercial – No Derivatives (CC BY NC ND)

Terms & Conditions applicable to all Elsevier Open Access articles:

Any reuse of the article must not represent the author as endorsing the adaptation of the article nor should the article be modified in such a way as to damage the author's honour or reputation.

The author(s) must be appropriately credited.

If any part of the material to be used (for example, figures) has appeared in our publication with credit or acknowledgement to another source it is the responsibility of the user to ensure their reuse complies with the terms and conditions determined by the rights holder.

Additional Terms & Conditions applicable to each Creative Commons user license:

CC BY: You may distribute and copy the article, create extracts, abstracts, and other revised versions, adaptations or derivative works of or from an article (such as a translation), to include in a collective work (such as an anthology), to text or data mine the article, including for commercial purposes without permission from Elsevier

CC BY NC SA: For non-commercial purposes you may distribute and copy the article, create extracts, abstracts and other revised versions, adaptations or derivative works of or from an article (such as a translation), to include in a collective work (such as an anthology), to text and data mine the article and license new adaptations or creations under identical terms without permission from Elsevier

CC BY NC ND: For non-commercial purposes you may distribute and copy the article and include it in a collective work (such as an anthology), provided you do not alter or modify the article, without permission from Elsevier

Any commercial reuse of Open Access articles published with a CC BY NC SA or CC BY NC ND license requires permission from Elsevier and will be subject to a fee.

Commercial reuse includes:

- Promotional purposes (advertising or marketing)
- Commercial exploitation (e.g. a product for sale or loan)
- Systematic distribution (for a fee or free of charge)

Please refer to Elsevier's Open Access Policy for further information.

21. **Other Conditions**:

v1.6

Questions? customercare@copyright.com or +1-855-239-3415 (toll free in the US) or +1-978-646-2777.

Gratis licenses (referencing $0 in the Total field) are free. Please retain this printable license for your reference. No payment is required.

JOHN WILEY AND SONS LICENSE TERMS AND CONDITIONS

Sep 18, 2014

This is a License Agreement between Michael Philben ("You") and John Wiley and Sons ("John Wiley and Sons") provided by Copyright Clearance Center ("CCC"). The license consists of your order details, the terms and conditions provided by John Wiley and Sons, and the payment terms and conditions.

All payments must be made in full to CCC. For payment instructions, please see information listed at the bottom of this form.

License Number

3471950679755

License date

Sep 18, 2014

Licensed content publisher

John Wiley and Sons

Licensed content publication

Journal of Geophysical Research: Biogeosciences

Licensed content title

Biochemical evidence for minimal vegetation change in peatlands of the West Siberian Lowland during the Medieval Climate Anomaly and Little Ice Age

Licensed copyright line

Licensed content author

Michael Philben,Karl Kaiser,Ronald Benner

Licensed content date

May 12, 2014

Start page

808

End page

825

Type of use

Dissertation/Thesis

Requestor type

Author of this Wiley article

Format

Print and electronic

Portion

Full article

Will you be translating?

No

Title of your thesis / dissertation

Climatic Controls on Organic Matter Decomposition in Boreal Peatlands

Expected completion date

Dec 2014

Expected size (number of pages)

150

Total

0.00 USD

Terms and Conditions

TERMS AND CONDITIONS

This copyrighted material is owned by or exclusively licensed to John Wiley & Sons, Inc. or one of its group companies (each a"Wiley Company") or handled on behalf of a society with which a Wiley Company has exclusive publishing rights in relation to a particular work (collectively "WILEY"). By clicking accept in connection with completing this licensing transaction, you agree that the following terms and conditions apply to this transaction (along with the billing and payment terms and conditions established by the Copyright Clearance Center Inc., ("CCC's Billing and Payment terms and conditions"), at the time that you opened your Rightslink account (these are available at any time athttp://myaccount.copyright.com).

Terms and Conditions

- The materials you have requested permission to reproduce or reuse (the "Wiley Materials") are protected by copyright.
- You are hereby granted a personal, non-exclusive, non-sub licensable (on a stand-alone basis), non-transferable, worldwide, limited license to reproduce the Wiley Materials for the purpose specified in the licensing process. This license is for a one-time use only and limited to any maximum distribution number specified in the license. The first instance of republication or reuse granted by this licence must be completed within two years of the date of the grant of this licence (although copies prepared before the end date may be distributed thereafter). The Wiley Materials shall not be used in any other manner or

for any other purpose, beyond what is granted in the license. Permission is granted subject to an appropriate acknowledgement given to the author, title of the material/book/journal and the publisher. You shall also duplicate the copyright notice that appears in the Wiley publication in your use of the Wiley Material. Permission is also granted on the understanding that nowhere in the text is a previously published source acknowledged for all or part of this Wiley Material. Any third party content is expressly excluded from this permission.

- With respect to the Wiley Materials, all rights are reserved. Except as expressly granted by the terms of the license, no part of the Wiley Materials may be copied, modified, adapted (except for minor reformatting required by the new Publication), translated, reproduced, transferred or distributed, in any form or by any means, and no derivative works may be made based on the Wiley Materials without the prior permission of the respective copyright owner. You may not alter, remove or suppress in any manner any copyright, trademark or other notices displayed by the Wiley Materials. You may not license, rent, sell, loan, lease, pledge, offer as security, transfer or assign the Wiley Materials on a stand-alone basis, or any of the rights granted to you hereunder to any other person.

- The Wiley Materials and all of the intellectual property rights therein shall at all times remain the exclusive property of John Wiley & Sons Inc, the Wiley Companies, or their respective licensors, and your interest therein is only that of having possession of and the right to reproduce the Wiley Materials pursuant to Section 2 herein during the continuance of this Agreement. You agree that you own no right, title or interest in or to the Wiley Materials or any of the intellectual property rights therein. You shall have no rights hereunder other than the license as provided for above in Section 2. No right, license or interest to any trademark, trade name, service mark or other branding ("Marks") of WILEY or its licensors is granted hereunder, and you agree that you shall not assert any such right, license or interest with respect thereto.

- NEITHER WILEY NOR ITS LICENSORS MAKES ANY WARRANTY OR REPRESENTATION OF ANY KIND TO YOU OR ANY THIRD PARTY, EXPRESS, IMPLIED OR STATUTORY, WITH RESPECT TO THE MATERIALS OR THE ACCURACY OF ANY INFORMATION CONTAINED IN THE MATERIALS, INCLUDING, WITHOUT LIMITATION, ANY IMPLIED WARRANTY OF MERCHANTABILITY, ACCURACY, SATISFACTORY QUALITY, FITNESS FOR A PARTICULAR PURPOSE, USABILITY, INTEGRATION OR NON-INFRINGEMENT AND ALL SUCH WARRANTIES ARE HEREBY EXCLUDED BY WILEY AND ITS LICENSORS AND WAIVED BY YOU

- WILEY shall have the right to terminate this Agreement immediately upon breach of this Agreement by you.
- You shall indemnify, defend and hold harmless WILEY, its Licensors and their respective directors, officers, agents and employees, from and against any actual or threatened claims, demands, causes of action or proceedings arising from any breach of this Agreement by you.

- IN NO EVENT SHALL WILEY OR ITS LICENSORS BE LIABLE TO YOU OR ANY OTHER PARTY OR ANY OTHER PERSON OR ENTITY FOR ANY SPECIAL, CONSEQUENTIAL, INCIDENTAL,

INDIRECT, EXEMPLARY OR PUNITIVE DAMAGES, HOWEVER CAUSED, ARISING OUT OF OR IN CONNECTION WITH THE DOWNLOADING, PROVISIONING, VIEWING OR USE OF THE MATERIALS REGARDLESS OF THE FORM OF ACTION, WHETHER FOR BREACH OF CONTRACT, BREACH OF WARRANTY, TORT, NEGLIGENCE, INFRINGEMENT OR OTHERWISE (INCLUDING, WITHOUT LIMITATION, DAMAGES BASED ON LOSS OF PROFITS, DATA, FILES, USE, BUSINESS OPPORTUNITY OR CLAIMS OF THIRD PARTIES), AND WHETHER OR NOT THE PARTY HAS BEEN ADVISED OF THE POSSIBILITY OF SUCH DAMAGES. THIS LIMITATION SHALL APPLY NOTWITHSTANDING ANY FAILURE OF ESSENTIAL PURPOSE OF ANY LIMITED REMEDY PROVIDED HEREIN.

- Should any provision of this Agreement be held by a court of competent jurisdiction to be illegal, invalid, or unenforceable, that provision shall be deemed amended to achieve as nearly as possible the same economic effect as the original provision, and the legality, validity and enforceability of the remaining provisions of this Agreement shall not be affected or impaired thereby.

- The failure of either party to enforce any term or condition of this Agreement shall not constitute a waiver of either party's right to enforce each and every term and condition of this Agreement. No breach under this agreement shall be deemed waived or excused by either party unless such waiver or consent is in writing signed by the party granting such waiver or consent. The waiver by or consent of a party to a breach of any provision of this Agreement shall not operate or be construed as a waiver of or consent to any other or subsequent breach by such other party.

- This Agreement may not be assigned (including by operation of law or otherwise) by you without WILEY's prior written consent.

- Any fee required for this permission shall be non-refundable after thirty (30) days from receipt by the CCC.

- These terms and conditions together with CCC&#65533;s Billing and Payment terms and conditions (which are incorporated herein) form the entire agreement between you and WILEY concerning this licensing transaction and (in the absence of fraud) supersedes all prior agreements and representations of the parties, oral or written. This Agreement may not be amended except in writing signed by both parties. This Agreement shall be binding upon and inure to the benefit of the parties' successors, legal representatives, and authorized assigns.

- In the event of any conflict between your obligations established by these terms and conditions and those established by CCC&#65533;s Billing and Payment terms and conditions, these terms and conditions shall prevail.

- WILEY expressly reserves all rights not specifically granted in the combination of (i) the license details provided by you and accepted in the course of this licensing transaction, (ii) these terms and conditions and (iii) CCC&#65533;s Billing and Payment terms and conditions.

- This Agreement will be void if the Type of Use, Format, Circulation, or Requestor Type was misrepresented during the licensing process.

- This Agreement shall be governed by and construed in accordance with the laws of the State of New York, USA, without regards to such state's conflict of law rules. Any legal action, suit or proceeding arising out of or relating to these Terms and Conditions or the breach thereof shall be instituted in a court of competent jurisdiction in New York County in the State of New York in the United States of America and each party hereby consents and submits to the personal jurisdiction of such court, waives any objection to venue in such court and consents to service of process by registered or certified mail, return receipt requested, at the last known address of such party.

WILEY OPEN ACCESS TERMS AND CONDITIONS

Wiley Publishes Open Access Articles in fully Open Access Journals and in Subscription journals offering Online Open. Although most of the fully Open Access journals publish open access articles under the terms of the Creative Commons Attribution (CC BY) License only, the subscription journals and a few of the Open Access Journals offer a choice of Creative Commons Licenses:: Creative Commons Attribution (CC-BY) license Creative Commons Attribution Non-Commercial (CC-BY-NC) license and Creative Commons Attribution Non-Commercial-NoDerivs (CC-BY-NC-ND) License. The license type is clearly identified on the article.

Copyright in any research article in a journal published as Open Access under a Creative Commons License is retained by the author(s). Authors grant Wiley a license to publish the article and identify itself as the original publisher. Authors also grant any third party the right to use the article freely as long as its integrity is maintained and its original authors, citation details and publisher are identified as follows: [Title of Article/Author/Journal Title and Volume/Issue. Copyright (c) [year] [copyright owner as specified in the Journal]. Links to the final article on Wiley's website are encouraged where applicable.

The Creative Commons Attribution License

The Creative Commons Attribution License (CC-BY) allows users to copy, distribute and transmit an article, adapt the article and make commercial use of the article. The CC-BY license permits commercial and non-commercial re-use of an open access article, as long as the author is properly attributed.

The Creative Commons Attribution License does not affect the moral rights of authors, including without limitation the right not to have their work subjected to derogatory treatment. It also does not affect any other rights held by authors or third parties in the article, including without limitation the rights of privacy and publicity. Use of the article must not assert or imply, whether implicitly or explicitly, any connection with, endorsement or sponsorship of such use by the author, publisher or any other party associated with the article.

For any reuse or distribution, users must include the copyright notice and make clear to others that the article is made available under a Creative Commons Attribution license, linking to the relevant Creative Commons web page.

To the fullest extent permitted by applicable law, the article is made available as is and without representation or warranties of any kind whether express, implied, statutory or otherwise and including, without limitation, warranties of title, merchantability, fitness for a particular purpose, non-infringement, absence of defects, accuracy, or the presence or absence of errors.

Creative Commons Attribution Non-Commercial License

The Creative Commons Attribution Non-Commercial (CC-BY-NC) License permits use, distribution and reproduction in any medium, provided the original work is properly cited and is not used for commercial purposes.(see below)

Creative Commons Attribution-Non-Commercial-NoDerivs License

The Creative Commons Attribution Non-Commercial-NoDerivs License (CC-BY-NC-ND) permits use, distribution and reproduction in any medium, provided the original work is properly cited, is not used for commercial purposes and no modifications or adaptations are made. (see below)

Use by non-commercial users

For non-commercial and non-promotional purposes, individual users may access, download, copy, display and redistribute to colleagues Wiley Open Access articles, as well as adapt, translate, text- and data-mine the content subject to the following conditions:

- The authors' moral rights are not compromised. These rights include the right of "paternity" (also known as "attribution" - the right for the author to be identified as such) and "integrity" (the right for the author not to have the work altered in such a way that the author's reputation or integrity may be impugned).

- Where content in the article is identified as belonging to a third party, it is the obligation of the user to ensure that any reuse complies with the copyright policies of the owner of that content.

- If article content is copied, downloaded or otherwise reused for non-commercial research and education purposes, a link to the appropriate bibliographic citation (authors, journal, article title, volume, issue, page numbers, DOI and the link to the definitive published version on **Wiley Online Library**) should be maintained. Copyright notices and disclaimers must not be deleted.

- Any translations, for which a prior translation agreement with Wiley has not been agreed, must prominently display the statement: "This is an unofficial translation of an

article that appeared in a Wiley publication. The publisher has not endorsed this translation."

Use by commercial "for-profit" organisations

Use of Wiley Open Access articles for commercial, promotional, or marketing purposes requires further explicit permission from Wiley and will be subject to a fee. Commercial purposes include:

- Copying or downloading of articles, or linking to such articles for further redistribution, sale or licensing;
- Copying, downloading or posting by a site or service that incorporates advertising with such content;
- The inclusion or incorporation of article content in other works or services (other than normal quotations with an appropriate citation) that is then available for sale or licensing, for a fee (for example, a compilation produced for marketing purposes, inclusion in a sales pack)
- Use of article content (other than normal quotations with appropriate citation) by for-profit organisations for promotional purposes
- Linking to article content in e-mails redistributed for promotional, marketing or educational purposes;
- Use for the purposes of monetary reward by means of sale, resale, licence, loan, transfer or other form of commercial exploitation such as marketing products
- Print reprints of Wiley Open Access articles can be purchased from:corporatesales@wiley.com

Further details can be found on Wiley Online Libraryhttp://olabout.wiley.com/WileyCDA/Section/id-410895.html

Other Terms and Conditions:

v1.9

Questions? customercare@copyright.com or +1-855-239-3415 (toll free in the US) or +1-978-646-2777.

Gratis licenses (referencing $0 in the Total field) are free. Please retain this printable license for your reference. No payment is required.

JOHN WILEY AND SONS LICENSE TERMS AND CONDITIONS

Sep 18, 2014

This is a License Agreement between Michael Philben ("You") and John Wiley and Sons ("John Wiley and Sons") provided by Copyright Clearance Center ("CCC"). The license consists of your order details, the terms and conditions provided by John Wiley and Sons, and the payment terms and conditions.

All payments must be made in full to CCC. For payment instructions, please see information listed at the bottom of this form.

License Number	3471950763641
License date	Sep 18, 2014
Licensed content publisher	John Wiley and Sons
Licensed content publication	Journal of Geophysical Research: Biogeosciences
Licensed content title	Does oxygen exposure time control the extent of organic matter decomposition in peatlands?
Licensed copyright line	©2014. American Geophysical Union. All Rights Reserved.
Licensed content author	Michael Philben,Karl Kaiser,Ronald Benner
Licensed content date	May 27, 2014
Start page	897
End page	909
Type of use	Dissertation/Thesis
Requestor type	Author of this Wiley article
Format	Print and electronic
Portion	Full article
Will you be translating?	No
Title of your thesis / dissertation	Climatic Controls on Organic Matter Decomposition in Boreal Peatlands
Expected completion date	Dec 2014
Expected size (number of pages)	150
Total	0.00 USD

TERMS AND CONDITIONS

This copyrighted material is owned by or exclusively licensed to John Wiley & Sons, Inc. or one of its group companies (each a"Wiley Company") or handled on behalf of a society with which a Wiley Company has exclusive publishing rights in relation to a particular work (collectively "WILEY"). By clicking accept in connection with completing this licensing transaction, you agree that the following terms and conditions apply to this transaction (along with the billing and payment terms and conditions established by the Copyright Clearance Center Inc., ("CCC's Billing and Payment terms and conditions"), at the time that you opened your Rightslink account (these are available at any time athttp://myaccount.copyright.com).

Terms and Conditions

- The materials you have requested permission to reproduce or reuse (the "Wiley Materials") are protected by copyright.

- You are hereby granted a personal, non-exclusive, non-sub licensable (on a stand-alone basis), non-transferable, worldwide, limited license to reproduce the Wiley Materials for the purpose specified in the licensing process. This license is for a one-time use only and limited to any maximum distribution number specified in the license. The first instance of republication or reuse granted by this licence must be completed within two years of the date of the grant of this licence (although copies prepared before the end date may be distributed thereafter). The Wiley Materials shall not be used in any other manner or for any other purpose, beyond what is granted in the license. Permission is granted subject to an appropriate acknowledgement given to the author, title of the material/book/journal and the publisher. You shall also duplicate the copyright notice that appears in the Wiley publication in your use of the Wiley Material. Permission is also granted on the understanding that nowhere in the text is a previously published source acknowledged for all or part of this Wiley Material. Any third party content is expressly excluded from this permission.

- With respect to the Wiley Materials, all rights are reserved. Except as expressly granted by the terms of the license, no part of the Wiley Materials may be copied, modified, adapted (except for minor reformatting required by the new Publication), translated, reproduced, transferred or distributed, in any form or by any means, and no derivative works may be made based on the Wiley Materials without the prior permission of the respective copyright owner. You may not alter, remove or suppress in any manner any copyright, trademark or other notices displayed by the Wiley Materials. You may not license, rent, sell, loan, lease, pledge, offer as security, transfer or assign the Wiley Materials on a stand-alone basis, or any of the rights granted to you hereunder to any other person.

- The Wiley Materials and all of the intellectual property rights therein shall at all times remain the exclusive property of John Wiley & Sons Inc, the Wiley Companies, or their

respective licensors, and your interest therein is only that of having possession of and the right to reproduce the Wiley Materials pursuant to Section 2 herein during the continuance of this Agreement. You agree that you own no right, title or interest in or to the Wiley Materials or any of the intellectual property rights therein. You shall have no rights hereunder other than the license as provided for above in Section 2. No right, license or interest to any trademark, trade name, service mark or other branding ("Marks") of WILEY or its licensors is granted hereunder, and you agree that you shall not assert any such right, license or interest with respect thereto.

- NEITHER WILEY NOR ITS LICENSORS MAKES ANY WARRANTY OR REPRESENTATION OF ANY KIND TO YOU OR ANY THIRD PARTY, EXPRESS, IMPLIED OR STATUTORY, WITH RESPECT TO THE MATERIALS OR THE ACCURACY OF ANY INFORMATION CONTAINED IN THE MATERIALS, INCLUDING, WITHOUT LIMITATION, ANY IMPLIED WARRANTY OF MERCHANTABILITY, ACCURACY, SATISFACTORY QUALITY, FITNESS FOR A PARTICULAR PURPOSE, USABILITY, INTEGRATION OR NON-INFRINGEMENT AND ALL SUCH WARRANTIES ARE HEREBY EXCLUDED BY WILEY AND ITS LICENSORS AND WAIVED BY YOU

- WILEY shall have the right to terminate this Agreement immediately upon breach of this Agreement by you.
- You shall indemnify, defend and hold harmless WILEY, its Licensors and their respective directors, officers, agents and employees, from and against any actual or threatened claims, demands, causes of action or proceedings arising from any breach of this Agreement by you.

- IN NO EVENT SHALL WILEY OR ITS LICENSORS BE LIABLE TO YOU OR ANY OTHER PARTY OR ANY OTHER PERSON OR ENTITY FOR ANY SPECIAL, CONSEQUENTIAL, INCIDENTAL, INDIRECT, EXEMPLARY OR PUNITIVE DAMAGES, HOWEVER CAUSED, ARISING OUT OF OR IN CONNECTION WITH THE DOWNLOADING, PROVISIONING, VIEWING OR USE OF THE MATERIALS REGARDLESS OF THE FORM OF ACTION, WHETHER FOR BREACH OF CONTRACT, BREACH OF WARRANTY, TORT, NEGLIGENCE, INFRINGEMENT OR OTHERWISE (INCLUDING, WITHOUT LIMITATION, DAMAGES BASED ON LOSS OF PROFITS, DATA, FILES, USE, BUSINESS OPPORTUNITY OR CLAIMS OF THIRD PARTIES), AND WHETHER OR NOT THE PARTY HAS BEEN ADVISED OF THE POSSIBILITY OF SUCH DAMAGES. THIS LIMITATION SHALL APPLY NOTWITHSTANDING ANY FAILURE OF ESSENTIAL PURPOSE OF ANY LIMITED REMEDY PROVIDED HEREIN.

- Should any provision of this Agreement be held by a court of competent jurisdiction to be illegal, invalid, or unenforceable, that provision shall be deemed amended to achieve as nearly as possible the same economic effect as the original provision, and the legality, validity and enforceability of the remaining provisions of this Agreement shall not be affected or impaired thereby.

- The failure of either party to enforce any term or condition of this Agreement shall not constitute a waiver of either party's right to enforce each and every term and condition of this Agreement. No breach under this agreement shall be deemed waived or excused by either party unless such waiver or consent is in writing signed by the party granting such waiver or consent. The waiver by or consent of a party to a breach of any provision of this Agreement shall not operate or be construed as a waiver of or consent to any other or

subsequent breach by such other party.

- This Agreement may not be assigned (including by operation of law or otherwise) by you without WILEY's prior written consent.

- Any fee required for this permission shall be non-refundable after thirty (30) days from receipt by the CCC.

- These terms and conditions together with CCC's Billing and Payment terms and conditions (which are incorporated herein) form the entire agreement between you and WILEY concerning this licensing transaction and (in the absence of fraud) supersedes all prior agreements and representations of the parties, oral or written. This Agreement may not be amended except in writing signed by both parties. This Agreement shall be binding upon and inure to the benefit of the parties' successors, legal representatives, and authorized assigns.

- In the event of any conflict between your obligations established by these terms and conditions and those established by CCC's Billing and Payment terms and conditions, these terms and conditions shall prevail.

- WILEY expressly reserves all rights not specifically granted in the combination of (i) the license details provided by you and accepted in the course of this licensing transaction, (ii) these terms and conditions and (iii) CCC's Billing and Payment terms and conditions.

- This Agreement will be void if the Type of Use, Format, Circulation, or Requestor Type was misrepresented during the licensing process.

- This Agreement shall be governed by and construed in accordance with the laws of the State of New York, USA, without regards to such state's conflict of law rules. Any legal action, suit or proceeding arising out of or relating to these Terms and Conditions or the breach thereof shall be instituted in a court of competent jurisdiction in New York County in the State of New York in the United States of America and each party hereby consents and submits to the personal jurisdiction of such court, waives any objection to venue in such court and consents to service of process by registered or certified mail, return receipt requested, at the last known address of such party.

WILEY OPEN ACCESS TERMS AND CONDITIONS

Wiley Publishes Open Access Articles in fully Open Access Journals and in Subscription journals offering Online Open. Although most of the fully Open Access journals publish open access articles under the terms of the Creative Commons Attribution (CC BY) License only, the subscription journals and a few of the Open Access Journals offer a choice of Creative Commons Licenses:: Creative Commons Attribution (CC-BY) license Creative Commons Attribution Non-Commercial (CC-BY-NC) license and Creative Commons Attribution Non-Commercial-NoDerivs (CC-BY-NC-ND) License. The license type is clearly identified on the article.

Use by non-commercial users

For non-commercial and non-promotional purposes, individual users may access, download, copy, display and redistribute to colleagues Wiley Open Access articles, as well as adapt, translate, text- and data-mine the content subject to the following conditions:

- The authors' moral rights are not compromised. These rights include the right of "paternity" (also known as "attribution" - the right for the author to be identified as such) and "integrity" (the right for the author not to have the work altered in such a way that the author's reputation or integrity may be impugned).

- Where content in the article is identified as belonging to a third party, it is the obligation of the user to ensure that any reuse complies with the copyright policies of the owner of that content.

- If article content is copied, downloaded or otherwise reused for non-commercial research and education purposes, a link to the appropriate bibliographic citation (authors, journal, article title, volume, issue, page numbers, DOI and the link to the definitive published version on **Wiley Online Library**) should be maintained. Copyright notices and disclaimers must not be deleted.

- Any translations, for which a prior translation agreement with Wiley has not been agreed, must prominently display the statement: "This is an unofficial translation of an article that appeared in a Wiley publication. The publisher has not endorsed this translation."

Use by commercial "for-profit" organisations

Use of Wiley Open Access articles for commercial, promotional, or marketing purposes requires further explicit permission from Wiley and will be subject to a fee. Commercial purposes include:

- Copying or downloading of articles, or linking to such articles for further redistribution, sale or licensing;

- Copying, downloading or posting by a site or service that incorporates advertising with such content;

- The inclusion or incorporation of article content in other works or services (other than normal quotations with an appropriate citation) that is then available for sale or licensing, for a fee (for example, a compilation produced for marketing purposes, inclusion in a sales pack)

- Use of article content (other than normal quotations with appropriate citation) by for-profit organisations for promotional purposes

- Linking to article content in e-mails redistributed for promotional, marketing or educational purposes;

- Use for the purposes of monetary reward by means of sale, resale, licence, loan, transfer or other form of commercial exploitation such as marketing products

- Print reprints of Wiley Open Access articles can be purchased from:corporatesales@wiley.com

Further details can be found on Wiley Online Libraryhttp://olabout.wiley.com/WileyCDA/Section/id-410895.html

Other Terms and Conditions:

v1.9

Questions? customercare@copyright.com or +1-855-239-3415 (toll free in the US) or +1-978-646-2777.

Gratis licenses (referencing $0 in the Total field) are free. Please retain this printable license for your reference. No payment is required.